

Climatic changes in short duration extreme precipitation and rapid onset flooding - implications for design values

NCCS report no. 1/2018



Photo: Arne Hamarsland, NVE

Editors

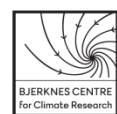
A. Sorteberg (UiB), D.Lawrence (NVE), A. V. Dyrrdal (MET), S. Mayer (UNI), K. Engeland (NVE)

Contributing Authors

A. V. Dyrrdal (MET), K. Engeland (NVE), E. Førland (MET), S. Johansen (UiB), D.Lawrence (NVE), S. Mayer (UNI), N.K. Orthe (NVE), M. I. Sandvik (UiB), L. Schlichting (NVE), R. G. Skaland (MET), T. Skaugen (NVE), A. Sorteberg (UiB), A. Voksø (NVE), K. Vormoor (NVE) og T. Væringstad (NVE)

The Norwegian Centre for Climate Services (NCCS) is a collaboration between the Norwegian Meteorological Institute, the Norwegian Water Resources and Energy Directorate, Uni Research and the Bjerknes Centre for Climate Research. The main purpose of NCCS is to provide decision makers in Norway with information relevant regarding climate change adaptation. In addition to the partners, the Norwegian Environment Agency is represented on the Board.

The NCCS report series includes reports where one or more authors are affiliated to the Centre, as well as reports initiated by the Centre. All reports in the series have undergone a professional assessment by at least one expert associated with the Centre. Reports in this series may also be included in report series from the institutions to which the authors are affiliated.



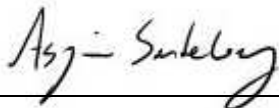
Title:	Date
Climatic changes in short duration extreme precipitation and rapid onset flooding - implications for design values	05.2018
ISSN no.	Report no.
2387-3027	1/2018
Authors	Classification
Editors A. Sorteberg (UiB), D. Lawrence (NVE), A.V. Dyrrdal (MET), S. Mayer (UNI), K. Engeland (NVE)	Free
Contributing Authors A. V. Dyrrdal (MET), K. Engeland (NVE), E. Førland (MET), S. Johansen (UiB), D.Lawrence (NVE), S. Mayer (UNI), N.K. Orthe (NVE), M. I. Sandvik (UiB), L. Schlichting (NVE), R. G. Skaland (MET), T. Skaugen (NVE), A. Sorteberg (UiB), A. Voksø (NVE), K. Vormoor (NVE) og T. Væringstad (NVE)	Clients The Norwegian Research Council, Norwegian Public Roads Administration, Norwegian Rail Administration

Abstract

Short duration extreme precipitation and rapid onset flooding have been the subject of the research project ExPrecFlood - Climatic changes in short duration extreme precipitation and rapid onset flooding - implications for design values. The project consortium consisted of five research partners: The Bjerknes Centre for Climate Research (Univ. of Bergen), the Norwegian Water Resources and Energy Directorate (NVE), the Norwegian Meteorological Institute (MET), Uni Research (UNI), and SINTEF. In addition, there were two user partners: The Norwegian National Rail Administration (Jernbaneverket) and the Norwegian Public Roads Administration (Statens Vegvesen). This is the final report for the project. Through 15 articles we summarize the current status of knowledge on observed trends in short duration extreme precipitation and rapid onset flooding, progress and uncertainties in the estimation of extreme values, possible future changes and newly developed tools and datasets that have been partly financed and become publically available during the project period.

Keywords

Return values, extreme value analysis, extreme precipitation, flood, climate change



Disciplinary signature



Responsible signature

TABLE of CONTENTS

1. Observed trends and statistical relationships

1.1 Trend analyses for short duration rainfall in Norway.....	11
<i>E. J. Førland and A. V. Dyrørdal.</i>	
1.2 Observed trends in the magnitude and frequency of high flow events in Norway during the past 50 years.....	21
<i>K. Vormoor and D. Lawrence</i>	
1.3 Investigating the statistical relationship between extreme rainfall events and peak flows in small catchments.....	29
<i>L. Schlichting, D. Lawrence, K. Engeland, A.V. Dyrørdal</i>	

2. Estimation of short term extreme precipitation

2.1 Estimation of return levels /precipitation design values at single sites in Norway.....	37
<i>A. V. Dyrørdal and E. J. Førland</i>	
2.2 Gridded return level estimates for extreme precipitation using Bayesian hierarchical modeling.	45
<i>A. V. Dyrørdal and E. J. Førland</i>	
2.3 Regionalization of rainfall return values for single sites in Norway.....	51
<i>E. J. Førland and A. V. Dyrørdal</i>	
2.4 Sensitivity of return value estimates to method and sites – a case study for Bergen.....	60
<i>A. Sorteberg and S. Johansen</i>	

3. Hydrological modelling –Datasets and model development

3.1 A high resolution 3-hourly precipitation and temperature forcing dataset for hydrological models.....	73
<i>T. Skaugen and A. V. Dyrørdal</i>	
3.2 The Distance Distribution Dynamics Model- Development for use in ungauged catchments.....	79
<i>T. Skaugen</i>	

4. Future changes in short-term extreme precipitation and flooding

4.1 Projected changes in future short-duration extreme precipitation events using EURO-CORDEX simulations: Stationary and non-stationary analysis..... <i>S. Mayer, A.V.Dyrrdal and R.G.Skaland</i>	91
4.2 Sensitivity of historical extreme precipitation events to a temperature change..... <i>A. Sorteberg and M. I. Sandvik</i>	101
4.3 Modelling the effects of projected changes in sub-daily precipitation intensities on flooding in small catchments..... <i>D. Lawrence</i>	109
4.4 Uncertainty introduced by flood frequency analysis in the estimation of climate change impacts on flooding..... <i>D. Lawrence</i>	121

5. New tools for design flood analysis

5.1 The Intensity-Duration-Frequency (IDF) tool – combining point and grid estimates..... <i>A. V. Dyrrdal and E. J. Førland</i>	131
5.2 NEVINA..... <i>K. Engeland, T. Væringstad, N.K. Orthe, A. Voksø, D. Lawrence</i>	137

Summary

Extreme precipitation and related flooding events have a major impact on Norwegian society's overall vulnerability to climate change and are currently a pressing issue for the transport infrastructure, urban water and sewage systems, buildings, agricultural drainage systems, as well as dam safety. However, our understanding of variability and long-term changes in short-duration extreme precipitation and rapid onset flooding suffers from limited theoretical and empirical knowledge contributing to increased uncertainty in future climate projections and related hydrological impact analyses. Additionally, there is a need for building national competence regarding how to take account of climate change effects in design values for short-duration extreme events. This report summarizes the progress made within the project *Climatic changes in short duration extreme precipitation and rapid onset flooding – Implications for design values (ExPrecFlood)* financed by the Research Council of Norway, the Norwegian Public Roads Administration and the Norwegian Rail Administration.

The report is divided in five parts covering the observed changes in short-duration extreme precipitation and rapid onset flooding, investigation into methods and uncertainties in estimation of short term extreme values in precipitation, model development and development of input datasets to hydrological modeling, future changes in short-term extremes and new tools for design flood analysis that have been made available for users during the project.

Main results:

- A majority of the longest time series of sub-daily precipitation shows positive trends for annual heavy rainfalls as well as for frequencies of high values. However, trend analysis is hampered by the fact that most pluviometers are only operative during the summer season (May-September), time series are short and serious data gaps exist.
- Overall, negative trends reflecting a decrease in flood magnitudes are detected more often than positive trends. Trend analyses distinguishing flood generating processes indicate that high flow events driven by rainfall have become more frequent over the past several decades in southern and western Norway. There is no evidence to suggest that their magnitude has increased. In northern Norway, both the magnitude and frequency of over threshold events have decreased in response to the diminishing role of snowmelt in flood generation.
- An analysis of the occurrence of events generated by rainfall vs. snowmelt indicates that rainfall has increased in importance in driving high flows during the period 1972-2012 in most regions.
- A Bayesian model has been developed and is used to provide spatially continuous maps of precipitation return levels with a high spatial resolution of 1x1 km. Maps for durations 10 – 1440 minutes and return periods of up to 200 years have been estimated and form the basis for new Intensity-Duration-Frequency curves.
- Norway was divided into seven regions and Intensity-Duration-Frequency statistics are calculated for each region. A survey of highest observed rainfall for different durations in the seven regions is presented. Rainfall for various durations is also described as fractions of estimated 1 hour

and 24 hours rainfall. These fractions combined with maps of 1 hour and 24 hours rainfall may be used to deduce rough estimates of rainfall design values.

- Investigation into the sensitivity of return values for extreme sub-daily precipitation to parameter estimation method, length of time series and representativeness of the station selected shows that length of time series and representativeness of the station are the main uncertainties.
- Statistical analyses of the relationship between extreme precipitation and extreme flows have been conducted in 138 small catchments (with area < 50 km²). Results suggest that in most cases there is no significant correlation between the highest observed precipitation intensities and the highest flows in individual catchments. This emphasizes the importance of the antecedent weather and soil wetness, but may partly be due to poor quality of the precipitation estimates.
- A 1*1 km² (seNorge grid) high temporal resolution, 3h, precipitation and temperature dataset covering all of Norway has been developed. It can be used as input to hydrological modelling and precipitation analysis. The daily values are constrained by the 24h seNorge data and disaggregated in time using the sub-daily cycle of precipitation and temperature from an atmospheric model.
- Model development has reduced the errors of predicting runoff at ungauged basins in the Distance Distribution Dynamics (DDD) model by 50% compared to the previous version.
- Analysis of modelled changes in future hourly and 3-hourly extreme precipitation suggests that increases in the 200-year event will be in the order of +40 to +50% at the end of the century given a high future emission scenario (rcp8.5).
- Simulations where the temperature of historical extreme precipitation events was increased to see the effect of a warmer atmosphere on the extreme precipitation have been conducted for a set of extreme events. Change in the intensity of the daily extreme precipitation was on average around 5% per degree warming with a distinct geographical pattern. The intensity of the most extreme hours within the extreme days changed considerably more. As these were autumn and winter extremes there was a large increase in rainfall (over 20% per degree) on the expense of snowfall.
- Hydrological projections of future streamflow for 65 small (< 160 km²), rapidly responding catchments have been conducted using the DDD hydrological model. Results point towards increases in the 200-yr 3-hr flow that are at least 20 - 25% higher than increases in the daily-averaged 200-yr flow. Simulations suggest that catchments with contributions from both rainfall and snowmelt can have increases in the annual maximum flood of over 40%. The results confirm previous speculations that in small catchments, the instantaneous flood can increase more than the daily flood under a future climate.
- A tool for downloading Intensity-Duration-Frequency curves for extreme precipitation for any point in the country for durations 10 – 1440 minutes and return periods of up to 200 years has been developed and is available at the Norwegian Center for Climate Service webpage (<https://klimaservicesenter.no/>)
- NEVINA (<http://nevina.nve.no/>) is a public, map-based service providing estimates of streamflow characteristics such as design flood values. Results from ExPrecFlood (and other projects) provide the basis for new algorithms for estimating design floods in ungauged catchments, new algorithms for estimating climate factors in ungauged catchments and a dynamic link to the hydrological database for extracting observed floods from quality controlled streamflow observations.

1 Observed trends and statistical relationships



1.1 Trend analyses for short duration rainfall in Norway

E. J. Førland and A. V. Dyrødal

Norwegian Meteorological Institute, Oslo, Norway

Summary

Sub-daily rainfall records in Norway begin in the late 1960s, but trend analysis is hampered by short data series and serious data gaps. A majority of the longest series shows positive trends for annual heavy rainfalls as well as for frequencies of high values. Studies of centennial series of 1-day rainfall confirm positive trends in recent decades, but also indicate a secondary maximum in the 1930s. Rather low maximum values of daily rainfall are recorded in the 1960s and 1970s. Because of decadal variability in rainfall intensities, one should be careful when basing IDF-statistics on short time series.

Introduction

Norwegian cities have experienced several events with heavy rainfall and urban flooding during the recent years. According to NOU 2015:16, there is a positive trend in costs and damages caused by storm water during 2008-2014. It is therefore important to know if there have also been changes in the observed intensity or frequency of heavy sub-daily rainfall events. Annual precipitation over Norway has increased since 1900 and particularly during the late 1970s (Hanssen-Bauer et al., 2015), but trend studies for short-term rainfall are complicated by relatively short and incomplete observation series for Norwegian pluviometer stations.

In the present study, trends have therefore also been studied for the more comprehensive number of series of daily rainfall.

Trends in sub-daily rainfall

Regular measurements of rainfall with sub-daily time resolution (pluviometer (Plu) recordings) started in the late 1960s. However, just a few stations have been running for more than 30 years, and most series contain several serious gaps (Table 1). The criterion for stations included in Table 1 is that they start before 1988; - i.e. more than 30 years ago; - and that the station has still been operative in recent years. Table 1 demonstrates that for several of the stations more than 30 % of the seasons are missing during the station period.

For the 14 long Plu-series in Table 1, most series have positive trends for the studied durations of 10, 30 and 60 minutes for both annual maximum series (AMS) and Peak over threshold (POT). For two of the stations in Oslo (Hausmannsgt and Blindern) the

positive AMS and POT trends are significant (95 % level). For the POT-series, statistical significant trends are found for six stations. Two stations (Øvrevoll and Time-Lye) have negative trends in the AMS-series. For five of the stations the gaps were too serious to allow POT-analysis.

AMS and POT time series for Ås-Rustadskogen and Oslo-Blindern are shown in Figure 1 and 2.

Station number and name	Period	Msg (%)*	Highest annual value			Peak over threshold		
			10min	30min	60min	10min	30min	60min
12290 Hamar	1968-2017	22						
17870 Ås-Rustadskogen	1974-2017	7						
18020 Oslo-Lambertseter	1985-2017	6						
18270 Oslo-Vestli	1974-2017	25						
18320 Oslo-Hausmannsgt	1984-2015	25						
18701 Oslo-Blindern	1968-2017	4						
19490 Gjøttum	1971-2017	40						
19510 Øvrevoll	1967-2017	31						
39150 Kristiansand-Sømskleiva	1975-2017	26						
44190 Time-Lye	1981-2017	27						
44730 Sandnes-Rovik	1974-2017	34						
47240 Karmøy-Brekkevann	1970-2015	36						
64300 Kristiansund-Karihola	1974-2017	30						
68230 Trondheim-Risvollan	1987-2017	10						

* Missing seasons (%) from start to present

Table 1. Trends in heavy sub-daily rainfall for durations 10, 30 and 60 minutes. Trend analysis is performed for Annual Maximum Series (AMS) and Peak Over Threshold (POT; threshold 5 mm/h). Blue indicate positive trend, red negative. For five stations there were too many gaps to allow POT-analysis. Dark colors indicate statistical significant trends (95% level, Mann-Kendall trend test).

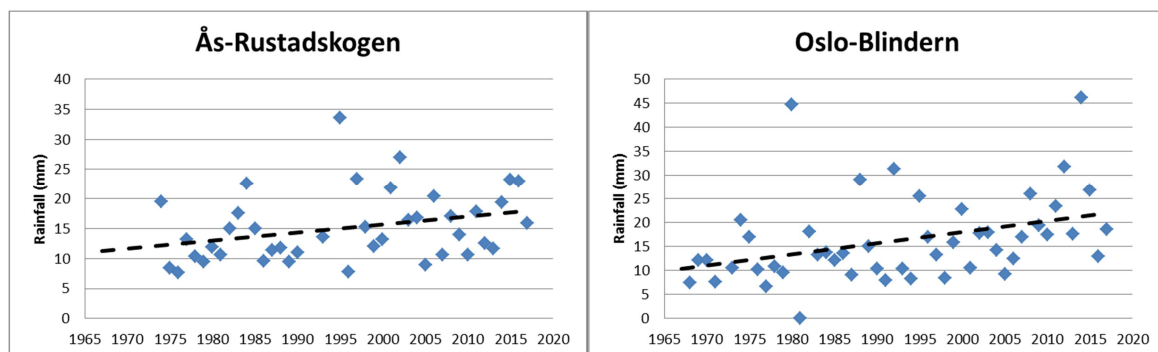


Figure 1. Highest annual 1-hour rainfall at Ås-Rustadskogen and Oslo-Blindern during 1968-2017

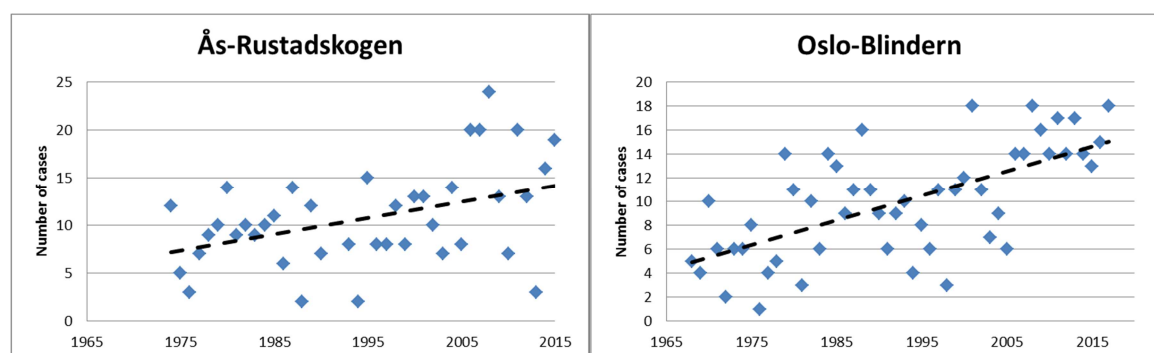


Figure 2. Annual number of 1-hourly rainfalls exceeding 5 mm at Ås-Rustadskogen and Oslo-Blindern during 1968-2017

Trends were also calculated for shorter Plu-series (series > 10 years), and figure 3 demonstrates that a majority of stations experienced positive trends for 60-minutes rainfall during 1967-2016 (left column). During the first part of the period (1967-1996) a majority of stations had negative trends (central column), while in the last part of the period (1987-2016) most of the stations had positive trends (right column). Almost no significant negative trends were found.

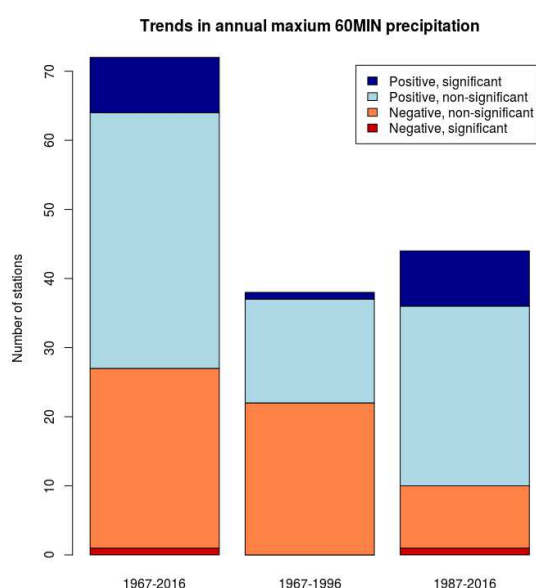


Figure 3. Trends in highest annual 60-minutes rainfall for 72 stations with series >10 years.

Trends in maximum 1 day rainfall (Rx1d)

Due to the limited number of long and complete sub-daily rainfall series, it is difficult to get an overall picture of trends for different durations and different regions in Norway. For 1-day rainfall, however, there are far more long data series from the regular MET network of precipitation stations. Therefore, in order to obtain a comparison with the trends from the pluviometer series, we analyzed trends in highest annual 1 day rainfall for the same period as there are pluviometer data; - i.e.

the period 1968-2016. As most pluviometers are just operative during the summer season, the analysis concentrated on the summer months May-September. Figure 4 shows trends for 142 series of maximum 1-day summer rainfall. Of these, 112 series (~80 %) have a positive trend, but especially in Western Norway there are some stations with negative trends. For 21 series, the positive trends are significant at a 95% confidence level. No stations have a statistically significant negative trend.

The trend analyses discussed above are based on Mann-Kendall tests on monotonic trends, but variability on different time scales can underlie this overall trend. On a decadal scale, Førland et al (1998) found that for the Nordic region; - except in western regions; there was a maximum in high 1-day rainfalls (Rx1d) in the 1930s, and a tendency for increasing Rx1d values during the 1980s and 1990s. The same tendencies in trends were found for frequencies of “extraordinary” precipitation events, i.e. 1-day rainfall higher than the 5-year return period value. For Norway the decades with maximum frequencies and magnitudes of heavy 1-day rainfall coincide with decades with high regional summer temperatures (Hanssen-Bauer et al., 2017).

Førland et al (1998) pointed out that series of Rx1d-values from single stations were not an ideal indicator for trend studies in extreme 1-day rainfall, and therefore recommended a regional grouping of series. For studies of long-term variations of annual and seasonal precipitation in Norway, the country is divided into 13 regions as shown in Figure 5 (Hanssen-Bauer et al., 2015). In the present study, these regions were also used for trend studies for Rx1d series. The analyses were restricted to stations still in operation, and with daily series of at least 70 years in length. In total 63 stations fulfilled this criterion, but unfortunately just one station is located in each of the northern regions 12 (Finnmarksvidda) and 13 (Varanger).

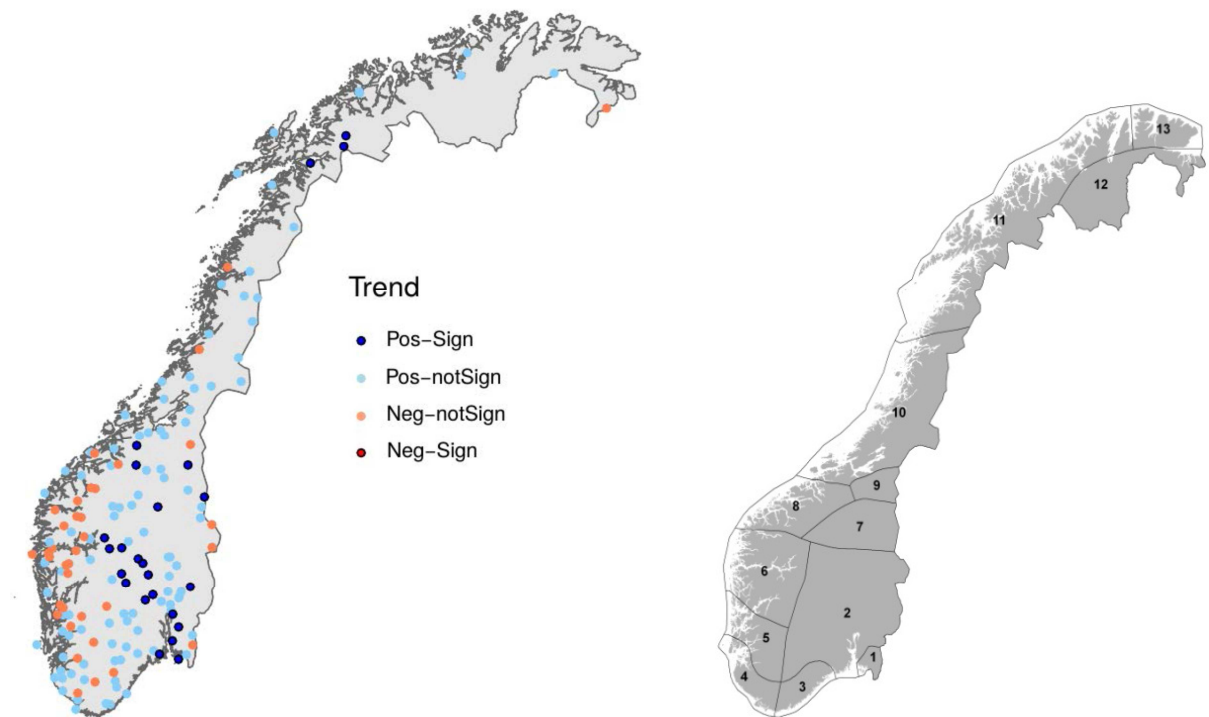


Figure 4 (Left). Trends (1968-2017) in summer (May-September) values of maximum 1-day rainfall. Figure 5 (Right). Norwegian precipitation regions.

There is a large span in Rx1d values for the selected stations: For the reference period 1971-2000 (see Hanssen-Bauer et al., 2017), the mean Rx1d-value for station 1566 Skjåk in region 7 was 21 mm while 80200 Lurøy in region 10 had 110 mm. In the grouping of series for each region, the Rx1d-values were therefore “standardized” for each station by dividing with the mean Rx1d value for the reference period 1971-2000. Table 2 shows ratios of Rx1d for each region relative to the period 1971-2000. For the southern and western regions (regions 3 - 6), the mean values for the period with complete records (1946-2017) and for the “standard normal period” 1961-1990 are lower than for the reference period 1971-1990; - i.e. the same features are shown as in Figure 4. For the most recent 30-year period (1988-2017) the mean values are higher than during 1971-2000 for all regions except region 3 and 8 where they are slightly lower.

Region	1	2	3	4	5	6	7	8	9	10	11	12+13
(Stations)	(3)	(14)	(8)	(5)	(6)	(9)	(2)	(3)	(2)	(5)	(4)	(2)
1946-2017	1,01	1,01	0,97	0,98	0,98	0,97	1,00	0,97	1,05	1,00	1,02	0,98
1961-1990	1,03	0,98	0,98	0,99	0,97	0,95	0,93	0,96	1,06	1,00	1,01	0,98
1988-2017	1,03	1,06	0,99	1,02	1,04	1,01	1,07	0,99	1,07	1,04	1,07	1,03

Table 2. Mean values of standardized Rx1d-values relative to 1971-2000 values.

The standardized station series for Rx1d were grouped within each of the precipitation regions (Figure 5), and mean values were calculated for each year based on available series. The number of series (see table 2) is increasing with time, and are complete from 1945 to present. The time series of regional means were smoothed by a Gaussian filter. Figure 6 demonstrates that most of the regions experienced high Rx1d values in the 1930s, and also that for most of the regions there has been increasing Rx1d values since the 1960s/1970s.

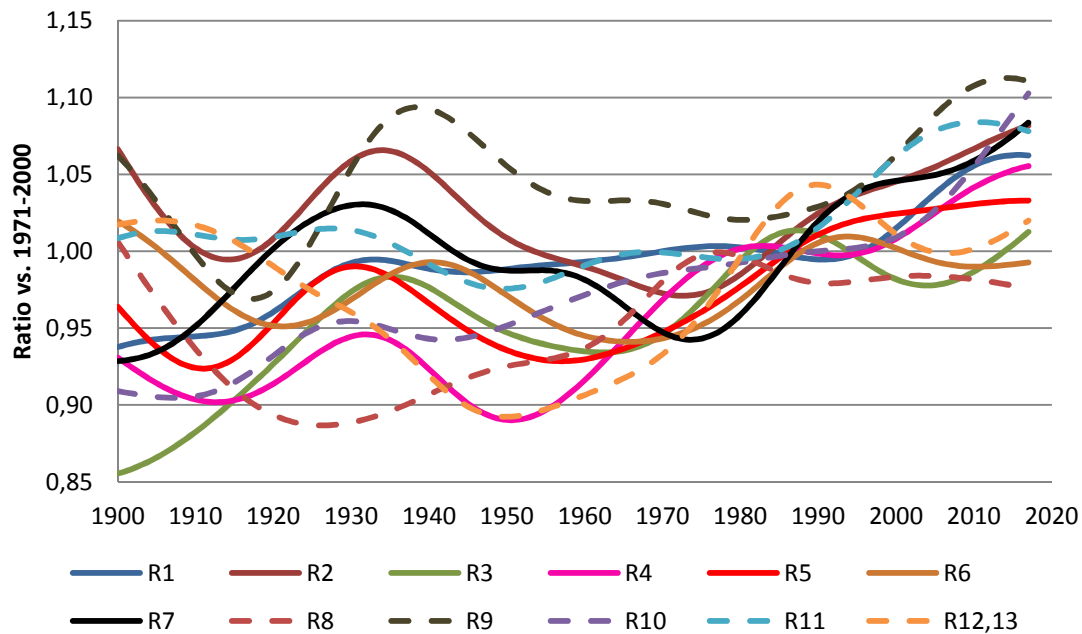


Figure 6. Time series of standardized regional values of maximum 1-day rainfall for different precipitation regions. The series are smoothed by a Gaussian filter to illustrate variability on a 30-year time scale.

To illustrate the large-scale variability in Rx1d-values, figure 7 shows results from a grouping of regional series: Southeastern Norway (Region 1+2), Western Norway (Region 4,5 and 6), Central Norway (Region 7,8 and 9) and Northern Norway except eastern parts of Finnmark county (Region 10 +11). The long-term variability for the southernmost region “Sørlandet” (Region 3) differs from the other regions, and this region is therefore not combined with neighboring regions. For regions 12 and 13 there is just one station in each region, and the graphs for these regions are thus probably not representative. The features from figure 6 is evident also in figure 7, i.e. for all parts of the country there is a secondary maximum for Rx1d values in the 1930s, and increasing values from the 1960s and 1970s. The present level is the highest since the start of the series, and for most regions is substantially higher than during the 1930s. But for southeastern Norway (R1+2) the Rx1d values during the 1930s were almost as high as the present values. Around 1910 and during the 1960s and early 1970s the Rx1d values were rather low. For Sørlandet (R3) there is a strong increase from the start of the series until the mid-1930s.

Figure 6 and 7 demonstrate that one should be very careful in drawing conclusions from linear trends. The sub-daily series start in the late 1960s and figure 6 and 7 show that this is in a period with rather low Rx1d-values. Linear Rx1d trends starting in the 1930s would show quite different results than trends starting in the late 1960s. The trend pattern shown in figure 4 is thus strictly just valid for the period 1968-2016.

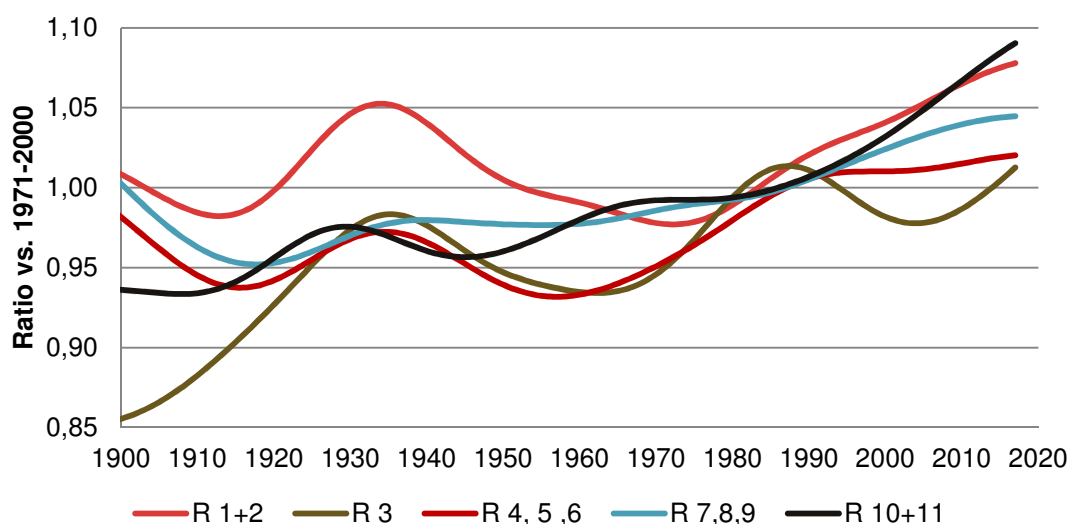


Figure 7. Time series of standardized regional values of maximum 1-day rainfall for different parts of Norway (e.g. R 1+2 is regions 1 and 2 (Figure 4), etc). The series are smoothed by a Gaussian filter to illustrate variability on a 30-year time scale.

Trends in design values (IDF-statistics)

As most short-term rainfall series are short, IDF-statistics at MET have been estimated if the series is longer than 10 years. The results discussed above illustrate that there are positive trends in maximum values for sub-daily rainfall as well as 1 day rainfall. A crucial question is whether there are also trends in IDF-values; -i.e. would the IDF-values be different if they are based on data from periods either in the start or end of the period of sub-daily measurements (1968-present), or if detrending were implemented.

Figure 8 shows graphs of sliding IDF-values for three Pluviometer stations (Hamar, Ås and Oslo-Blindern) with long time series and rather few data gaps. The estimates are performed for four overlapping 20-year time periods 1968-1987, 1978-1997, 1988-2007 and 1998-2017, and for return periods 2, 5, 10, 20, 25, 50, 100 and 200 years. These three stations show different developments in IDF-estimates: At Oslo-Blindern the estimates of 100 year return period values are 12 % lower for 1968-1987 than for the most recent 20-year period, while at Ås they are 8 % higher. For Hamar they are quite stable.

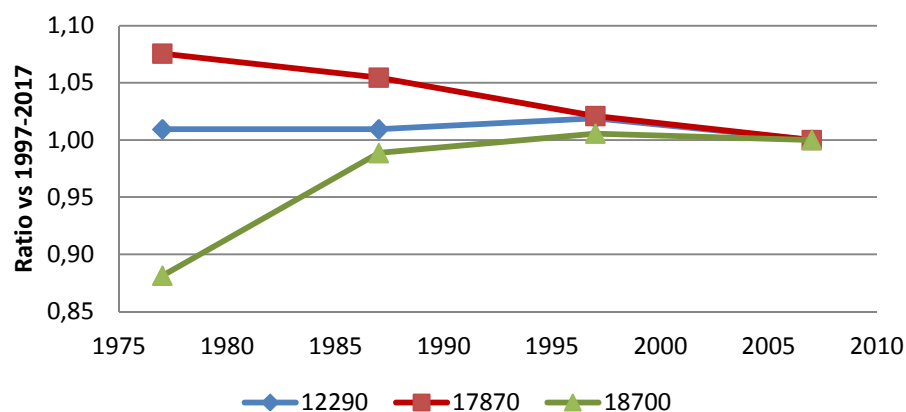


Figure 8. 100 year return period estimates for maximum 1 hourly rainfall for three pluviometer stations (12290 Hamar, 17870 Ås and 18700 Oslo-Blindern). The estimates are based on sliding 20-year periods, and are shown as ratios to 100 year values for the period 1998-2017.

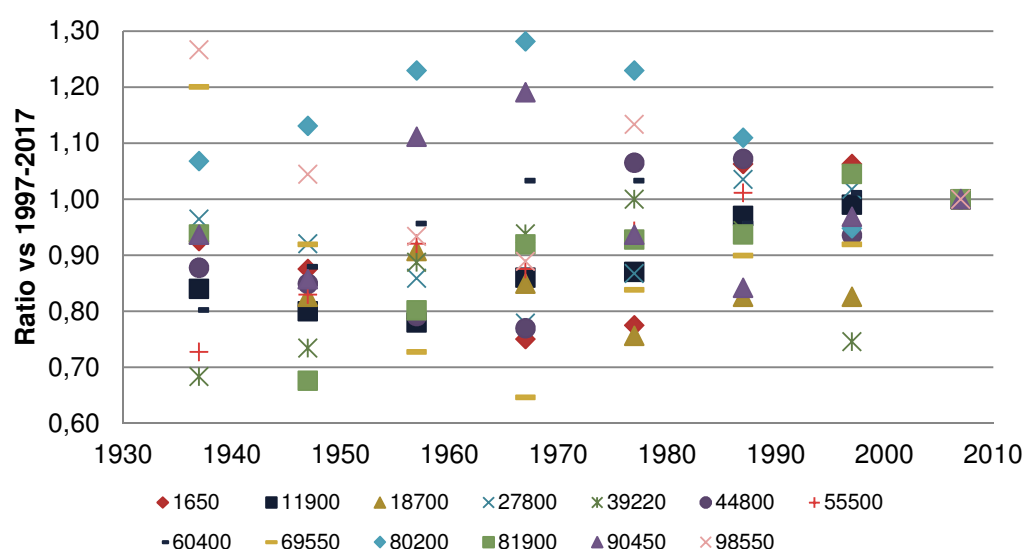


Figure 9. 100 year return period estimates for maximum 1-day rainfall. The estimates are based on sliding 20-year periods, and are shown as ratios relative to 100 year values for the period 1998-2017. The stations are identified by MET station number, and belong to the following regions (Figure 5). 01650 (R1), 11900 (R2), 18700 (R2), 27800 (R2), 39220 (R3), 44800 (R4), 55500 (R6), 60400 (R8), 69550 (R9), 80200 (R10), 81900 (R10), 90450 (R11), 98550 (R13).

Figure 9 is similar to Figure 8, but shows thirteen long series of 1-day rainfall. The figure indicates that for most stations the 100 year return period values are higher for the most recent three 20-year periods than earlier in the century. For most stations there is a minimum for the periods 1938-1957 and 1948-1967, and relatively high values during 1928-1947, i.e. similar features as those shown for the smoothed series shown in Figure 6 and 7. Figure 9 also demonstrates that for some stations the IDF-values deviate by more than 20 % from the present level. This is in line with the results from Førland et al (1998), who found that even for 30 year long series; a majority of 5-year return period values for Rx1d differed more than 15 % from IDF-

estimates based on complete century-long series. This emphasizes that one should be cautious when basing IDF-estimates on short data series.

Discussion and conclusions

During the last fifty years frequency and intensity of short duration rainfall have increased at a majority of the Norwegian measuring sites. This positive trend also affects rainfall design values (IDF-estimates). Projections indicate increasing rainfall intensities up to the end of this century. For the next few decades natural variations will largely dominate over the “climate signal” resulting from an enhanced greenhouse effect. For design of measures or constructions with a life time horizon of 10 – 20 years, the Norwegian Centre for Climate Services thus recommends to use updated observations rather than climate projections (Hanssen-Bauer et al., 2017).

As MET Norway estimates IDF-values for all sub-daily rainfall series longer than 10 years, IDF-estimates based on data from recent years will tend to be higher than estimates based on long-term series, or short series from the 1960s and 1970s. A crucial question is thus whether IDF-statistics should be adjusted to the rainfall climate observed during the most recent decades. The trend studies of 1-day rainfall shown here demonstrate that the positive trend is not monotonic; i.e. that there is decadal variability superposed on the long-term trend. The centennial long-term variability of heavy 1-day rainfall reveals high values in the 1930s and low values in the 1960s and 1970s. It is thus not unlikely that the present high level of heavy rainfall events will be followed by decades with lower values. Consequently IDF-estimates based on observations from the most recent decade(s) may tend to be biased compared to estimates for 30-years reference periods, e.g. 1971-2000. Users of IDF-estimates should be aware of this possible bias, but until further notice the IDF-estimates at the MET Norway and NCCS's web-sites (see article 5.1, this report) are not trend-adjusted.

References

- Førland, E.J., H Alexandersson, A. Drebs, I. Hanssen-Bauer, H. Vedin and O.E. Tveito, 1998: Trends in maximum 1-day precipitation in the Nordic region (Reward), MET Norway Report KLIMA 14/98
- Førland, E.J., J. Mamen, L. Grinde, A.V. Dyrddal and S. Myrabø, 2015: Dimensjonerende korttidsnedbør (In English: Design values for short-term rainfall), MET Norway Report 24/2015
- Hanssen-Bauer, I., E.J. Førland, I. Haddeland, H. Hisdal, S. Mayer, A. Nesje, J.E. Ø. Nilsen, S. Sandven, A.B. Sandø, A. Sorteberg and B. Ådlandsvik, 2015: Klima i Norge 2100 – Kunnskapsgrunnlag for Klimatilpasning, oppdatert i 2015. (In English: Climate in Norway 2100 – Knowledge base for climate adaptation, updated in 2015). Norwegian Centre for Climate Services, Report 2/2015.
- Hanssen-Bauer et al., 2017 I. Hanssen-Bauer, E.J. Førland, I. Haddeland, H. Hisdal, D. Lawrence, S. Mayer, A. Nesje, J.E. Ø. Nilsen, S. Sandven, A.B. Sandø, A. Sorteberg and B. Ådlandsvik, 2017: Climate in Norway 2100 – a knowledge base for climate adaptation. Norwegian Centre for Climate Services, Report 1/2017

NOU 2015: 16, 2016: Overvann i byer og tettsteder — Som problem og ressurs. (In English: Stormwater in cities and towns - As a problem and resource). Official Norwegian Reports, 2015:16.

1.2 Observed trends in the magnitude and frequency of high flow events in Norway during the past 50 years

K. Vormoor^{a,b} and D. Lawrence^a

^aNorwegian Water Resources and Energy Directorate, Norway

^bInstitute of Earth and Environmental Science, University of Potsdam, Germany

Summary

Trend analyses distinguishing flood generating processes indicate that high flow events driven by rainfall have become more frequent over the past several decades in southern and western Norway although there is no evidence to suggest that their magnitude has increased. Overall, negative trends reflecting a decrease in flood magnitudes are detected more often than positive trends. In northern Norway, both the magnitude and frequency of over threshold events have decreased in response to the diminishing role of snowmelt in flood generation. An analysis of the occurrence of over threshold events generated by rainfall vs. snowmelt in six runoff regions in Norway indicates that rainfall has increased in importance in driving high flows during the period 1972-2012 in most regions.

Introduction

It is often assumed that observed increases in precipitation intensities during recent decades, such as those reported by Dyrddal, et al. (2012 and article 1.1, this report), have resulted in similar patterns in flood magnitudes in Norway. A recent study of trends in peak flows in small catchments (Wilson et al., 2014), however, suggests that statistically significant positive trends in flow magnitudes in Norway are the exception, rather than the norm. This finding is consistent with an earlier study considering a wider range of catchments in the Nordic region (Wilson et al., 2010).

An important factor contributing to the lack of correspondence between changes in precipitation and in flooding is that both snowmelt and rainfall contribute to high flows in cold climates. Under a warming

climate, reduced snow volumes and an earlier peak snowmelt can change the magnitude and seasonality of high flows derived from snowmelt. If a trend analysis is performed on a discharge series subject to changes in both rainfall and snowmelt inputs, the response of the catchment to the increased heavy rainfall may be masked by a decreasing trend in the volume of runoff generated by snowmelt. This effect is taken partly into account in earlier studies that use seasonal analyses. In Norway, however, both rainfall and snowmelt can potentially contribute to high flows during much of the year, and a season-based analysis does not necessarily distinguish high flows generated by rainfall vs. snowmelt. Therefore, a process-orientated approach

was developed to distinguish observed high flow events with regard to their dominant generation processes (i.e. snowmelt and rainfall). A comprehensive trend analysis based on up to 211 catchments was then conducted to assess changes in the magnitude and frequency of rainfall vs. snowmelt driven floods during three different time periods (1962-2012, 1972-2012, and 1982-2012). Full details of the analysis are reported in Vormoor et al. (2016) and a shorter summary of that work is given here, including the data and methods used, key results and a discussion of their implications.

Data and methods

Data for discharge, rainfall and snowmelt

Daily discharge data from 211 gauging stations for catchments with negligible or no regulation and stable land use conditions were compiled for the trend analyses. The choice of a daily, rather than a shorter, sub-daily temporal resolution for the analysis is in response to the results of Wilson et al. (2014) which compare the results of trend analyses for daily vs. instantaneous annual maxima in Norway. No significant differences in the results as a function of the higher temporal resolution were found, even though the analyses were performed for small catchments (31 catchments with area < 60 km²). Daily discharge data were therefore used here, as this gives a much larger and more comprehensive dataset and supports a discussion of regional variations. Daily precipitation, temperature and snowmelt data were also required so that the dominant flood generating process (FGP) could be determined for individual high flow events. These data were extracted from 1 x 1 km² gridded maps for Norway (www.seNorge.no) for each catchment, and a temperature threshold of 0.5°C was used to create a rainfall series from the precipitation data.

Detection and attribution of peak over threshold (POT) events

A peak over threshold (POT) discharge series was extracted using the 98th streamflow percentile as a threshold and an independence criteria based on the 'normal flood duration' (Vormoor et al., 2015, 2016) for each station. The threshold value was chosen to ensure that, on average, at least one independent peak per year was selected. A higher threshold would indeed focus on events that are more extreme than those that occur, on average, once a year. This would lead, however, to an insufficient number of events for the trend analysis, if rigorous statistical methods are to be

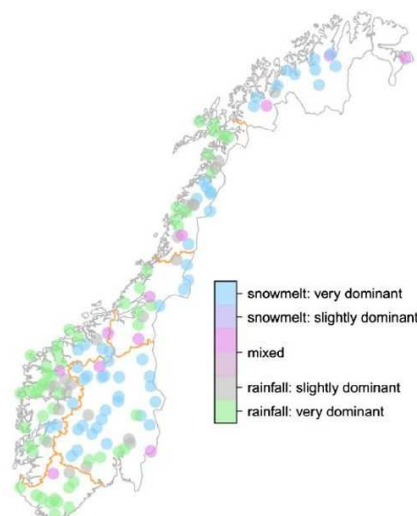


Figure 1: Dominant flood generating processes for the period 1971-2000 for 140 catchments (from Vormoor et al., 2016). Used with permission from Elsevier.

applied. Each extracted POT event was analysed to determine the relative contributions of rainfall vs. snowmelt to the volume accumulated during and immediately before the event. An event is classified as 'rainfall generated' if at least 67% of the volume comes from rain and 'snowmelt generated' if at least 67% comes from snowmelt. Events between these two end members are classified as 'mixed'. A regional overview of the dominant flood generating processes during the normal period 1971-2000 is shown in Figure 1 for the 140 catchments with records covering that period.

Trend analysis and target variables

The Mann-Kendall (MK) test (Kendall, 1975) was used to analyse trends in the magnitude of the POT events over time. This non-parametric statistic uses a rank-transformed time series to test for the presence of a trend and requires no assumptions regarding the underlying statistical distribution of the series, which is its principal advantage over parametric tests. Trends in the frequency of over threshold events were tested using Poisson regression (PR), which is based on a generalised linear model and treats the frequency series as count data (number of events per year) which follow a Poisson distribution. The MK test has been widely used in previous studies investigating trends in precipitation and flooding (see, for example, Madsen, 2014 for a review), and PR has been more recently introduced as a suitable method for assessing trends in the frequency of events (e.g. Gregersen et al., 2010; Mallakpour and Villarini, 2015). The POT series were tested for serial autocorrelation, but this was found to be negligible, reflecting the stringent independence criterion used for selecting the individual events. A bootstrap procedure (Burn and Elnur, 2002) was also used to assess the potential effect that cross correlation between sites can have on the number of sites indicating significant trends, so that the field significance of the results can also be quantified and reported.

As trend analyses are often sensitive to the time periods and period lengths considered (Hannaford et al., 2013), a minimum record length of 25 years is recommended (Burn and Elnur, 2002). Three time periods were therefore used in this study: (1) 1962-2012, (2) 1972-2012, and (3) 1982-2012. Analyses were conducted separately for series consisting of a) rainfall generated events, b) snowmelt generated events, and c) all events. Discharge records with 10 or fewer events for series a) or b) were discarded from that particular analysis. The number of series available for each analysis varies between a minimum of 75 series (for snowmelt generated events during the period 1962-2012) and a maximum of 211 series (for all events during the period 1982-2012). To assess how stable significant trends are over time, a robustness index was defined (Vormoor et al., 2016), and a 30-year moving window was sequentially applied from the period 1962-1992 to the period 1982-2012. The Wald-Wolfowitz runs test (Wald and Wolfowitz, 1940) was used to establish that the sequence of trends differs significantly from that which would be generated by random sampling.

Results

Trends in flood magnitude and frequency

Results for all three periods and the three flood series are summarised in Figure 2, which shows the percentage of the catchments with positive or negative trends (at the 90% significance level) for each case. The percentage required to establish that a group of results is field significant is also shown (shaded bars) and indicates that 16 of the 18 groups are field significant, although the two groups representing trends in the magnitude of snowmelt dominated events for the periods 1972-2012 and 1982-2012 are not. The majority of stations (i.e. 77 – 93% for individual groups) do not show significant trends in the magnitude or the frequency of POT events. For trends in flood magnitude (Fig. 2a), more catchments show significant negative trends (indicating a decrease in magnitude) than significant positive trends.

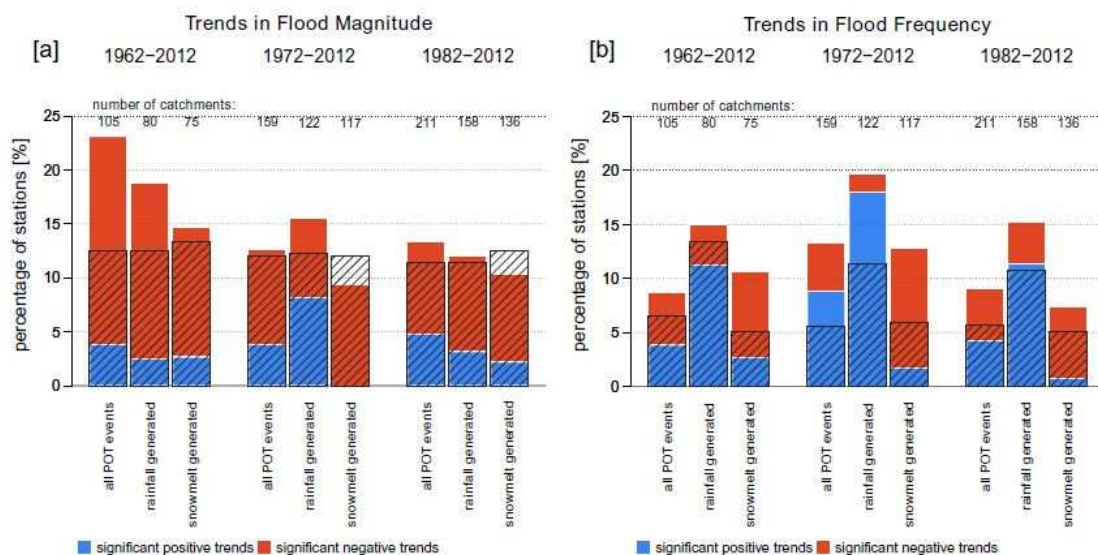


Figure 2: Percentage of stations with significant positive (blue) and negative (red) trends at the 90% confidence level. Shading indicates the number of stations needed to verify that significant trends are field significant. From Vormoor et al., 2016. Used with permission from Elsevier.

An exception to this is the series representing rainfall driven events during the period 1972-2012 for which the number of catchments with positive trends is slightly larger than the number with negative trends. For trends in the frequency of over threshold events (Fig. 2b), the number of catchments with positive vs. negative trends is approximately equal for the series for all POT events during the periods 1962-2012 and 1982-2012, and for the period 1972-2012 there are a larger number of positive trends than negative. For rainfall generated events in all three periods, there are a considerably larger number of significant positive trends than negative, indicating an increase in the frequency of high flows generated by rainfall. Snowmelt generated events show the opposite tendency in all three periods, i.e. most catchments with significant trends have negative trends.

Spatial distribution of trends

The spatial pattern of the results for the 18 groups in Figure 2 can be found in Vormoor et al. (2016) and are not reproduced here. Those results distinguish between stations with strong trends (95% significance level) and weak trends (90% significance level). There are no consistent spatial patterns of positive trends in flood magnitude that persist for all three time periods, as might be expected from the grouped results in Figure 2a. Negative robust trends in magnitude, persisting through the three time periods, are found for a number of stations in central, eastern and western Norway and one station in northern Norway. For the longest time period, 1962-2012, an additional four stations in northern Norway have significant negative trends. A share of these persistent negative trends results from decreasing magnitudes of rainfall dominated events, although in most cases it is hardly possible to match the spatial patterns of significant trends in all POT event with significant trends in rainfall and snowmelt dominated events, respectively.

Significant trends in the frequency of over threshold events show a very different spatial distribution than those for magnitude. For the series representing all POT events and the series for rainfall generated events, the majority of stations in the southern half of Norway showing significant trends have positive trends. This is seen for all three time periods. In addition, there are pronounced clusters with strong positive trends in the frequency of rainfall generated events in south-eastern Norway during the two more recent time periods (1972-2012 and 1982-2012). In northern Norway, the series for all POT events have uniformly negative trends for all three time periods, and the significant trends in the series for rainfall generated events are mixed (i.e. both positive and negative trends), although there are only few stations with significant trends during the two shorter time periods (1972-2012 and 1982-2012). Most stations, both in southern and northern Norway, with significant trends in the series for snowmelt generated events have negative trends. This is the case for all three time periods.

Changes in flood generating processes

Changes in the dominant flood generating process were analysed by calculating the fraction of rainfall events or snowmelt events (of the total number of POT events) for individual catchments for 10-year periods between 1972-1982 to 2002-2012. Catchments were then grouped into six standard runoff regions (Finnmark/Troms, Nordland, Trøndelag, Vestlandet, Sørlandet and Østlandet) and the median and interquantile range for the catchments in each region were plotted over time. Figure 3 illustrates the results for two of these regions, Østlandet and Nordland, and the results for the other four regions can be found in Vormoor et al., 2016. Both Østlandet and Nordland show an increase in the fractional number of over threshold events generated by rainfall and a decrease in those generated by snowmelt over time. The majority of catchments in the region Østlandet have a higher fraction of high flow events generated by snowmelt during the earlier periods, and in recent years, a higher fraction that can be attributed to rainfall. Nordland also shows a

decrease in the importance of snowmelt as a driving component of flooding over the periods considered. In western and southern Norway (Vestlandet and Sørlandet, not shown), rainfall dominates the generation of over threshold flows throughout the 1972-2012 period, and in Sørlandet the fraction of events generated by snowmelt is minimal in the most recent 10-year periods. In mid-Norway (Trøndelag, not shown), rainfall generated events are slightly more important than snowmelt generated events in most catchments throughout the full 1972-2012 period, although the role of snowmelt decreases from the mid-1970's but then slightly increases in more recent periods. Finnmark/Troms (not shown) is the only region in which snowmelt dominates high flow generation throughout the 1972-2012 period, although there is evidence for a decrease in the fractional number of snowmelt generated events and an increase in rainfall generated events beginning with the 1995-2005 period.

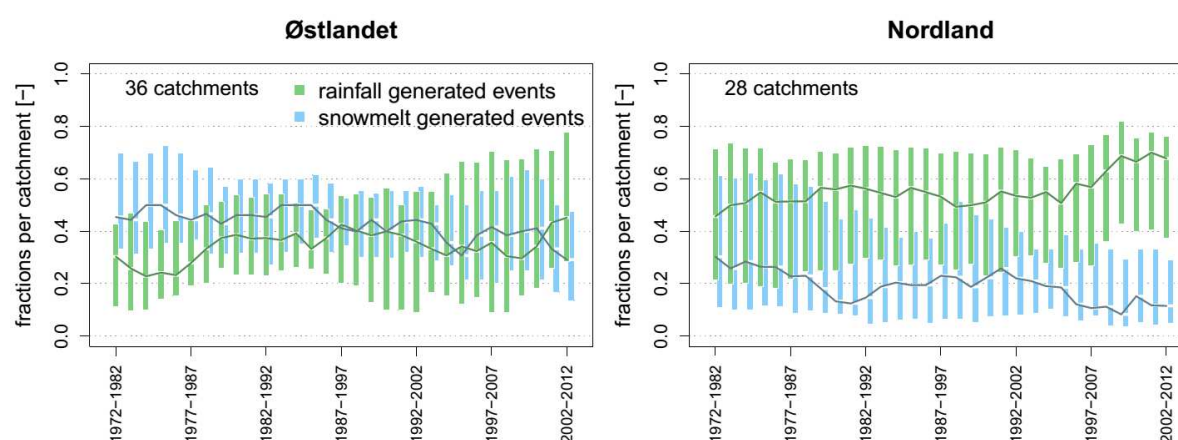


Figure 3: Interquartile ranges and median values of the fractions of rainfall and snowmelt generated events out of all POT events for catchments in two runoff regions. From Vormoor et al., 2016. Used with permission from Elsevier.

Discussion and conclusions

The results of the trend analyses indicate that changes in the frequency of high flows are more evident than changes in the magnitude of these flows. This agrees with the results of Dyrødal et al. (2012) and article 1.1 (this report), who found more pronounced changes in the frequency of extreme precipitation than in precipitation intensity, and with recent studies of high flows in central USA (Mallakpour and Villarini, 2015) and Canada (Burn and Whitfield, 2015). The work presented here also confirms the study by Wilson et al. (2014) for small catchments, i.e. that most stations in Norway show no significant trend either in the magnitude or in the frequency of high flow events. We have also found that stations with significant trends in high flow magnitude are, in most cases, more likely to have negative than positive trends, even when flood series are distinguished based on the flood generating process (i.e. rainfall vs. snowmelt). The results for the frequency of over threshold flows are in contrast with this, particularly for high flows generated by rainfall, i.e. significant trends tend to be positive. Taken together, it can be concluded that although flood

magnitudes are found to be increasing at very few stations over the periods considered, the occurrence of high flows generated by rainfall is more frequent at many stations. Simultaneously, over threshold flows generated by snowmelt have decreased both in magnitude and frequency at most stations showing significant trends in these variables. The results suggest that rainfall has become increasingly important for flood generation in most regions in Norway, in comparison with snowmelt, over the period 1972-2012. In regions in which rainfall generated flows have dominated extreme flows throughout the period considered, the fractions of high flow events generated by snowmelt have become even smaller in recent years. In Finnmark/Troms, which is snowmelt dominated throughout the period considered, the fractions of high flow events caused by rainfall increases towards the end of the period. These regional results are also consistent with projections for future changes in flooding in Norway (Vormoor et al., 2015; Lawrence, 2016), which suggest that rainfall will increasingly replace snowmelt as the dominant factor driving flooding under a future climate in most regions.

References

- Burn, D. H. and M. A. H. Elnur (2002), Detection of hydrologic trends and variability, *Journal of Hydrology*, 255, 107-122.
- Burn, D. H. and P.H. Whitfield (2015), Changes in floods and flood regimes in Canada, *Canadian Water Resources Journal*, 1784, 1-12.
- Dyrørdal, A., K. Isaksen, H. Hygen and N. Meyer (2012), Changes in meteorological variables that can trigger natural hazards in Norway, *Climate Research*, 55, 153-165.
- Gregersen, I. B., K. Arnbjerg-Nielsen and H. Madsen (2010), Parametric analysis of regional trends in observed extreme rainfall in Denmark, *International Workshop on Advances in Statistical Hydrology*, Taormina, 1-8.
- Hannaford, J., G. Buys, K. Stahl and L.M. Tallaksen (2013), The influence of decadal-scale variability on trends in long European streamflow records, *Hydrology and Earth System Sciences*, 17, 2717-2733.
- Kendall, M. G. (1975), *Rank Correlation Measures*, Charles Griffin, London.
- Lawrence, D. (2016), *Klimaendring og framtidige flommer i Norge (Climate change and future floods in Norway)*, NVE Rapport 81/2016.
- Madsen, H., D. Lawrence, M. Lang, M. Martinkova, and T. R. Kjeldsen (2014), Review of trend analysis and climate change projections of extreme precipitation and floods in Europe, *Journal of Hydrology*, 519, 3634-3650.
- Mallakpour, I. and G. Villarini (2015), The changing nature of flooding across the central United States, *Nature Climate Change*, 5, 250-254.
- Vormoor, K., D. Lawrence, M. Heistermann, and A. Bronstert (2015), Climate change impacts on the seasonality and generation processes of floods – projections and uncertainties for catchments with mixed snowmelt/rainfall regimes. *Hydrology and Earth System Sciences*, 19, 913-931.
- Vormoor, K., D. Lawrence, L. Schlichting, D. Wilson and W. K. Wai (2015), Evidence for changes in the magnitude and frequency of observed rainfall vs. snowmelt driven floods in Norway. *Journal of Hydrology*, 538, 33-48.
- Wald, A. and J. Wolfowitz (1940), On a test whether two samples are from the same population, *Annals of Mathematical Statistics*, 11, 147-162.
- Wilson, D., H. Hisdal and D. Lawrence (2010), Has streamflow change in the Nordic countries? Recent trends and comparisons to hydrological projections. *Journal of Hydrology*, 394, 334-346.
- Wilson, D., H. Hisdal and D. Lawrence (2014), Trends in floods in small Norwegian catchments – instantaneous vs. daily peaks, *Hydrology in a Changing World: Environmental and Human Dimensions*, 42-47.

1.3 Investigating the statistical relationship between extreme rainfall events and peak flows in small catchments

L. Schlichting^a, D. Lawrence^a, K. Engeland^a, A.V. Dyrda^b

^aHydrology Department, Norwegian Water Resources and Energy Directorate (NVE), Norway

^aNorwegian Meteorological Institute, Norway

Summary

Statistical analyses of the relationship between extreme precipitation and extreme flows in 138 small catchments (with area < 50 km²) indicate that in most cases there is no significant correlation between the highest observed precipitation intensities and the highest flows in individual catchments. This is despite the fact that events comprising the peak over threshold series analyzed are caused primarily by rainfall, rather than snowmelt. The few catchments with the correlations > 0.5 between the highest observed flows and precipitation intensities tend to be located in south to southwestern Norway, whilst catchments with the strongest correlations between the highest observed precipitation intensities and the corresponding streamflow are located in western Norway. Analyses based on the return periods of the events also indicate that 40% of the catchments have at least one discharge event with a return period ≥ 5 years which is caused by a rainfall event with a return period ≥ 5 years.

Introduction

Event-based methods for extreme flood estimation, such as those used for design flood analyses in Norway (see Midttømme et al., 2011 or Filipova et al., 2016), often assume that a precipitation sequence representing a given return period produces a flood discharge with the same return period. This is an important assumption that significantly simplifies the estimation procedure. As long as the estimate is not compared with more complex modelling approaches or statistically-based flood frequency analyses (e.g. Lawrence et al., 2014), the approach appears to provide a consistent methodology for estimating high flood quantiles. It is recognized that either soil moisture deficits or snowmelt can undermine a direct one-to-one correspondence between the return period of a rainfall sequence and the streamflow response. Nevertheless, it is thought that for smaller catchments, the relationship should approximately hold, at least for events in which the contribution of

snowmelt is negligible. The assumption, i.e. that an extreme precipitation event of a given return period produces a runoff event of approximately the same return period, has however very rarely been tested. The few examples which can be found in the

literature (e.g. Harr, 1981) are often concerned with other issues. This is undoubtedly due to a lack of data series of sufficient length to empirically test the precipitation and flood quantiles of interest. Nevertheless, it can be instructive to evaluate more generally the statistical relationship between extreme precipitation and extreme discharge, and this is the starting point for the work presented here. In particular, three questions are considered: 1) is there a correlation between the highest observed flows and the precipitation intensities driving them?; 2) is there a correlation between the highest observed precipitation intensities and the magnitude of the flows they produce; and 3) is there a correlation between the return periods of observed high flows and those of precipitation intensities?

Data and methods

Gridded precipitation data disaggregated to a 3-hr timestep (Vormoor and Skaugen, 2013) were extracted for 160 catchments. These are small catchments having an area of $< 50 \text{ km}^2$ and an estimated concentration time (representing the lag between rainfall input and peak flow response) of < 24 hours. Streamflow data with a sub-daily temporal resolution were also extracted for the catchments. Streamflow records having years with more than five consecutive days of missing data were deleted from the analysis, thus reducing the number of gauging records to 138. Independent over threshold events were extracted from both the precipitation and discharge series using a threshold such that the number of events for each series was equal to two times the length of the series. The discharge peaks were assumed to be independent if they were separated by at least 24 hours (i.e. the maximum concentration time) and the minimum inter-peak discharge was less than 60% of the previous peak value. Rainfall maxima were assumed to be independent if they were separated by at least 8 days.

As this analysis focuses on the relationship between extreme rainfall and flooding, it is important to exclude events in which snowmelt plays a significant role. This was done by estimating the relative contribution of rainfall vs. snowmelt to the flood volume generated during an event using seNorge precipitation, temperature and snowmelt data for each catchment and following the procedure described in Vormoor et al. (2016). Flood events were discarded from the analysis if the estimated contribution from snowmelt was greater than 50%.

After the final selection of the precipitation and discharge event series, the corresponding discharge events for the precipitation series and the precipitation events for the discharge series were also extracted. The statistical methods applied to analyze the series include a) correlation analysis using the Pearson coefficient, linear regression, and ANOVA analysis to investigate the relationship between precipitation and discharge series, and b) flood frequency analysis using an exponential distribution to estimate return levels of precipitation and discharge from the over-threshold series.

Results

Correlations between rainfall events and high flows

Correlations between a) the maximum discharge series and the series of simultaneous precipitation events, and b) the maximum precipitation series and the corresponding discharge event series were estimated for each case in each catchment. The Pearson coefficient was used to assess the strength of the correlation. An example of the correlations and the individual events for each series are shown for a catchment located in Sør-Trøndelag in Fig. 1. The diagram on the left-hand side shows the correlation between the maximum discharge series and the simultaneous precipitation events, and indicates a moderate level of correlation (0.54) between these two sets of values. The right-hand side shows the maximum precipitation events and the corresponding discharge values. In this case, there is no correlation between the two variables (0.03). Colours are used to indicate the estimated fractional contribution of rain (vs. snowmelt) to each event and confirm that most of the high flow events are driven by rainfall.

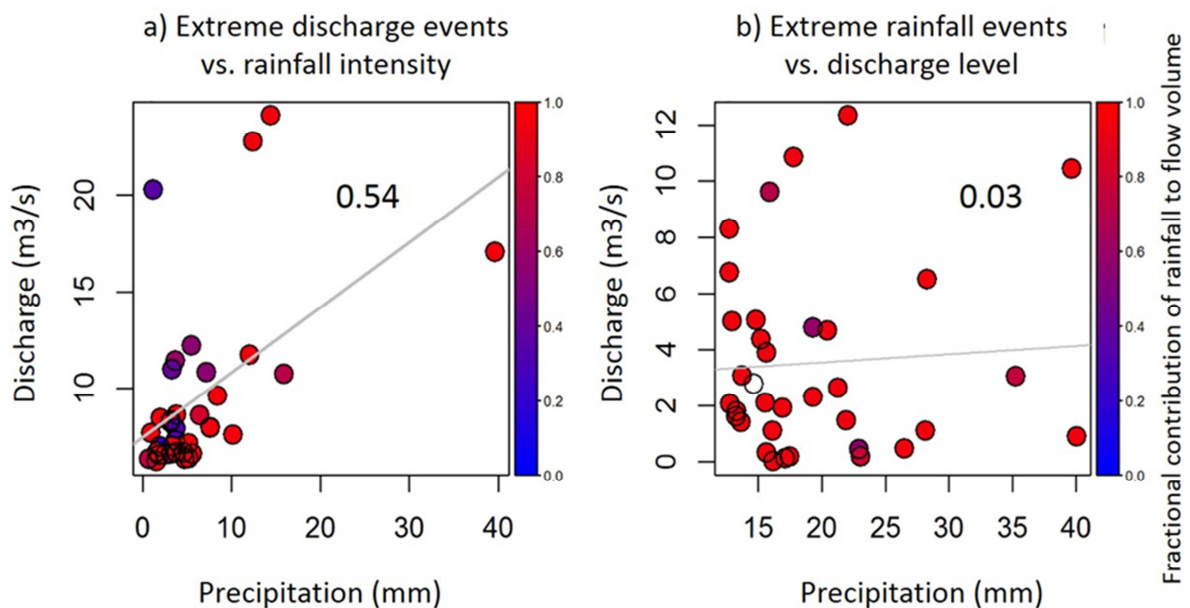


Figure 1: Correlations between a) extreme discharge events and the associated rainfall intensity, and b) extreme rainfall events and the associated streamflow for gauging station 117.4 Valen (Laksvatnet), Hitra, Sør-Trøndelag. The colours indicate the fractional contribution of rainfall to the total flow volume during the event.

The Pearson coefficients for all catchments for both case a) and case b) are shown in Fig. 2. The results indicate that 22 catchments have coefficients > 0.5 (and 5 have coefficients > 0.75) for case a), while 17 catchments have coefficients > 0.5 (and 3 > 0.75) for case b). In other words, most catchments have relatively weak or no

correlation between the values in the series considered. The highest correlations between the extreme discharge events and the corresponding rainfall intensities are generally found in south to southwestern Norway, but correlations > 0.5 are also found in Møre og Romsdal, Sør-Trøndelag (i.e. the example illustrated in Fig. 1), Nordland and in Finnmark. In contrast, there are better correlations between the extreme precipitation series and the corresponding discharge events in western Norway than in southernmost and south-eastern Norway. The same two analyses were also conducted using the logarithmic value of discharge. The results were very similar for case a), with 23 (cf. 22) having coefficients > 0.5 , but were worse for case b), with only 8 (cf. 17) catchments having coefficients > 0.5 . The regional patterns of correlation were similar to those shown in Fig. 2 in both cases.

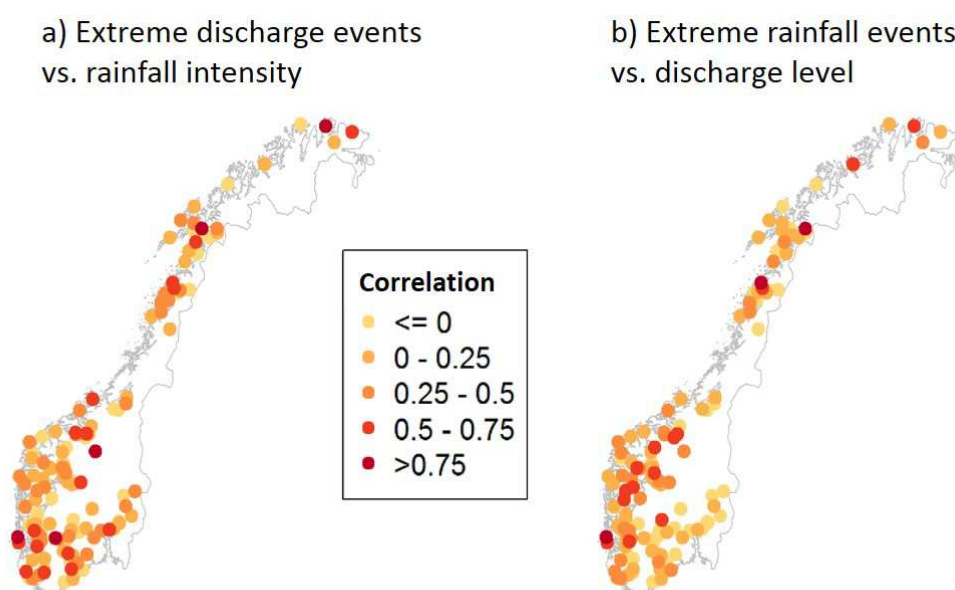


Figure 2: Correlations between a) extreme discharge events and the associated rainfall intensity, and b) extreme rainfall events and the associated streamflow. The colours indicate the value of the Pearson coefficient of correlation between the two variables.

ANOVA tables were also constructed by grouping values of precipitation and discharge into classes and using the classes as explanatory variables. It was again found that there is more often a significant relationship between the maximum discharge events and the class of rainfall intensity that produced them than between maximum rainfall intensities and the class of the discharge in response to the rainfall. In particular, 20 stations showed a significant relationship (for a significance level of $p=0.05$) for the first case, and 9 stations for the latter case.

The results for both the correlation analyses (illustrated in Figs. 1 and 2) and the ANOVA analysis suggest that it is more often the case that extreme high flow events are generated by high precipitation intensities than vice versa (i.e. that high

precipitation intensities lead to extreme flow events). However, the two analyses also confirm that significant relationships between the two variables are the exception rather than the rule, and that in most catchments there appears to be no relationship between precipitation intensities and discharge levels.

Analyses based on return levels

Exponential distributions were used to model the over threshold extreme value series for precipitation and for discharge for each catchment. The return periods for the extreme discharge and precipitation events were extracted from the extreme value model fits, as were the return periods for the corresponding precipitation and discharge values. However, in many cases (i.e. for up to 40% of the stations) the return period for a 'corresponding' precipitation or discharge value were below the lower bound of the extreme value distribution curve and so could not be estimated.

Correlation analyses were performed for the series of return levels for the two cases, i.e. a) the return periods of the events in this maximum discharge series and those of the corresponding precipitation events, and b) the return periods of the events in the maximum precipitation series and those of the corresponding discharge series. The results indicated that 20% of the catchments have a correlation coefficient > 0.5 for case a), representing the correlation between the return period of the over threshold flows and the return period of the corresponding precipitation. A larger percentage of the catchments (27%) have a correlation coefficient > 0.5 for case b), representing the correlation between the return period of maximum precipitation events and the corresponding discharge value.

Empirical return levels were used to determine the fractional number of flooding events with a return period of 5 years or longer caused by a precipitation event with a return period ≥ 5 years. The results are illustrated in Fig. 3 and confirm that this occurs (at least once) in 40% of the catchments. The inverse case (i.e. that a precipitation event with a return period of 5 years or longer leads to a flooding event with a return period ≥ 5 years) occurs at least once in 41% of the catchments. The spatial distribution of the results are illustrated in Fig. 4 and suggests

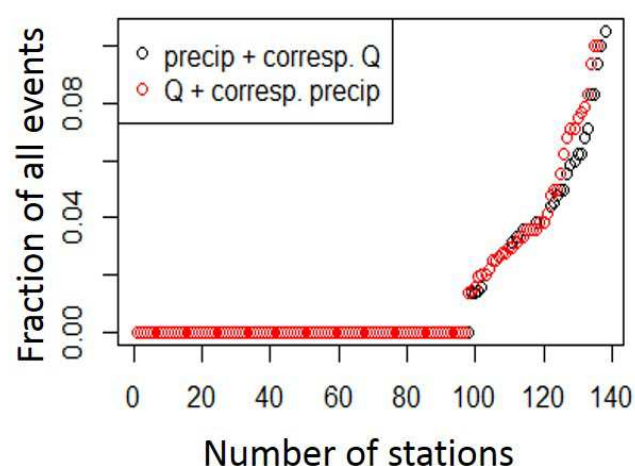


Figure 3. Fraction of events for which a) flooding events with a return period of ≥ 5 years is caused by a rainfall event with a return period of ≥ 5 years (red) and vice versa (black).

that the majority of catchments having at least one event which fulfills the criteria considered tend to lie in more coastal locations. The catchments with the highest occurrence of events are mostly found in southwestern Norway and in Nordland.

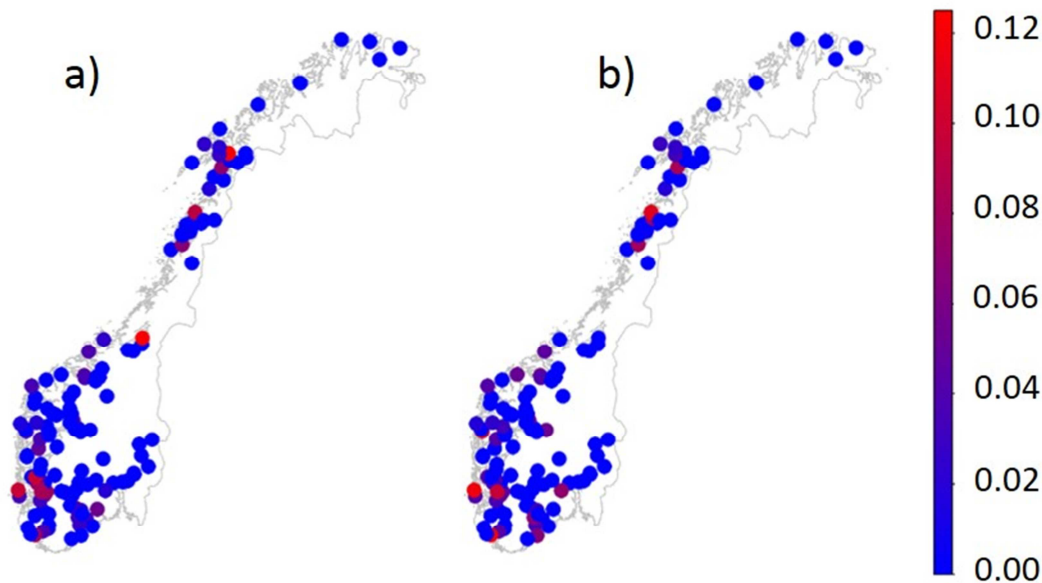


Figure 4. Fractional number of events for which a) discharge events with a return period ≥ 5 years are caused by rainfall with a return period ≥ 5 years, and b) precipitation events with a return period ≥ 5 years produce a discharge with a return period ≥ 5 years.

References

- Filipova, V., D. Lawrence, H. Klempe, (2016), Regionalisation of the parameters of the rainfall-runoff model PQRUT, *Hydrology Research* 47, 748-766.
- Harr, R. D., (1981), Some characteristics and consequences of snowmelt during rainfall in western Oregon, *Journal of Hydrology*, 53, 277-304.
- Lawrence, D., E. Paquet, J. Gailhard, A. Fleig, (2014), Stochastic semi-continuous simulation for extreme flood estimation in catchments with combined rainfall-snowmelt flood regimes, *Natural Hazards and Earth System Science*, 14, 1283-1298.
- Midttømme, G. H and L. E. Pettersson (Eds.), (2011), Retningslinjer for flomberegninger, NVE Retningslinjer nr. 4/2011.
- Vormoor, K. and T. Skaugen, (2013), Temporal disaggregation of daily temperature and precipitation grid data for Norway, *Journal of Hydrometeorology*, 14, 989-999.
- Vormoor, K., D. Lawrence, L. Schlichting, D. Wilson, W. K. Wong, (2016) Evidence for changes in the magnitude and frequency of observed rainfall vs. snowmelt driven floods, *Journal of Hydrology*, 538, 33-48.

2. Estimation of short term extreme precipitation



2.1 Estimation of return levels /precipitation design values at single sites in Norway

A. V. Dyrødal and E. J. Førland

Norwegian Meteorological Institute (MET), Norway

Summary

In the planning and design of important infrastructure in Norway, precipitation return levels estimates from meteorological measuring sites are applied. Estimates are derived using extreme value analysis, but depending on the choice of input data, extremal distribution type and parameter estimation method, we can arrive at very different values. The uncertainty increases for short time series and long return periods.

Introduction

To withstand typical and heavy precipitation events, infrastructure in Norway is designed according to statistical estimates of precipitation for the site in question. These statistical estimates represent the probability that a certain precipitation amount (return level) will occur at a specific site, and how often it occurs on average (return period). The choice of return period in number of years depends on the type of construction and consequences of damage. In this article we present the current

methodology for estimating such precipitation return levels in Norway.

Extreme value analysis

Extreme value analysis deals with estimating the tail of a probability distribution, often presented as return levels for design purposes. There are basically three steps in a return level estimate:

1. Extracting values of measured “extreme” precipitation to be fit to an extreme value distribution.
2. Choosing the best extreme value distribution.
3. Estimating the parameters of the extreme value distribution.

A widely used method for extreme value analysis is the fitting of a Generalized Extreme Value (GEV) distribution to a block maximum series, usually the annual maxima (e.g. Coles, 2001). A special version of the GEV distribution is the simpler Gumbel distribution. Another popular method is the fitting of Peak-Over-Threshold (POT) values to a Generalized Pareto Distribution (GPD), but this method requires very high quality time series and a well-selected threshold.

The GEV distribution

Fitting annual maxima to a GEV distribution involves estimating three parameters; location, scale and shape. Location represents the average, scale represents the variability, while shape describes the thickness of the tail. The GEV distribution is divided into three families, depending on the sign of the shape parameter. GEV type I (Gumbel; shape = 0), GEV type II (Fréchet, shape > 0), and GEV type III (Weibull; shape < 0). In the first two types there is no upper bound on the return levels, but Gumbel converges slowly to infinity compared to Fréchet. Weibull has a theoretical upper limit, towards which estimated return levels converge.

Several studies have shown that for daily precipitation at a point, extremes follow a Fréchet distribution (e.g. Wilks, 1993; Koutsoyiannis, 2004a). This distribution also represents the lowest risk for design as return levels tend to be higher than for Gumbel and Weibull. The parameter estimation becomes unstable as time series become short, thus caution must be taken when extrapolating to long return periods. We have seen examples in which the 200-year rainfall has almost become the 100-year rainfall after an extreme event.

Comparing estimation methods

At MET a version of the Gumbel distribution has been fitted to the n highest occurrences in a station series, where n is the number of years for which the station has measured precipitation on a given temporal resolution. In recent years, the more traditional version with annual maximum series (AMS) is has been applied at MET.

Depending on the selected measurements, the type of distribution, as well as the parameter estimation method, the estimated return level can differ quite significantly, in particular for short time series and long return periods. Given that we would like to use the block maximum method, there is still a choice of GEV versus Gumbel, and even different versions of GEV where the difficult shape parameter can be partially controlled through use of prior information. The prior suggested in Martins and Stedinger (2000) has been tested at MET, showing promising results and more stable return levels. In the third step there exist several parameter estimation methods, the most common being Maximum Likelihood Estimation (MLE) and different moment methods, as well as more recent Bayesian methods.

MET and NVE have compared three methods for estimating the 200-year return level for daily precipitation at 14 stations with relatively long time series. A difference of up to 22 % was seen, with average differences of 3 and 8 %. All methods used annual maxima as input data. For shorter durations and shorter time series, the differences become much larger.

Intensity – Duration - Frequency

Return levels for different return periods and durations are summarized in so-called Intensity-Duration-Frequency (IDF) curves. As an example of an IDF-curve from the Oslo-Blindern meteorological station is shown in Figure 1, including the highest observed precipitation amount for each duration at one of the meteorological stations in Oslo. At MET, a typical IDF-curve presents estimated precipitation return levels for the following durations and return periods: 1, 2, 3, 5, 10, 15, 20, 30, 45, 60, 90, 120, 180, 360, 720, 1440 minutes, and for 2, 5, 10, 20, 25, 50, 100, 200 years.

Return levels are presented in mm or in liters per second per hectare (l/sha), and are also available as tables.

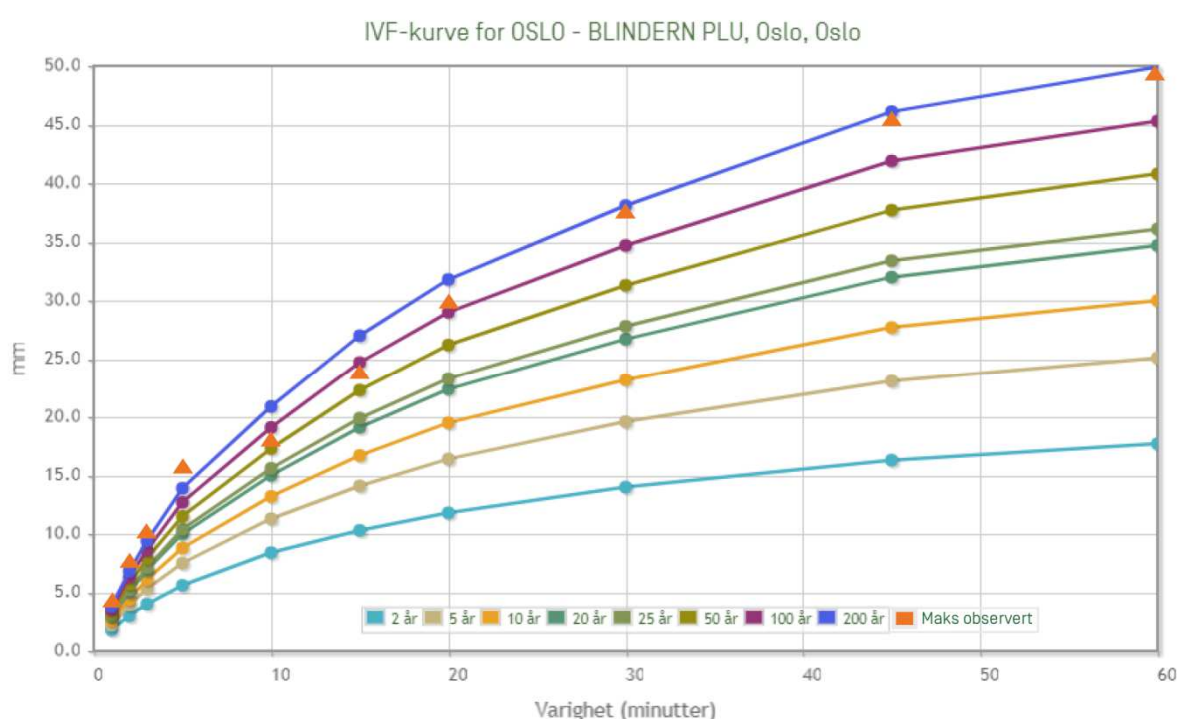


Figure 1: IDF-curve for Oslo – Blindern meteorological station, including max observed precipitation in Oslo (orange triangles).

Probability of extreme precipitation

A precipitation return level can be interpreted as the precipitation intensity with a certain probability of occurrence. For instance, a 10-year return level has a 10% probability of occurring each year. During a random 10-year period there is a 5% probability for a 200-year event (or higher) to occur. See Table 1 below for the probability of exceedance for other period lengths and return periods.

Return period (years)	Period length (years)					
	10	50	100	200	500	1000
10	65	99	100	100	100	100
50	18	64	87	98	100	100
100	10	40	63	87	99	100
200	5	22	39	63	92	99
500	2	10	18	33	63	86
1000	1	5	10	15	39	63

Table 1: Probability (%) for exceedance of T-year precipitation for different period lengths. (From NVE (2011) and Førland et al.(2015).

Measured exceedances

Table 2 shows exceedances of the 10-year return level at seven selected stations with 36-48 years of sub-daily precipitation measurements. We expect the 10-year value to be exceeded approximately 3-5 times during such period lengths, which is confirmed in the table for durations of 10, 30 and 60 minutes. The average number of exceedances for the seven stations is four. The 50-year return level is exceeded 0 – 2 times at the same stations, while the 200-year return level is not exceeded at any of the stations.

10-year return period						
	Station	# years	10 min	30 min	60 min	Average
18701	Oslo-Blindern	48	4	5	4	4.3
12290	Hamar	43	6	5	4	5.0
4781	Gardermoen	43	4	5	6	5.0
3810	Askim	40	5	4	3	4.0
17870	Ås	39	4	5	3	4.0
47240	Karmøy	38	3	2	3	2.7
39150	Kristiansand	36	2	3	4	3.0
	Average					4.0

Table 2: Exceedances of the 10-year return level for 10, 30 and 60 minutes at seven selected stations.

Statistics in a point

One must keep in mind that measured precipitation at a meteorological station essentially only represents the precipitation climate at a single point during the time period with available measurements. As seen in article 1.1 (this report) the precipitation climate in Norway has varied over the last 100 or so years, and the latest decades have shown increased heavy precipitation, both in terms of frequency and intensity. Heavy precipitation of shorter durations (< 1 hour) is often a result of small-scale summer showers, and whether these hit a meteorological station is partly arbitrary, but is also determined by local conditions. Although a 200-year event has a small probability of occurrence in a single site, the probability of such an event to occur within a larger area is much higher. This means that the more stations, the higher the frequency of recorded extreme events. In the light of this knowledge, for planning purposes it is recommended that one checks all available precipitation statistics in the area. As seen in Figure 1, according to statistics at Blindern 100-200 year events are observed some location in Oslo for all durations.

Statistics in a catchment

Precipitation return levels for a catchment are smaller than for a point (station site), because it does not rain simultaneously with the same intensity over the entire catchment. Figure 2 demonstrates this for two different rainfall events; 1: a large-scale frontal system and 2: small-scale summer showers. The former shows a rather uniform distribution of precipitation over the catchment (in blue), and the mean areal precipitation is relatively similar to the precipitation amounts at the point of highest intensity. In the second event, on the other hand, there is large variability over the catchment and mean areal precipitation is lower than point precipitation.

To estimate return levels for a catchment an Areal Reduction Factor (ARF) is traditionally applied. An ARF describes how return levels in an area of a certain size relates to return levels in a representative point. Figure 3 shows typical ARF values for heavy daily and hourly precipitation, which often results from event type 1 and type 2 (Figure 2), respectively. For daily duration, longer gridded datasets are available from which we can compute return levels directly, without the use of ARFs.

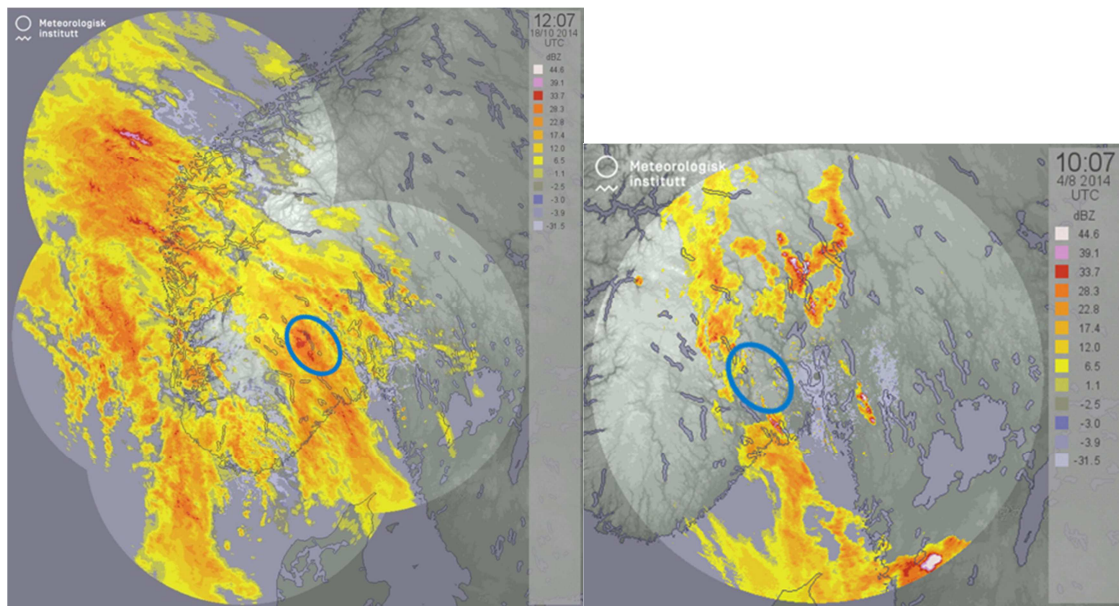


Figure 2: Radar image from a large-scale frontal system (left) and small-scale summer showers (right).

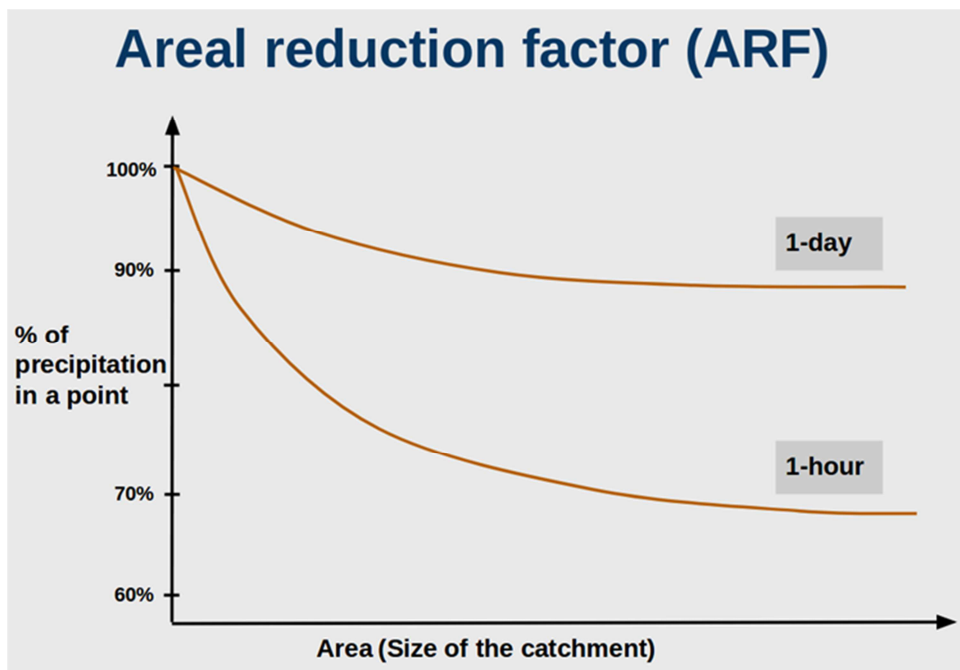


Figure 3: Typical areal reduction factors for 1-day and 1-hour precipitation, with increasing area on the x-axis.

References

- Coles, S.G., 2001: An Introduction to Statistical Modeling of Extreme Values. Springer Series in Statistics: Springer-Verlag London.
- Førland, E.J., Mamen, J., Dyrddal, A.V., Grinde, L., and Myrabø, S.: Dimensjonerende korttidsnedbør. MET report 24/2015.
- Koutsoyiannis, D., 2004: Statistics of extremes and estimation of extreme rainfall: II. Empirical investigation of long rainfall records. *Hydrological Sciences* 49(4):591-610.
- Martins, E. S. and J. R. Stedinger (2000). "Generalized maximum-likelihood generalized extreme-value quantile estimators for hydrologic data." *Water Resources Research* **36**(3): 737-744.
- NVE, 2011: Retningslinjer for flomberegninger. NVE - Retningslinjer nr. 4/2011.
- Wilks, D.S., 1993: Comparison of three-parameter probability distributions for representing annual extreme and partial duration precipitation series. *Water Resour. Res.*, 29(10):3543-3549.

2.2 Gridded return level estimates for extreme precipitation using Bayesian hierarchical modeling.

A. V. Dyrddal and E. J. Førland

Norwegian Meteorological Institute (MET), Norway

Summary

Local precipitation design values given as return levels are important in the planning and design of infrastructure in Norway. We have developed a Bayesian model to provide spatially continuous maps of precipitation return levels with a high spatial resolution of 1x1 km. Maps for durations 10 – 1440 minutes and return periods of up to 200 years are available, and the model provides a framework for developing local Intensity-Duration-Frequency curves.

Introduction

Intense short-duration precipitation over Norway often causes damage to infrastructure and thus represents an economic challenge as well as a threat to human safety. In the planning and design of infrastructure, specifically urban drainage and sewage systems, roads and railways, there is a need for precipitation return levels in terms of Intensity-Duration-Frequency (IDF) statistics. Due to large spatial variability and the relatively sparse network of

conventional meteorological stations measuring short duration precipitation is not able to capture the locality of intense precipitation events. Thus, estimates for ungauged areas have long been requested by the users. We present here the development of gridded return levels with a 1 x 1 km² resolution, covering the entire Norwegian mainland, using a Bayesian hierarchical model. Norway is, to our knowledge, the first country in the world to provide spatially continuous, high resolution maps of precipitation design values in terms of return levels, from which local IDF-statistics are generated.

The BMA-model

As described in Dyrddal et al.(2015), we defined a Bayesian hierarchical model, estimated via Markov chain Monte Carlo (MCMC) methods, which spatially interpolates the parameters of a Generalized Extreme Value (GEV) distribution (e.g. Coles, 2001) for precipitation in Norway. The interpolation applies the relationship between GEV parameters; location, scale and shape, and well-known geographical and meteorological covariates on a high resolution grid. This implies a structure similar to generalized linear modelling. Gaussian fields on the GEV parameters capture additional unexplained spatial heterogeneity, and a Bayesian Model

Averaging (BMA) component over all possible regression models directly assesses estimation uncertainty. We hereby refer to the model as the BMA-model.

The BMA-model is coded by the Norwegian Computing Centre, and is freely available on their github account as an R-package; SpatGEVBMA. Input to the model include measured annual maximum precipitation at stations with at least 10 years of data, coordinates of the same stations, and covariates on a similar grid to seNorge2-data; the official gridded temperature and precipitation data at MET (Lussana and Tveito, 2014). For fitting the simplified two-parameter GEV distribution, i.e. the Gumbel distribution, the shape parameter can be set to zero prior to running the model.

Station measurements

For durations of 60 minutes and up to 1440 minutes, 133 stations in Norway have at least 10 years of annual maxima during the period 1968-present, and are thus included as input in the BMA-model. For durations < 60 minutes (down to 10 minutes), 75 stations fulfil the same criteria. The stations that are included are shown in Figure 1, which also demonstrates that the station network is biased towards low altitudes and residential areas. This leaves large areas, particularly in the north and in mountainous regions, uncovered. As observational series become longer and more and more stations are included in the model, the uncertainty associated with estimated return levels becomes lower.

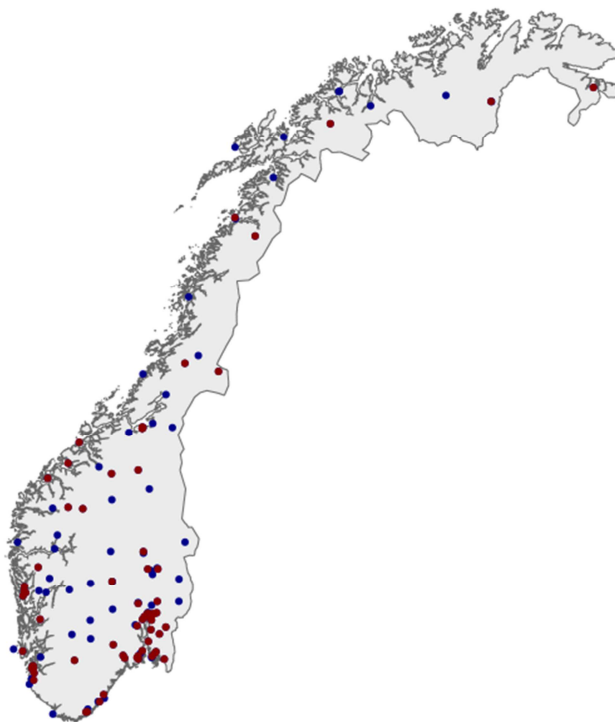


Figure 1: Station network providing precipitation measurements as input to the BMA-model. Red =all durations, blue + red = durations ≥ 60 minutes.

Covariates

We have used 4 geographical variables; latitude, longitude, elevation and distance to sea, and 15 meteorological covariates. The latter include climatological variables derived from seNorge2 gridded temperature and precipitation data from the period 1957-present, such as seasonal means, wet day frequencies, 5-year return levels, and temperature range. All covariates are defined on a 1 x 1 km² grid. For shorter durations, it is expected that many extreme precipitation events are a result of convective summer showers, thus a good covariate for those durations in affected areas is summer temperature.

A way to improve the return level estimates is through better covariates, and for heavy short-duration precipitation a spatial description of the orographic effect and of the occurrence of lightning are two variables worth exploring in the future.

Return level maps

The output of the BMA-model is Norwegian maps of return levels for the duration in question on a similar grid to the input covariates. We have run the model for the following durations and return periods, to deliver IDF-curves similar to those estimated directly at the meteorological stations (but starting from 10 minutes rather than 1 minute): 10, 20, 30, 45, 60, 90, 120, 180, 360, 720 and 1440 minutes for 2, 5, 10, 20, 25, 50, 100 and 200 year return periods.

Figure 2 below shows the estimated 20-year return levels for 60-minute precipitation and Figure 3 shows an example of an IDF-curve from an arbitrary 1 x 1 km grid point. IDF-curves from stations and from arbitrary points based on the maps presented here are combined in a new interactive tool on the web sites of the Norwegian Center for Climate Services (NCCS). See article 5.2 (this report) for more details on the IDF-tool.

Evaluation

In Dyrddal et al.(2015) the BMA-model was compared to 3 other model setups, where a leave-one-out cross-validation showed that the BMA approach performs better than the alternatives in both estimating the “bulk” of the predictive distribution and its tail. As seen in Figure 2, the model is able to reproduce a reasonable pattern of 60-minute return values, with the largest values found along the southern coast, including the Oslofjord-region. Dyrddal et al. (2015) showed that the 20-year return levels compared well with GEV-estimates made directly at the stations. In later evaluations of other durations and longer return periods, we also see good correspondence with station estimates. However, the separate modelling of the different durations creates unrealistic “dips” in IDF-curves some places for long return periods, mainly due to unstable estimates of the GEV shape parameter for

short time series (see article 2.1, this report). This should be addressed in a further development of the model.

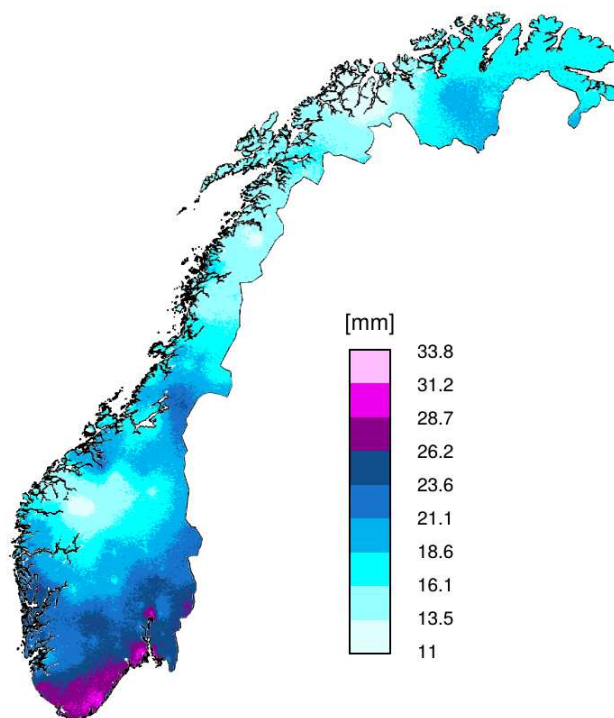


Figure 2: 20-year return levels for 60-minute precipitation as estimated by the BMA-model (Gumbel distribution).

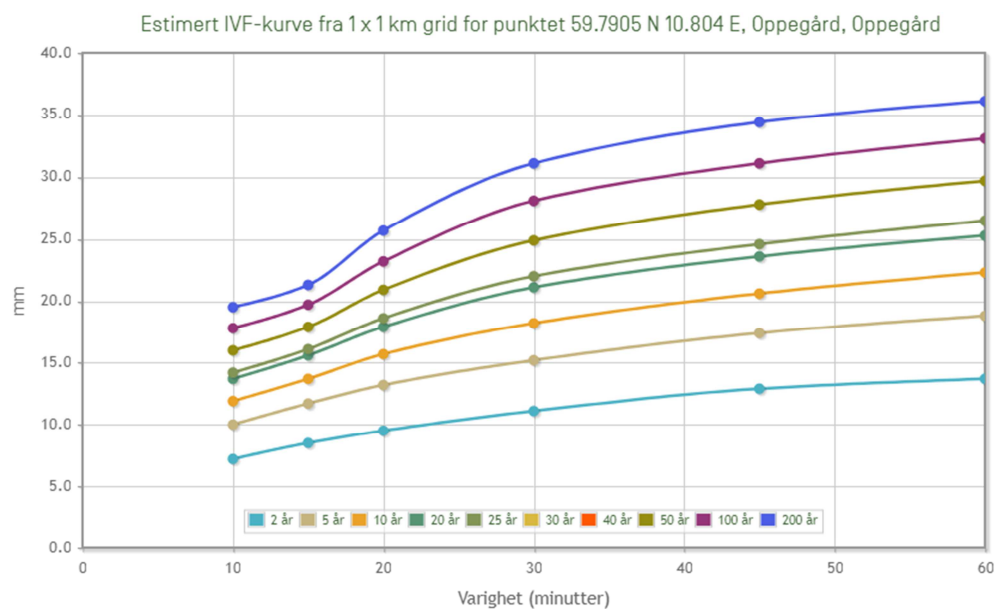


Figure 3: An example of IDF-curves estimated by the BMA-model, for a grid cell in Oppegård.

Further development

Future development of the BMA-model includes implementing the choice of a prior on the shape parameter similar to the one suggested in Martins and Stedinger (2000). This to constraint the shape parameter to reasonable values, and overcome some of the inconsistency between different durations for long return periods. This might also help harmonizing grid and station estimates (see article 2.1, this report). We would like the different durations to be modelled together, to ensure strictly increasing values. Also we want to build a spatio-temporal model to account for non-stationarity in the GEV parameters due to trends in the data (see article 1.1, this report).

References

- Coles, S.G., 2001: An Introduction to Statistical Modeling of Extreme Values, Springer Series in Statistics: Springer-Verlag London.
- Dyrddal, A.V., Lenkoski, A., Thorarinsdottir, T.L., and Stordal, F., 2015: Bayesian hierarchical modeling of extreme hourly precipitation in Norway. *Environmetrics*, 26(2), 89-106.
- Lussana, C. and Tveito, O-E., 2014: Spatial Interpolation of Precipitation using Bayesian methods. Internal research note, MET Norway.
- Martins, E. S. and J. R. Stedinger (2000). "Generalized maximum-likelihood generalized extreme-value quantile estimators for hydrologic data." *Water Resources Research* **36**(3): 737-744.

2.3 Regionalization of rainfall return values for single sites in Norway

E. J. Førland and A. V. Dyrødal

Norwegian Meteorological Institute, Oslo, Norway

Summary

For quality assessment, rainfall design values should be compared to neighboring stations or to “regional estimates”. To get a robust measure of “regional estimates”, Norway was divided into seven regions. IDF-statistics is calculated for each region, and a survey is given of highest observed rainfall for different durations. Rainfall for various durations is also described as fractions of estimated 1 hour and 24 hours rainfall. These fractions combined with maps of 1 hour and 24 hours rainfall may be used to deduce rough estimates of rainfall design values.

Introduction

Rainfall design values (Intensity-Duration-Frequency (IDF) estimates) for single stations can be affected by the rainfall climate during the period the stations were operative (e.g. in periods with many / few heavy rainfall events), or by local “outliers” leading to biased IDF statistics. As the pluviometer series are relatively short (the longest ~ 50 years, see article 1.1, this report), it is thus not obvious that the estimated IDF-values for a single station provide a representative picture of rainfall design values. This is particularly the case for long return periods. To evaluate the representativeness of IDF-estimates

for single sites, the estimates should therefore be compared to neighboring stations or possibly rough “regional IDF estimates”.

Grouping of IDF-estimates into geographical regions

In order to get a robust measure of “regional IDF estimates”, an attempt has been made to group the Norwegian IDF curves for the 200-year return period rainfall into different regions. The reason for focusing on the 200 years return period is that it is recommended to design urban water systems for a 200 year flood (NOU 2015:16). The grouping is partly based on the geographical distribution of 200 year estimates for 1-hour rainfall (background map in Figure 1), and partly on the graphs of 200-year return values for durations 1 minute to 24 hours for each of the measurement stations. The IDF estimates for all series longer than 10 years were divided into seven regions (Figure 1). For the Oslofjord area (R1), the large number of IDF-series allowed one to use only series longer than 15 years in the grouping. In order to

include all IDF series in the grouping and on the other hand to avoid too many groups, regions R3, R6 and R7 cover large areas. In large parts of these regions there is a low station density, and thus difficult to map local variations.

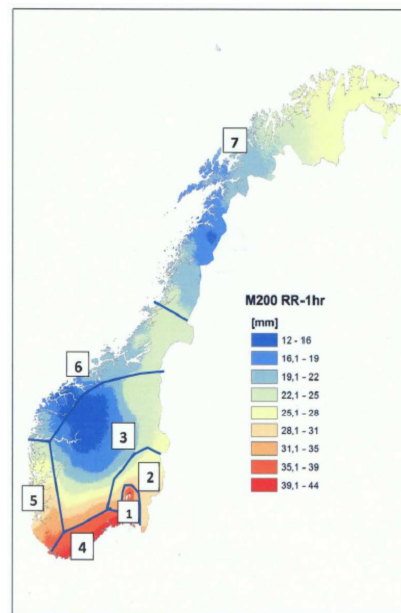


Figure 2: Tentative IDF-regions Background map shows 200 year return period values for 1h rainfall

The ensemble of IDF graphs for each of the regions (see examples in Figure 2 and 3) provides a measure of the spread of 200-year IDF values, as well as an indicator of the highest and lowest estimated 200-year rainfall in the region. The figures also show the highest recorded rainfall values for a number of durations. The maximum recorded values in all regions are summarized in Table 1

Reg- ion	Duration									
	1 min	10 min	30 min	1 hour	1 h (wt)*	2 hrs	6 hrs	12 hrs	24 hrs	1 day**
1	4,1	19,5	42,0	54,9	49,8	59,3	77,7	92,7	104,8	104,3
2	4,3	16,7	21,1	26,2	32,0	28,4	41,4	64,3	81,4	149,5
3	2,6	15,0	18,7	25,6	30,9	27,4	48,4	58,6	77,4	113,2
4	3,8	19,9	32,6	44,9	32,8	64,4	87,4	121,0	143,4	173,2
5	3,3	17,8	38,1	41,9	42,1	47,2	83,2	144,0	159,6	229,6
6	4,3	25,5	28,3	28,9	27,3	29,1	41,9	67,6	87,8	178,5
7	3,6	11,3	16,1	22,4	21,6	30,0	60,4	84,6	113,8	184,3

* 1-hour values for weight pluviometers are adjusted by a factor of 1,12 to be valid for sliding 60 minutes (Førland et al., 2015). ** Measurements from METs regular manual precipitation stations (data from 1895-present).

Table 1. Highest recorded rainfall (mm) in different IDF-regions

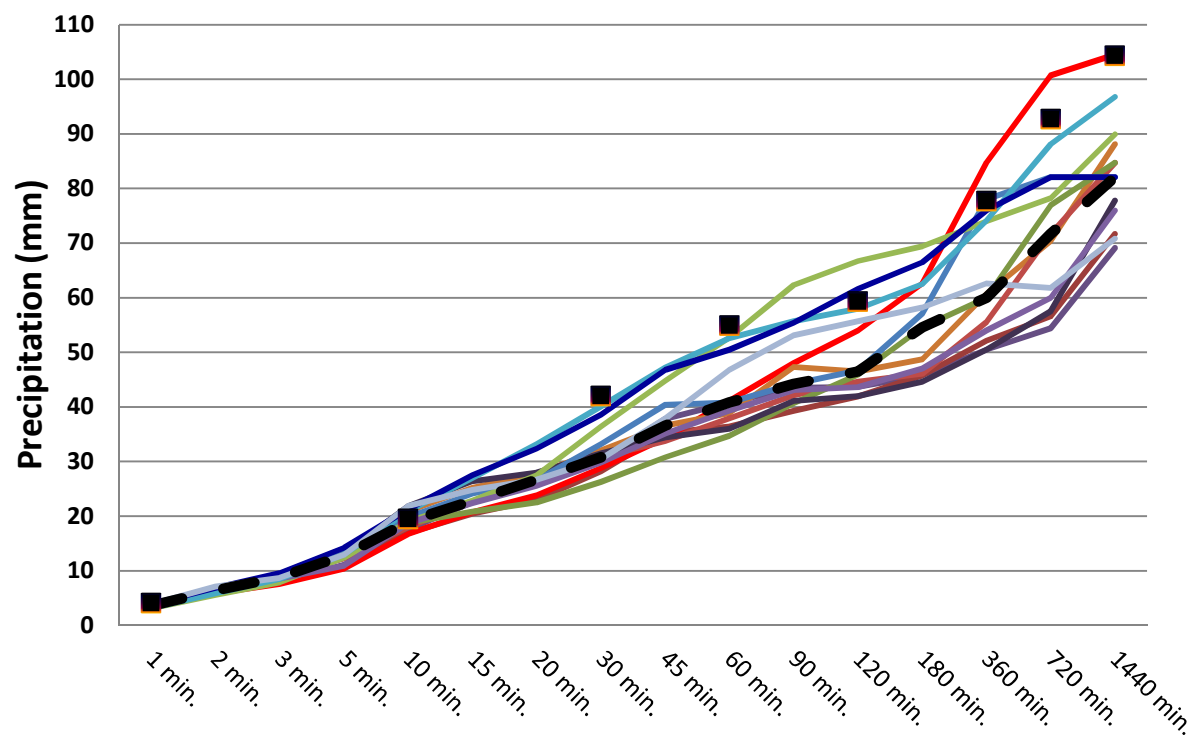


Figure 2. Estimated 200-year rainfall values for durations 1 – 1440 minutes for 13 stations in Region 1: «Oslofjorden». Black squares indicate the highest measured values. The dashed line represents the median values for the region.

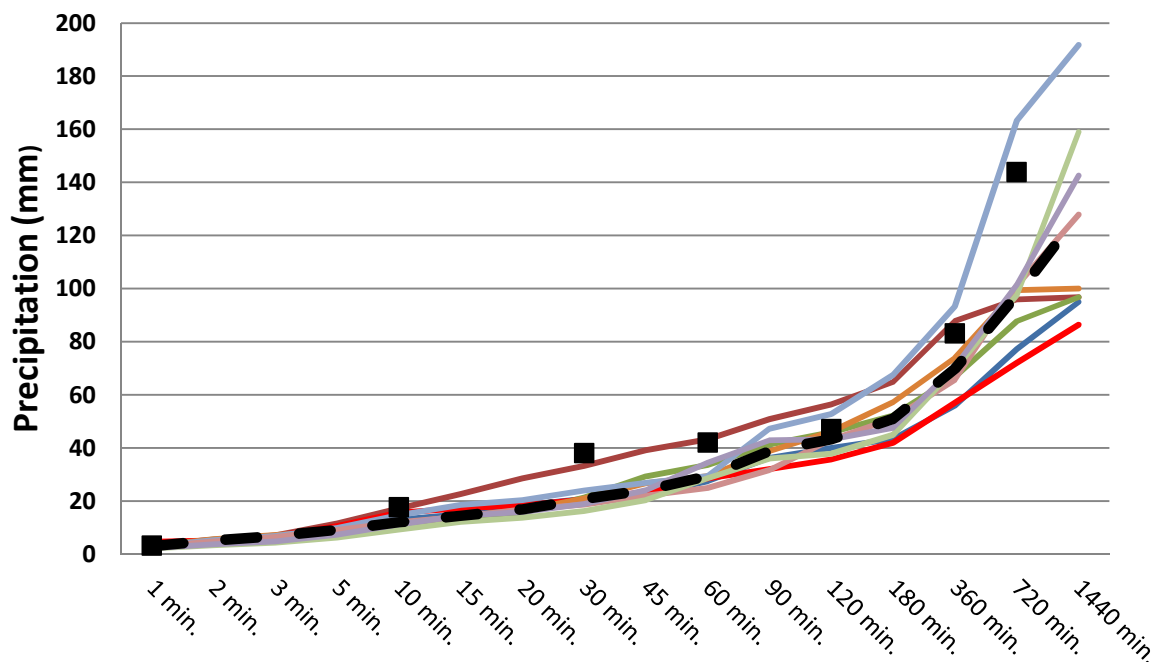


Figure 3. Estimated 200-year rainfall for durations 1 – 1440 minutes for 9 stations in Region 5: «Vestlandet». Black squares indicate the highest measured values. The dashed line represents the median values for the region.

Based on the ensemble of IDF-estimates, median 200 year return period values were calculated for each region (Table 2, Figure 4). In Figure 4 also the highest recorded values in Norway are indicated. For durations of 1 minute and up to approx. 4 hours the highest values are found in regions R1 (Oslofjorden) and R4 (Sørlandet). For durations beyond 4 hours Sørlandet has higher values than the Oslofjorden area. Region R2 (Østlandet-SE) also has high values for up to approx. 10 minutes duration, but for longer periods, the values for this region are significantly lower than for the Oslofjorden and Sørlandet regions. Region R5 (Vestlandet) has the highest values for durations higher than approx. 4 hours but lower values than Region R1, R2 and R4 for short durations. The regions R3 (Innlandet), R6 (Møre/Romsdal/Trøndelag) and R7 (Northern Norway) have approximately identical values up to ca. 12 hours duration.

As described in articles 2.2 and 1.1 (this report), the geographical distribution of IDF values over Norway is related to summer temperatures. The main reason for this is that the potential amount of precipitable water increases with increasing temperatures. The higher rainfall values in Figure 1 for the Oslofjorden region (R1) and along the southernmost coastline (R4) are probably connected with the advection of moist air from surrounding sea areas, where the summer air and sea surface temperatures are higher than for the rest of Norway. In large parts of Norway the most intense sub-daily rainfalls occur in weather situations with high convective

activity (summer showers), but for Western Norway (R5) and the coast of Nordland (western part of R7) orographically enhanced rainfall during strong onshore winds may cause high rainfall amounts even for short durations.

Figure 4 demonstrates that the highest observed values in Norway are significantly higher than the median 200-year estimates for the regions. However, in most regions there are single stations with 200-year estimates at the same level as the highest observed values; cf. Figure 2 and 3 for regions 1 and 5. Private observations indicate values that are far higher than those recorded at METs pluviometer stations (Førland et al., 2015). However, it is not inconsistent with IDF statistics that intensities that far exceed the 200-year estimates may also occur even for short data series.

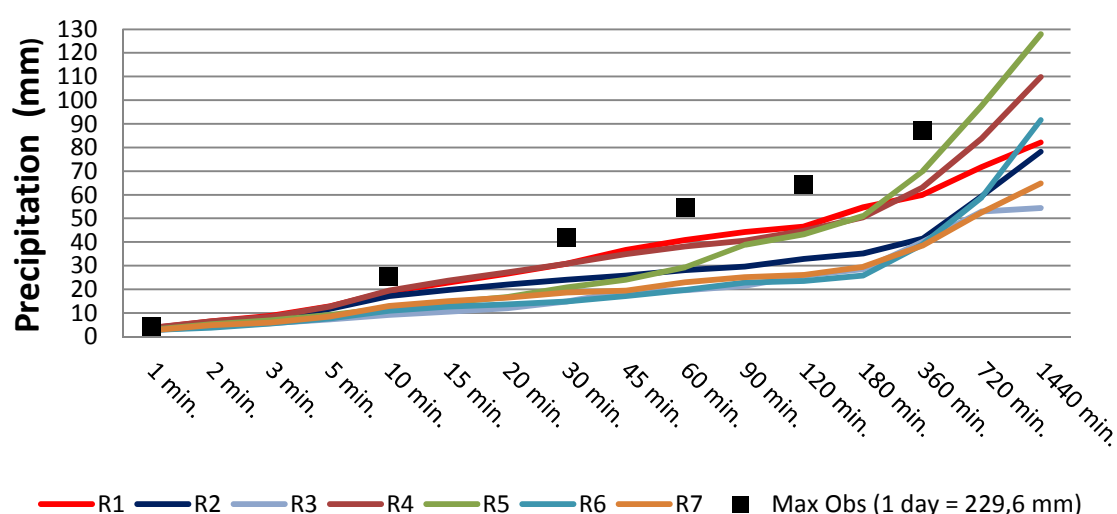


Figure 4. Median values of estimated 200-years rainfall for different regions. Black squares indicate the highest observed rainfall intensities for Norwegian stations.

Duration	Region						
Minutes	1	2	3	4	5	6	7
1	3,6	3,3	2,7	3,8	3,0	2,8	2,7
2	6,4	5,7	4,3	6,5	5,2	3,8	4,8
3	8,8	8,2	5,7	8,4	6,9	5,5	5,9
5	12,8	11,8	7,3	12,7	9,2	7,7	8,5
10	19,0	17,2	9,2	19,4	12,0	10,9	12,9
15	22,8	19,7	10,5	23,7	14,4	12,7	15,1
20	26,7	22,0	12,0	27,2	16,8	13,6	16,5
30	30,8	24,1	14,8	30,9	20,8	14,8	18,6
45	36,6	25,8	19,2	34,9	24,1	17,1	19,5
60	40,8	28,2	19,6	38,1	29,4	19,7	23,0
90	44,2	29,6	21,6	40,6	38,8	22,8	25,2
120	46,5	32,9	25,8	44,8	43,3	23,5	26,2
180	54,6	35,1	28,6	50,4	51,0	25,8	29,5
360	60,0	41,5	40,0	63,1	69,8	38,9	38,4
720	71,7	59,4	53,0	83,8	97,6	58,8	52,5
1440	82,1	78,2	54,5	109,7	127,9	91,6	64,8

Table 2. Median values for estimated 200-years rainfall (mm) for different regions (cf. Figure 1).

Rainfall for different durations as fractions of 1-h and 24-h rainfall

The most comprehensive datasets from which design values can be estimated are found for durations of 1 hour and 1 day. The 1-day estimates may be based on time series from a large number of long-term manual precipitation stations. Because of several sources of “noise” (e.g. false registrations) in the pluviometer series, MET has focused quality control on 1-hour values. Mapping of IDF-estimates for durations 1-hour and 1-day is thus based on more stations and is more robust than for other sub-daily durations.

In order to provide rough estimates of design values for rainfall for durations other than 1-hour and 1-day, rainfall for other durations has been analyzed as percentages of 1-hour (24-hour) rainfall. Regional fractions have been based on the regional values shown in Figure 4 and Table 2.

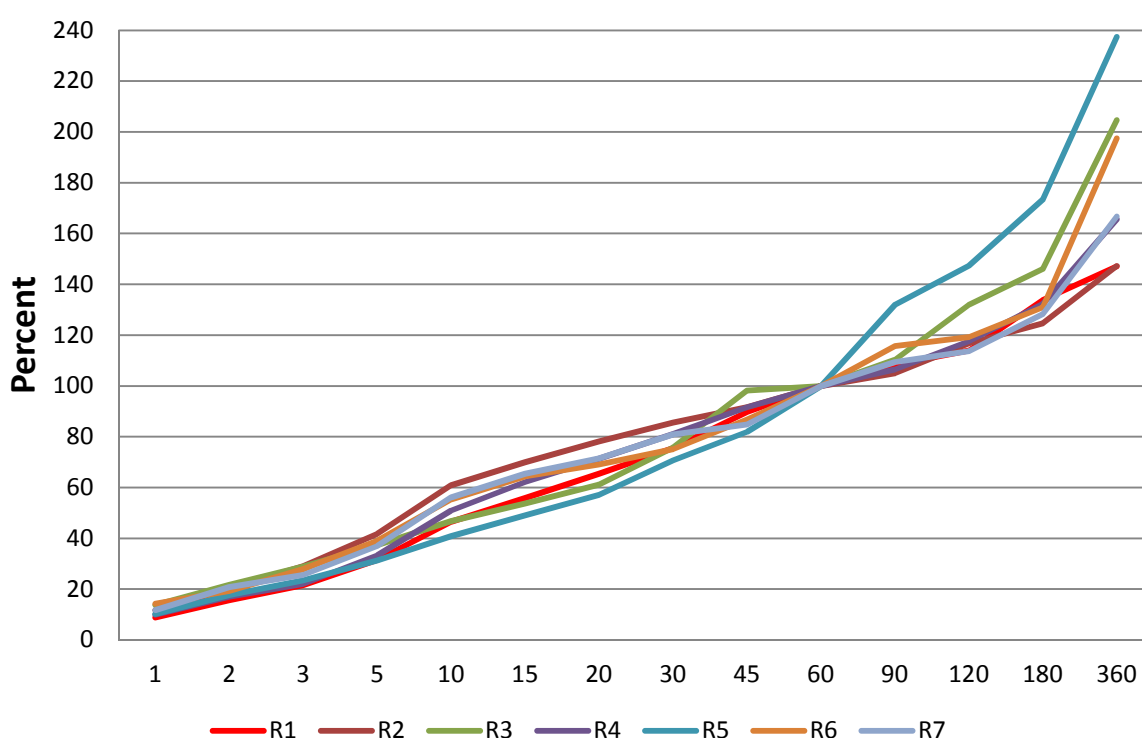
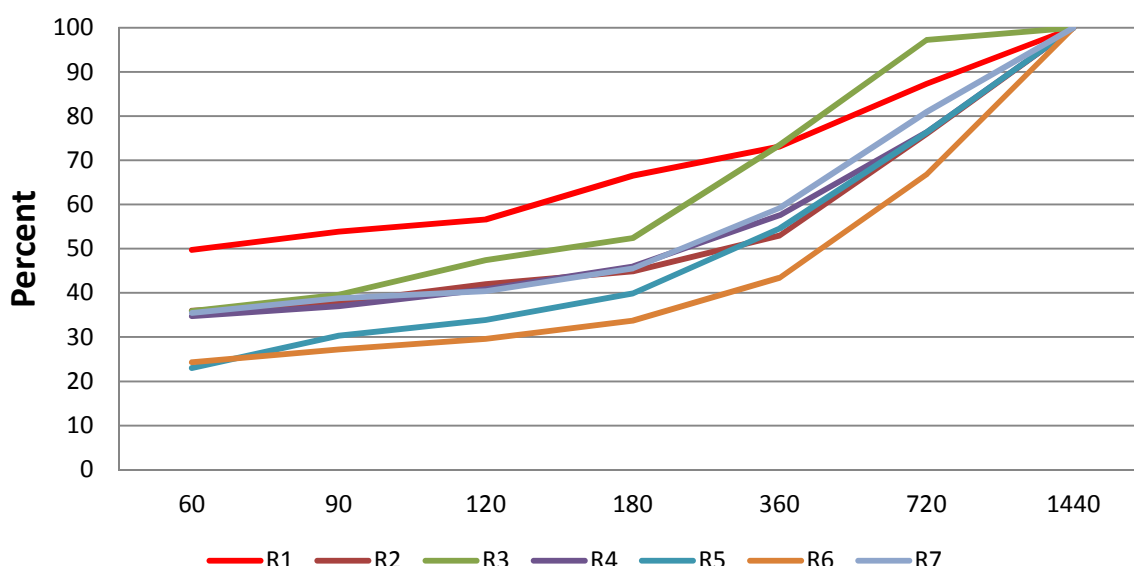


Figure 5. 200-year rainfall for durations 1-360 minutes as a fraction of rainfall during 60 minutes. *The graphs are based on the values in Table 2.*

Figure 5 shows that for rainfall with a return period of 200 years, the 1-minute value is approximately 10-15% of the 1-hour value, while 10-minute rainfall is 40-60%. For durations of up to 1-hour, Western Norway has the lowest percentages, while southeastern parts of Eastern Norway have the highest values. For the latter region, the precipitation value for 20 minutes is 80 % of the 1-hour value, while for Western Norway it is lower than 60 %. For periods exceeding 1 hour, Western Norway has the highest percentages; - the estimated 6-hour rainfall amounts to 240% of the 1-hour

value, while for Eastern Norway it is 140%. The reason for these differences is that in Southeastern Norway a large part of heavy rainfalls is caused by short duration showers. In Western Norway, however, in weather conditions with high humidity and strong onshore winds, - relatively high precipitation intensity may persist over longer periods. By combining the regional fractions in Figure 5 with the map of 1-hour rainfall (Figure 1), it is possible to deduce rough estimates of the 200-years rainfall for durations of 1 to 360 minutes.



Figur 6. Rainfall with duration 60-1440 minutes as a fraction of 1-day (1440 minutes) rainfall. The graphs are based on the regional values in Table2.

Figure 6 shows the 200-year rainfall down to 1-hour duration as a fraction of the 1-day (1440 minutes) value. A map of estimated 1-day precipitation with return period 200 years is shown in Figure 7. It appears that for the Oslofjord region the 1-hour value is half the 1-day value, while in western Norway and in Møre / Romsdal / Trøndelag it amounts to approx. 25%. These are rough estimates; - there may be major deviations from the median curves within each of the regions. Among other features it is apparent from Førland (1992) that precipitation for n hours as a fraction of 1-day rainfall also depends on the mean annual rainfall.

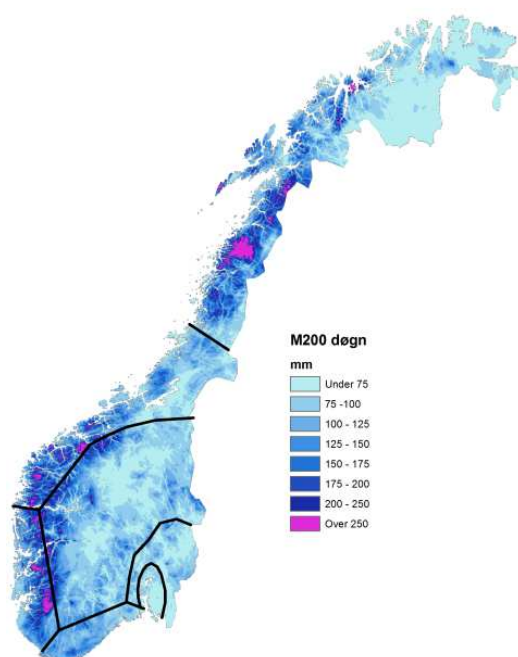


Figure 7. Estimated 1-day rainfall (mm) with return period 200 years.

Rough estimates and quality assessment of IDF estimates

From maps of 1-hour precipitation (Figure 1) and precipitation fractions outlined in Figure 5, it is possible to obtain rough estimates of the 200 year rainfall for various duration (1 - 360 minutes) for arbitrary locations. Similarly, map of 1-day rainfall (Figure 7) and the precipitation fractions in Figure 6 can be used to estimate the 200-year rainfall for 1 to 24 hours for different locations all over Norway.

It should be emphasized that the above methodology only provides very rough estimates; - there may be major deviations from the median curves within each of the regions. An indicator of the spread of IDF estimates within each of the regions is shown by Førland et al. (2015).

For quality assurance of IDF values from sites in areas with good coverage of pluviometer stations, regional statistics may be a useful basis for comparison. For estimates in areas with poor station coverage, a combination of the results in Figure 1/5 and 6/7 may be used to provide rough estimates.

As a result of the ExPrecFlood-project, a web-based tool for estimating IDF-values for arbitrary sites all over Norway was developed and implemented in collaboration with the Norwegian Centre for Climate Services (see www.klimaservicesenter.no). This new tool is described in article 5.1 (this report), and should be the main source for IDF-estimates for planning purposes. However, the IDF-estimates behind this tool

are based on a limited number of pluviometer series, and are hampered by large uncertainties in many regions. Consequently estimates extracted through this tool should be quality checked by comparing to the regional IDF-estimates outlined above.

References

- Førland, E.J., 1992: Manual for beregning av påregnelige ekstreme nedbørverdier. (In English: Manual for estimating probable extreme precipitation values). MET Norway Report 02/1992
- Førland, E.J., J. Mamen, L. Grinde, A.V. Dyrddal and S.Myrabø , 2015: Dimensjonerende korttidsnedbør (In English: Design values for short-term rainfall), MET Norway Report 24/2015
- NOU 2015: 16: Overvann i byer og tettsteder — Som problem og ressurs (In English: Surface water in cities and towns - As a problem and resource). Norwegian Ministry of Climate and Environment, December 2015

2.4 Sensitivity of return value estimates to method and sites – a case study for Bergen

A Sorteberg and S. Johansen

Geophysical Institute and Bjernes Center for Climate Research, University of Bergen, Norway

Summary

100-year return values from 2 minutes to 48 hours duration has been calculated for four stations close to Bergen based on yearly maxima using generalized extreme value distributions with several parameter estimation methods. We discuss how sensitive the return values are to selection of parameter estimation method and how much they differ between the different stations. Results suggest that even for short time series, the spread among the stations are much larger than the spread due to parameter estimation method. This emphasizes the need to thoroughly investigate the representativeness of the station selected when doing extreme value analysis.

Introduction

Extreme value analysis is about modelling the tail of a distribution, often with the aim of extrapolating the observed data to gain knowledge about rare events that has not yet been observed. Traditionally there has been two ways to look at extreme value analysis. One is that extreme events are given as maximum values over a given time period – often a year (*block maxima* methods). The other is that extreme events are events over a given threshold (*peak over threshold* methods). The extreme value distribution is often defined by three parameters. The location parameter μ , the scale parameter σ and the shape parameter ξ which all have to be estimated in order to fit a theoretical distribution curve to

the observations. Simply put, the effect of the location parameter μ is to shift the distribution left or right on the horizontal axis (see Figure 1). The effect of the scale parameter σ is to stretch or shrink the distribution while the shape parameter ξ affects the *shape* of the distribution by controlling the behavior of the probability of a really extreme event (i.e. the upper tail of the distribution) relative to the probability of less extreme events.

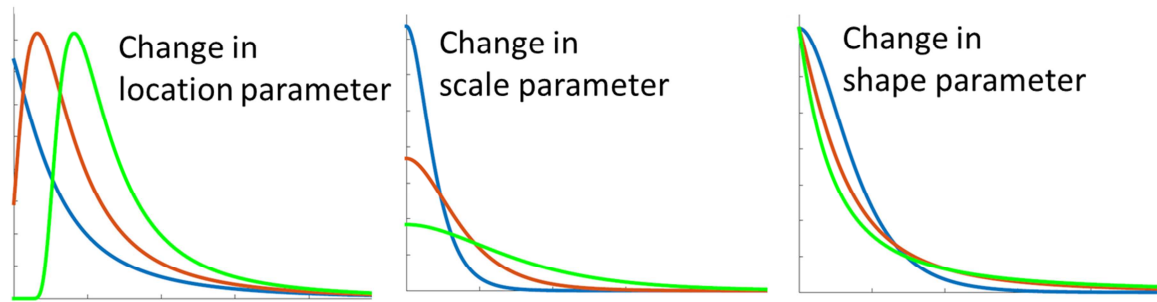


Figure 1: Examples showing the change in the probability density function when only the location (a), scale (b) and shape (c) factor are changed for a generalized extreme value (GEV) distribution.

The probability of extreme events exceeding a given threshold x_T , $P(x > x_T)$, is given as

$$P(x > x_T) = \frac{k}{m}$$

where k is the number of exceedances ($x > x_T$) in m number of observations. It is often convenient to have the probabilities of exceeding a given threshold for a given period T in years instead of a given number of observations m . If T is measured in years: the probability that $x > x_T$ is exceeded at least once in one year is $1/T$:

$$P(x > x_T) = \frac{1}{T}$$

where x_T is called *the return level* or the *return value* and T the return period. If $T \gg 1$ year this is equivalent to saying that x exceeds x_T on average once in T years.

Finding *return values using extreme value distributions* is an attempt to model the probability $P(x > x_T)$ for different *return values* x_T by assuming that the probability can be fitted to a given set of functions that has three parameters (the location parameter μ , the scale parameter σ and the shape parameter ξ). Numerical techniques must be used to find the best fit of the function to the available data.

$$P(x > x_T) = f(\mu, \sigma, \xi)$$

The three parameters can be estimated based on the observational data by a variety of techniques. The four most common techniques are probably maximum likelihood estimation (ML), L-moments (LMOM), Probability Weighted Moments (PWM) and Bayesian Markov Chain Monte Carlo (MCMC) methods.

In traditional extreme value theory the data is assumed to be stationary (i.e. to have means, variances and covariances that do not change with time) and the three parameters are estimated as constants. Stationary data will lead to a one-to-one relationship between the T-year return value (x_T) and the T-year return period (T). This leads to two possible interpretations of the 'T-year event' which under the assumption of stationarity are both correct:

1. The expected number of events in T years is 1.
2. The expected waiting time until the next exceedance is T years.

However, time series are often non-stationary (i.e. have means, variances and covariances that change over time). Typical non-stationary behaviors can be trends or cycles. In this case the one-to-one relationship breaks down as the expected waiting time till the next exceedance will not be the expected number of events in T years calculated from the observations. In the non-stationary case the extreme value distribution will change with time and a general theory about non-stationary extreme value analysis has not yet been formulated. The literature describes several possible methodologies which rely on the standard extreme value theory as the starting point:

- An established technique is to make one or more of the three parameters a function of time ($P(x > x_T) = f(\mu(t), \sigma(t), \xi(t))$). The function to use is unknown and has to be selected. A linear function is often used. T drawback of this approach is that there is no general way to formulate the function and often many functions have to be tested to find the best fit.
- A commonly used approach for dealing with nonstationary series is to divide them into quasi-stationary slices and apply the stationary theory to each slice. This has the drawback of reducing the size of the sample used for the extreme value analysis which leads to much larger uncertainty in the return value estimates.
- Another approach recently proposed is to transform the non-stationary time series into a stationary series and perform a classical stationary extreme value analysis, and then back-transforming the resulting extreme value distribution into a time-dependent one.

Here we will compare estimated 100-year return values based on stationary and non-stationary methods for a station near Bergen (Sandsli) which has data beginning in 1982. In addition, we will investigate how different methods of parameter estimation methods (maximum likelihood estimation and Bayesian Markov Chain Monte Carlo) affect the results.

We will also investigate how methods of parameter estimation affect the results for very short time series (Florida, Åsane and Sædalen). Finally we will look on the sensitivity of the estimates to location by comparing stations within Bergen (Sandsli, Florida, Åsane and Sædalen). Many of the results are part of the master thesis

Ekstremveridianalyse av nedbør og oppdatering av intensitet - varighet – frekvens kurver i Bergen Kommune (Johansen, 2016) and details may be found in the thesis.

Method

Four stations close to Bergen are used in the analysis. One is a relative long time series while the three others are shorter (see Table 1 and Figure 2).

Return values for durations of 2 minutes to 48 hours based on yearly maxima using generalized extreme value distributions were calculated based on three parameter estimation methods:

- Stationary block maxima (max per year) using maximum likelihood (ML) to estimate the parameters (called *ML stationary* in figures).
- Stationary block maxima (max per year) using maximum likelihood to estimate the parameters using a Bayesian Markov Chain Monte Carlo (Bayes-MCMC) method (called *Bayes stationary* in figures).
- Non-stationary block maxima (max per year) using maximum likelihood to estimate the parameters using a Bayesian Markov Chain Monte Carlo (Bayes-MCMC) method where the location parameter (μ) is assumed to be a linear function of time $\mu(t) = \mu_0 + \mu_1 t$ (called *Bayes non-stationary* in figures). The scale and shape parameters are assumed to be constants. The reason for this choice is that if scale and shape parameters should also be a function of time, much more data would be needed to get stable estimates.

In the analysis we also add the return values that can be downloaded from the Norwegian Centre for Climate Services (noted *NCCS* in the figures). The procedure used for these estimates are outlined in article 2.2 in this report.

Station name	Elev.	Time period	Highest values observed in the common time period 2004 - 2015			
			5 min	10 min	1 hour	12 hour
Florida	12	2004 - 2015	8,2 02.08.2014	11,4 20.09.2007	26,6 31.10.2007	119,4 13.09.2005
Åsane	95	2004 - 2015	7,0 02.08.2014	10,1 02.08.2014	26,7 25.08.2012	77,2 13.09.2005
Sædalen	200	2004 - 2015	6,6 02.08.2013	11,6 30.04.2014	23,6 22.08.2012	108,5 13.09.2005
Sandsli	40	1982 - 2015	7,2 02.08.2014	9,3 02.08.2014	21,7 22.08.2012	90,7 13.09.2005

Table 1: List of maximum observed values and dates for selected durations for the four stations used in this study.

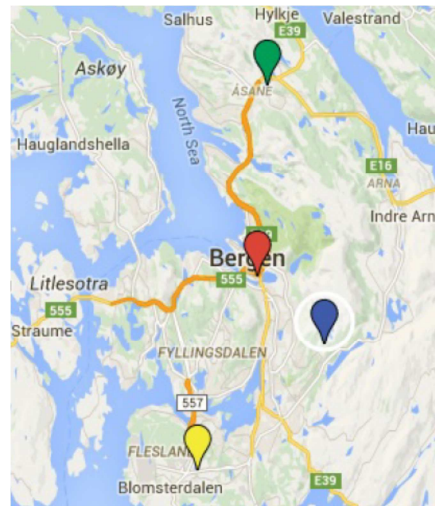


Figure 2: Map showing the location of the stations analyzed. Sandsli (yellow), Florida (red), Åsane (green) and Sædalen (blue).

Sensitivity of the return values to parameter estimation method

For Sandsli having 34 years of data, the choice of parameter estimation method did not change the 100-year return values much for durations from 2 min to 48 hours. The deviations are typically only a few percentage points. This is encouraging and indicates that in time series spanning 3-4 decades the choice of method to estimate the parameters are not the most important concern. This is in line with the analysis of several stations with relatively long time series using different stationary estimates (See article 2.1 this report). As will be shown below this result does not hold for shorter time series.

In the non-stationary case where the location parameter is $\mu(t) = \mu_0 + \mu_1 t$, we can extrapolate the location parameter forward in time and look at the hypothetical 100-year return value in 2100 under the assumption that the location parameter changes at the same rate as seen during the last 34 years. This is of course very hypothetical as there is no a priori reason to believe that climate change will make the extreme value probability behave in such a linear manner. Never the less this approach provides alternative information that can be used alongside climate factors derived purely from climate models. In the Sandsli case the time series has non-significant positive trends for all durations analyzed which translates into higher return values in the future if the trend continues (dashed line figure 3). Translating this into climate factors (defined as the ratio between 100-year return period for 2100 and the 100-year return period for the observed period) gives factors in the order in +20 to +35% for the durations of up to 3 hours and. +40 to +50% for 6 hours and higher durations.

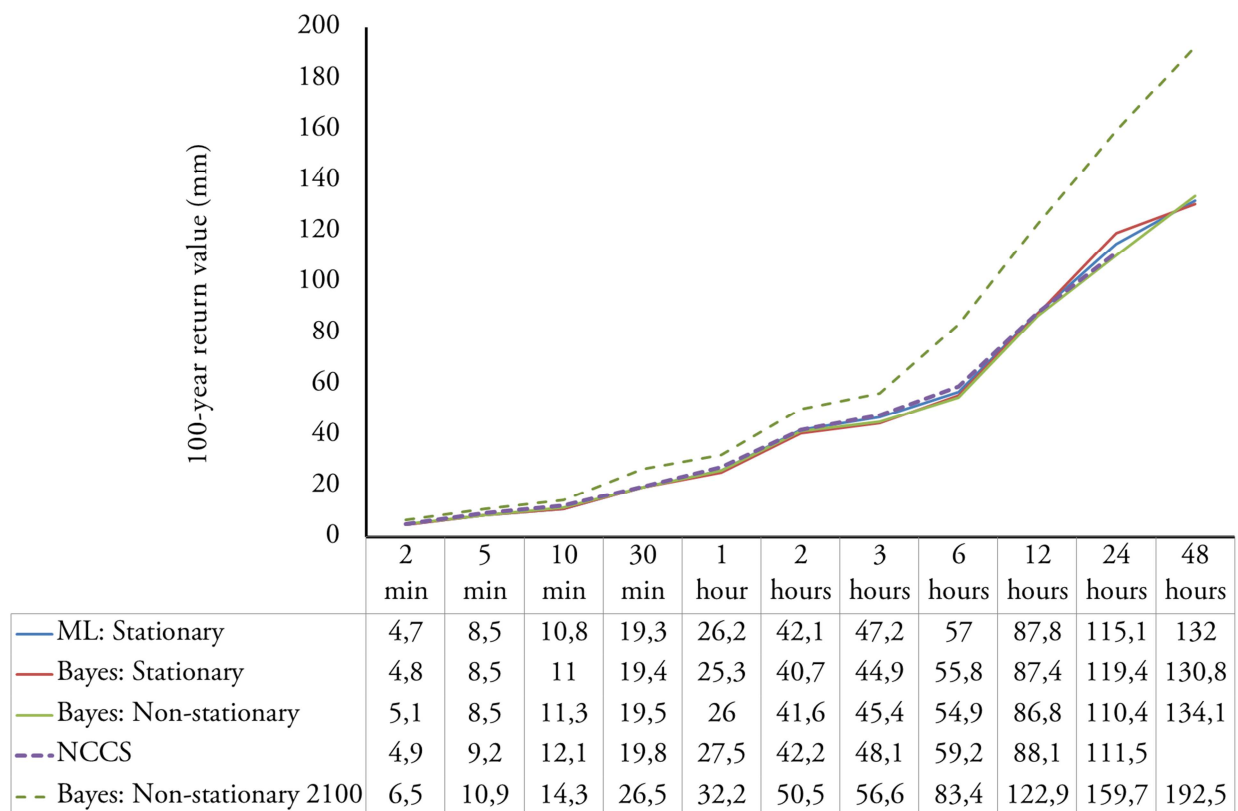


Figure 3: 100-year return values (mm) using observations from Sandsli (1982-2015) for different durations and parameter estimation methods. An extrapolation of the non-stationary estimate to year 2100 assuming that the location parameter changes at the same rate as seen during the observational period is also shown. ML stationary: Stationary block maxima (max per year) using the maximum likelihood method. Bayes stationary: Stationary block maxima using the Bayesian Markov Chain Monte Carlo (MCMC) method. Bayes non-stationary: Non-stationary block maxima using the MCMC method and taking the median of the location parameter (the 1999 value) for the observation period. NCCS: Method used in Norwegian Centre for Climate Services estimates. Bayes non-stationary 2100: Non-stationary block maxima using the MCMC method and taking the location parameter based on the observation period and extrapolate it to year 2100.

For the short time series at Florida, Sædalen and Åsane a non-stationary approach makes little sense, thus we will only compare the stationary estimates using the maximum likelihood, Bayes and the NCCS methods (Figure 3). We see that in the case of short time series the estimates become much more dependent on the choice of estimation method. For durations up to 3 hours the mean deviation between the maximum likelihood and the Bayes method is typically 10-15%. This increases to 30-60% for the longer durations (6 to 24 hours) and is a good example of the risk of parameter estimation becoming unstable as time series become short. None of the models gave more consistent lower or higher values than the others. Both the ML and Bayes method typically estimated values that are 15-40% higher than the highest observation during the 11 years of data for short durations.

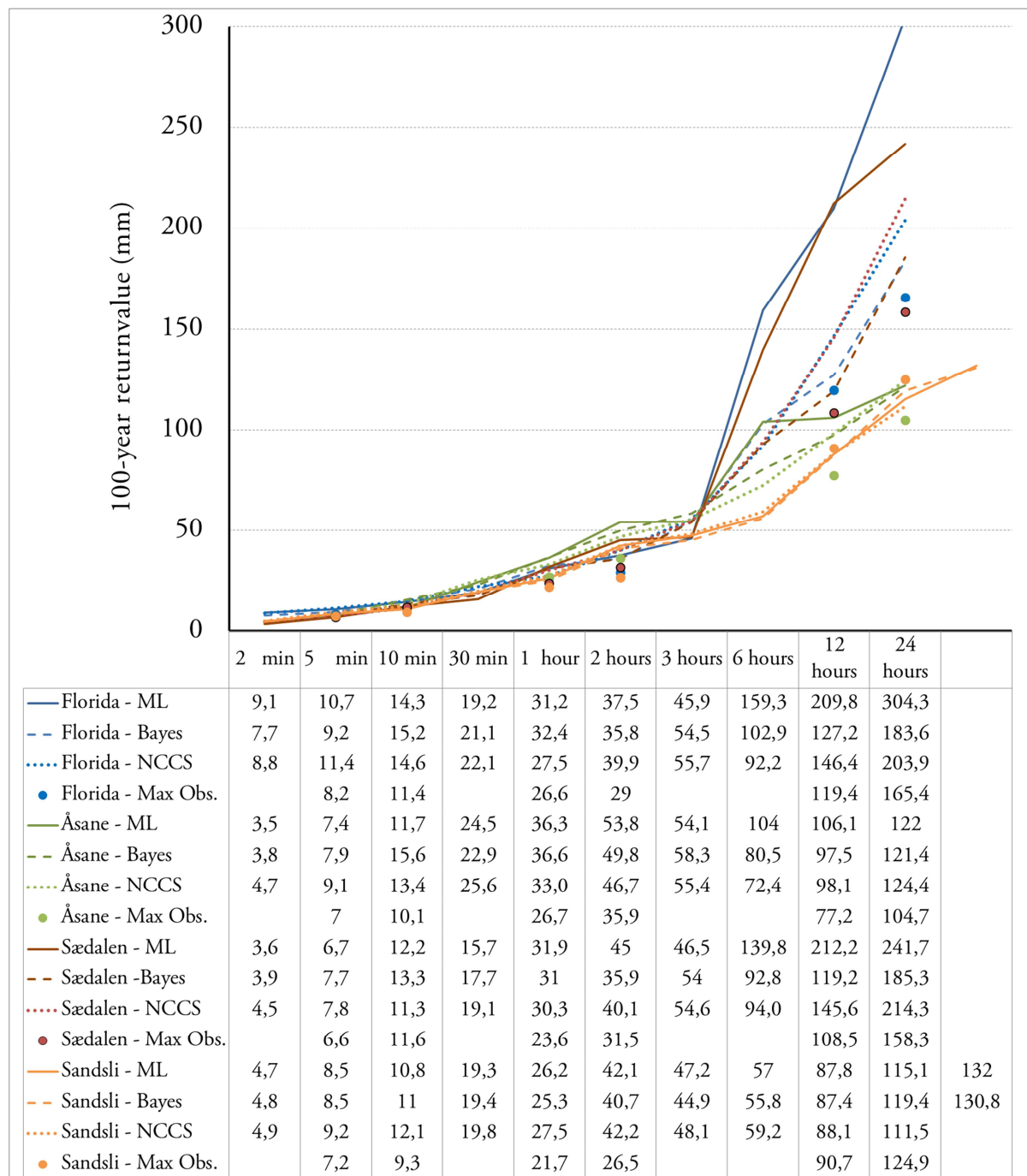


Figure 4: 100-year return values (mm) using observations from Florida, Åsane and Sædalen (2004-2015) and Sandsli (1982-2015) for different durations and parameter estimation methods (ML: stationary max. likelihood, Bayes: Stationary Bayesian Markov Chain Monte Carlo method. NCCS: Norwegian Centre for Climate Services estimates (Dyrddal and Førland section 2.2 this report). The maximum observed value (points) for selected durations is also shown.

Sensitivity of the return values to station - representativeness

In Norway there are few long time series for precipitation durations below 24 hours (see article 1.1 in this report for an overview) and their representativeness is often unclear. The Sandsli data are based on the 34 years available and are often used for estimating design values in the region. If there was no systematic difference between the sites and the data were stationary one should think that the Sandsli data would have the highest maximum values just because the observational period is three times as long as the other stations and therefore the probability of detecting a high value is larger. But as seen in Figure 3 the maximum values at Sandsli are the lowest among the stations for all durations between 10 minutes and 2 hours and are also much lower than the two stations in the city center for higher durations. The spread in the return values among the different stations are considerably larger than the spread due to choice of parameter estimation method (with the exception of the longer durations where the parameter estimation became unstable). The spread is typically 30-40%, but is over 100% for some durations.

Thus, it seems clear that representativeness is a somewhat greater issue than the choice of parameter estimation method and one should therefore be cautious in using the Sandsli data directly to estimate return values for Bergen city center without discussing how representative this station is. This also demonstrates the value of having relatively short time series that one would hesitate to calculate return values from, but which can be very valuable in a discussion of the representativeness of the longer time series.

Summary

100-year return values from 2 minutes to 48 hours duration at four stations close to Bergen have been calculated based on yearly maxima using generalized extreme value distributions with several parameter estimation methods. The main results are:

- The choice of parameter estimation method did not change the 100-year return values for the long time series (Sandsli) more than a few percent. The spread was considerably larger for the short time series and is typically 10-15% for the short durations and more for the longer (6 to 24 hours).
- We have demonstrated how non-stationary estimates can be used for long time series to gain additional information about future changes that can supplement climate factors derived from climate models.
- The spread in return values was found to be greater among the sites than the spread due to parameter estimation method for most durations. Even for the sites having short time series. The spread between sites was typically 30-40%, but over 100% for some durations.
- We emphasize the importance of investigating the representativeness of a selected station when stations relatively far from the area of interest are used and show how relatively short time series are valuable in the discussion of the representativeness for longer time series.

References

Johansen S. (2016): Ekstremverdianalyse av nedbør og oppdatering av intensitet - varighet - frekvenskurver i Bergen Kommune. Master thesis Geophysical Institute, University of Bergen.
<http://bora.uib.no/bitstream/handle/1956/12610/145000819.pdf?sequence=1>

3. Hydrological modelling – Datasets and model development

3.1 A high resolution 3-hourly precipitation and temperature forcing dataset for hydrological models

T. Skaugen^a and A. V. Dyrda^b

^aNorwegian Water Resources and Energy Directorate, Norway

^bNorwegian Meteorological Institute, Norway

Summary

A grid covering all of Norway with a high temporal resolution, 3h, for precipitation and temperature has been developed and used as input to hydrological modelling and precipitation analysis. The grid is basically a disaggregation of the 24h seNorge meteorological grid where the 24h values are disaggregated in time using the sub-daily pattern of precipitation and temperature of the reanalyzed HIRLAM model. When the seNorge 3h grid is used as forcing in hydrological models, there is no drop in performance skill compared against models that are forced by the seNorge24h grid and higher flood peaks are obtained for small catchments. In addition, precipitation values of the 5-year return period estimated from seNorge3h show a similar spatial pattern to that of a stochastic model used for estimating extreme values for all of Norway.

Introduction

The temporal resolution of hydrological modelling has to be, in some way, adjusted to the spatial scale of the catchment to be modelled. The time of concentration (Blöschl and Sivapalan, 1995) is often mentioned as a suitable temporal scale of a catchment, and is defined as “the time it takes water to travel from the hydraulically most distant part of the contributing area to the outlet” (Dingman, 2002, p.401). This definition is problematic for at least two reasons. 1) The timing of response will surely vary given different levels of saturation in the catchment. When the catchment is wet, the response to additional rainfall is quicker than when dry. 2) Is it really water that travels when we register a response, or is the response a manifestation of a wave reaching the outlet and

the wave velocity being a function of saturation? (Beven, 1982). Both these arguments suggest that it is more reasonable to link the term “time of concentration” to individual events rather than to treat it as a characteristic of a catchment. Furthermore, the temporal resolution of hydrological modelling should be as small as possible in order to account for different catchment scales and levels of saturation prior to the event.

Since hydrological rainfall-runoff (RR) models usually are calibrated against observed, historical data, the main obstacle for running RR models at finer temporal resolution has been the availability of suitable historical data on a national scale. This includes runoff, precipitation and temperature. For daily resolution, the operational RR models used in the flood forecasting service of the Norwegian Water Resources and Energy Directorate (NVE) are forced by a meteorological grid (1X1 km²) of precipitation and temperature provided by the Norwegian Meteorological Institute (MET Norway), called seNorge (www.senorge.no). seNorge interpolates data from temperature and precipitation gauges to the grid and has data from 1957 to the present. In addition, meteorological forecasts for 1 to 9 days ahead from MET Norway are produced using the same format. The meteorological station network is far more comprehensive both in time and space for daily- than subdaily observations (i.e. hourly) so the interpolation approach used for daily values is not appropriate for hourly values. Vormoor and Skaugen (2013) addressed this problem by disaggregating the daily seNorge fields of precipitation and temperature by imposing the temporal distribution obtained from 1-h, 10X10 km² fields of hindcast series (NORA10) obtained by the High Resolution Limited Area Model (HIRLAM) downscaling reanalyses data (ERA-40, 1957-2002) and operational European Centre for Medium Range Weather Forecasts (ECMWF) forecasts (2002-2010). The rationale behind such an approach was to accept the daily interpolated values from seNorge as the best possible estimates, but to adopt the temporal distribution as simulated by HIRLAM as reasonable and probable. As a tentative compromise between computational costs and the need for hydrological detail a 3h disaggregation scheme was chosen. This paper briefly reviews the disaggregation method and describes some of the applications of the 3h gridded data set of precipitation and temperature.

Disaggregation method

The method for disaggregation is very simple and intuitive. Since the HIRLAM model is available on a 10 X 10 km² grid these values were downscaled and geospatially adjusted to the Universal Transverse Mercator (UTM) 33 grid which is used by seNorge. From a HIRLAM grid cell the resulting 10 1X1 km² values were assigned equal HIRLAM values.

Temperature disaggregation

One must be aware that the seNorge value for date d, really represent the average temperature/precipitation sum over 0600 UTC the previous day (d-1) to 0600 UTC the current day (d). 3-h values of temperature for the eight time intervals 09, 12, 15, 18, 21, 24, 03, 06 are calculated as follows:

If $9 \leq t \leq 24$

$$T_{3h}(d-1, t) = \frac{\sum_{t-2}^t T_{H1h}(d-1, t)}{3} + \left(T_{24h}(d) - \frac{1}{24} \left(\sum_{09}^{24} T_{H1, d-1}(t) + \sum_{03}^{06} T_{H1h, d}(t) \right) \right)$$

If $03 \leq t \leq 06$

$$T_{3h}(d, t) = \frac{\sum_{t-2}^t T_{H1h}(d, t)}{3} + \left(T_{24h}(d) - \frac{1}{24} \left(\sum_{09}^{24} T_{H1, d-1}(t) + \sum_{03}^{06} T_{H1h, d}(t) \right) \right)$$

where T_{3h} is the disaggregated 3 h temperature, T_{24h} is the seNorge temperature, and T_{H1h} is HIRLAM 1 h temperature. Note that the difference between HIRLAM and seNorge is a constant correction term for the disaggregated values at all time intervals.

Precipitation disaggregation

3-h values of precipitation are computed/estimated by calculating the ratio between HIRLAM precipitation for the current time interval and the precipitation sum for that day. Here we also need to apply the, slightly cumbersome, time-labelling system:

If $9 \leq t \leq 24$

$$P_{3h}(d-1, t) = P_{24h}(d) \times \left(\frac{\sum_{t-2}^t P_{H1h}(d-1, t)}{\sum_{09}^{24} P_{H1h}(d-1, t) + \sum_{03}^{06} P_{H1h}(d, t)} \right)$$

If $03 \leq t \leq 06$

$$P_{3h}(d, t) = P_{24h}(d) \times \left(\frac{\sum_{t-2}^t P_{H1h}(d, t)}{\sum_{09}^{24} P_{H1h}(d-1, t) + \sum_{03}^{06} P_{H1h}(d, t)} \right)$$

where P_{3h} is the disaggregated 3 h precipitation, P_{24h} is the seNorge precipitation, and P_{H1h} is HIRLAM precipitation. In the case where HIRLAM has zero precipitation whereas seNorge has positive precipitation, the seNorge precipitation is distributed uniformly across all time intervals.

Validation of the 3 h meteorological grid

Vormoor and Skaugen (2013) validated the disaggregated grid (seNorge3h) at 5 sites where precipitation and temperature were recorded at a 1 h interval. These values were then aggregated to 3 hours. The meteorological stations were Furuneset and Tromsø, representing a wet, maritime climate, Lillehammer representing a dry inland climate and Blindern and Trondheim representing an intermediate climate.. When comparing time series of HIRLAM and seNorge3h against observed temperature, it was found that seNorge3h had better scores for correlation (r), mean absolute error (MAE) and root mean square error (RMSE) for all stations. For precipitation, seNorge3h had better r for all stations, MAE for 4 stations and RMSE

for 3 stations. When the 10 % highest precipitation values were compared against observed, it was found that seNorge3h had a cumulative distribution function closer to the observed for Lillehammer, Tromsø and Furuneset. For Blindern and Trondheim (of intermediate climate) the performance of seNorge3h and HIRLAM was similar. The Distance Distribution Dynamics (DDD) (Skaugen and Onof, 2014) was calibrated with the 3h data. Figure 1 shows a comparison of the skill score, Nash-Sutcliffe Efficiency criterion (NSE: Nash and Sutcliffe, 1970) for the model calibrated on 24h and 3h meteorological grid. We observe no significant loss in skill using the disaggregated 3h data.

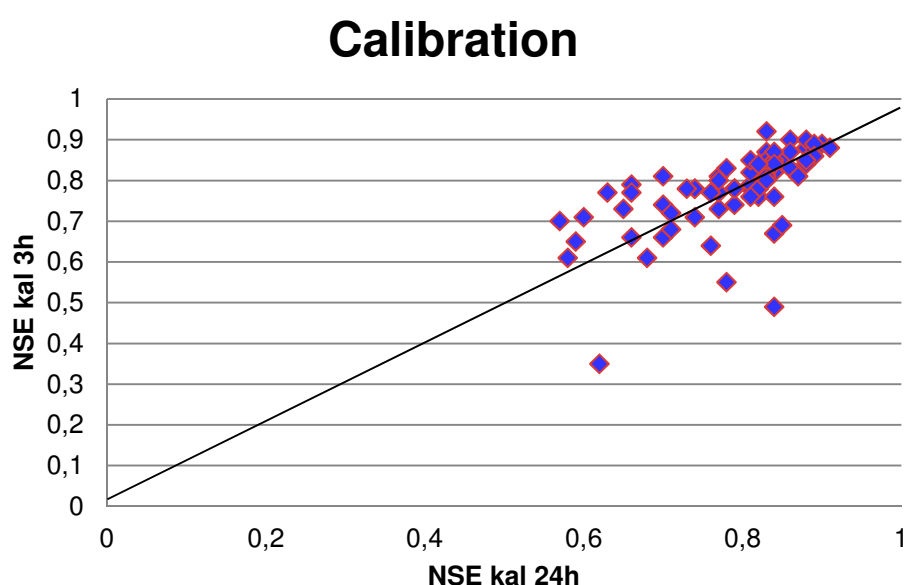


Figure 1. NSE skill score for the DDD model calibrated on 24 h and 3h meteorological grids.

Applications of the 3 h meteorological grid

Runoff simulations

Figure 2 demonstrates the potential benefits of applying finer temporal resolutions, at least for smaller catchments. The figure shows observed runoff at 3h resolution for the Røykenes catchment (50 km²), situated close to Bergen on the west coast of Norway. In addition, we have plotted simulated runoff at 24h and 3h resolution together with lines indicating flood levels for 24h and for culmination (i.e. at the temporal resolution at which the runoff data is collected, usually 1h).

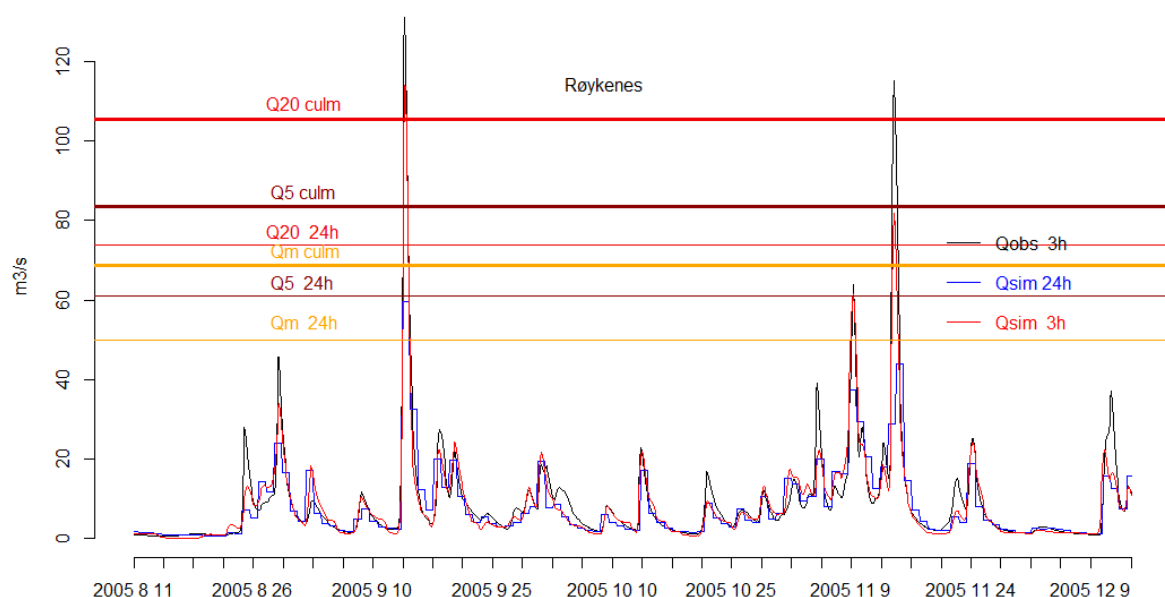


Figure 2. Observed (3h resolution) and simulated (24h and 3h resolution) runoff for the Røykenes catchment (50 km²). The horizontal lines show flood levels for mean annual flood (Qm), the five year flood (Q5) and the twenty year flood (Q20) at 24h resolution and at culmination (usually 1h).

If we look closer at the event in September 2005 we see that, at 24h resolution, the model simulates the Qm, but fails to simulate Q5 and Q20. At 3h resolution, however, the model simulates Q20. This example demonstrates quite clearly that, for small catchments, we face the risk of underestimating extreme events if the temporal scales of the response of the catchment and that of the meteorological input do not match.

Precipitation analysis

As it represents a unique source of spatially continuous information on short duration precipitation, seNorge3h has a range of applications. Summer precipitation from seNorge3h has been used as a reference dataset in the evaluation of EURO-CORDEX (Jacob et al., 2014) regional climate model simulations over Norway in Dyrørdal et al.(2017). Whereas the official meteorological station network only includes 19 stations within the time period of EURO-CORDEX evaluation runs (1989-2008), the seNorge3h gridded dataset enables a spatial evaluation of the simulations.

Recently, sliding 180-minute precipitation design values have been estimated on a similar 1x1 km grid to seNorge3h, based on a Bayesian Hierarchical model described in Dyrørdal et al.(2015) and referred to as the BMA-model. 5-year return levels (M5) from these maps have been compared to M5 estimated from seNorge3h precipitation. Figure 3 of the two M5-maps shows some deviance in values in

Nordland county and mountain regions in the south, but the general spatial distribution is quite similar.

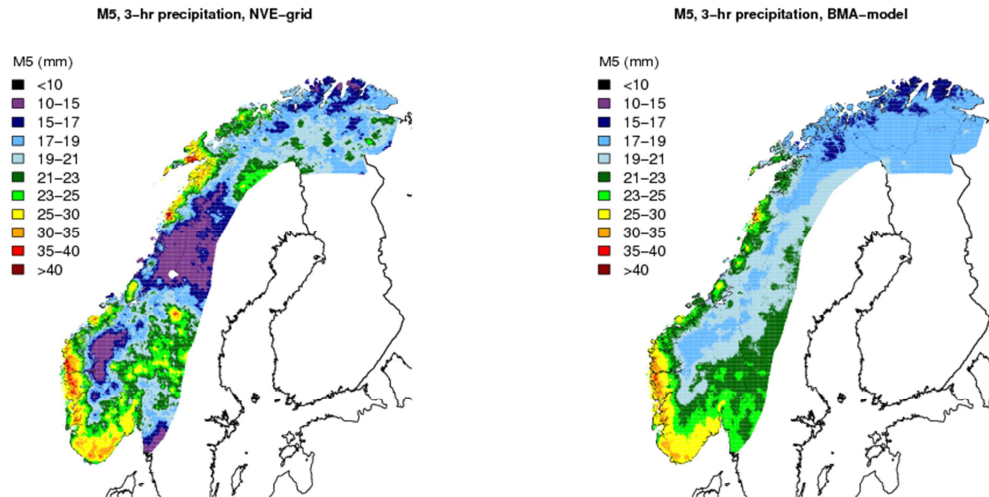


Figure 3. Spatial distribution of M5 for 3-hourly precipitation. seNorge3h (left), BMA-model (right).

References

- Dingman, S. L. (2002): Physical hydrology, Prentice Hall, New Jersey, USA
- Dyrrdal, A.V., Stordal, F., and Lussana, C., 2017: Evaluation of summer precipitation from EURO-CORDEX fine-scale RCM simulations over Norway. *International Journal of Climatology*. DOI: 10.1002/joc.5287.
- Dyrrdal, A.V., Lenkoski, A., Thorarinsdottir, T.L., and Stordal, F., 2015: Bayesian hierarchical modeling of extreme hourly precipitation in Norway. *Environmetrics*, 26(2), 89-106.
- Beven, K.J., 1982. On subsurface stormflow: an analysis of response times. *Hydrol. Sci. J.*, **4**, 505-521.
- Blöschl, G. and M. Sivapalan, (1995): Scale issues in hydrological modelling: a review. *Hydrol. Process.*, 9 (3-4), 251-290.
- Nash, J. E. and Sutcliffe, J.V.(1970). River flow forecasting through conceptual models, Part 1 – a discussion of principles, *J. Hydrol.*, 10, 282-290.
- Skaugen T. and Onof, C.(2014). A rainfall runoff model parameterized from GIS and runoff data. *Hydrol. Process.* 28, 4529-4542, DOI:10.1002/hyp.9968.
- Vormoor K. and T. Skaugen, (2013). Temporal disaggregation of daily temperature and precipitation grid data for Norway. *J. Hydrometeor.*, 14, 989-999, doi: <http://dx.doi.org/10.1175/JHM-D-12-0139.1>.

3.2 The Distance Distribution Dynamics Model- Development for use in ungauged catchments

T. Skaugen

Norwegian Water Resources and Energy Directorate, Norway

Summary

The hydrological rainfall-runoff model, Distance Distribution Dynamics model (DDD) is parsimonious in terms of the number parameters that must be calibrated. The development of the model has been driven by an intention to keep the model parameters as physically meaningful as possible. This has made it possible to estimate DDD's model parameters from catchment information derived from GIS. This paper show the results of prediction in ungauged basins for the current version of DDD where two processes have parameters estimated from observations instead of through calibration. The errors in predicting runoff at ungauged basins to the current DDD model has been reduced by 50% as compared with the previous version and the mean Nash-Sutcliffe efficiency criterion is now at an acceptable level, i.e. NSE=0.7.

Introduction

Hydrological information is needed for solving problems at sites where no one had the foresight or perhaps the resources to set up measurement equipment decades prior to the formulation of the problem. Such problems may involve design of infrastructure, such as bridges and roads, or may involve studies of the interaction between flora/fauna and freshwater (Nilsson et al., 2011). To predict hydrology at such ungauged sites has long been recognised as one of the major challenges in scientific and operational hydrology. The possible benefits of being able to provide hydrological information anywhere are numerous, and have been the motivation for the international initiative launched by the Association of Hydrological Sciences (IAHS) during the decade 2003-2012 for

advancements in the Prediction in Ungauged Basins (PUB) (Sivapalan, 2003; Blöschl et al., 2013; Hrachowitz et al. 2013). Hydrological models have been the usual tool to provide detailed hydrological information at ungauged sites and a fundamental problem has been to regionalise the model parameters. Since many hydrological models rely heavily on calibrated relationships, i.e. with numerous model parameters representing as many processes are calibrated against very little information (usually a time series of observed runoff). Through this calibration process, the model parameters lose their association to the processes they are supposed to represent as

they work together and compensate for errors in data and in model structures to optimize the simulated runoff (Kirchner, 2006). Such a system has a high flexibility and this is why we often find that many different parameter sets may provide equally good fits to the calibration runoff data (the equifinality problem discussed by Beven and Binley, 1992). The objective in ExPrecFlood with respect to PUB has been to provide flood estimates in small, ungauged catchments due to extreme precipitation. In light of the above we have chosen to use a hydrological model which has been developed with the aim minimizing the use of calibration parameters, and to estimate as many model parameters as possible from measureable catchment characteristics (CC's), such as the river network, fractions of wetlands, bare-rock, forest etc. The Distance Distribution Dynamics (DDD) model (Skaugen and Onof, 2014; Skaugen and Mengistu, 2016), relies on a detailed Geographical Information Systems (GIS) analysis of digitized maps for the determination of many of its parameters. Such information, however, is available for almost anywhere, and in Skaugen et al. (2015), the DDD model was used to provide time series of hydrological variables for 145 ungauged nesting sites of the national bird of Norway, the White Throated Dipper. The DDD model was calibrated for 84 gauged catchments and a correlation analysis between model parameters and CC's showed that all model parameters were significantly correlated with CC's. Model parameters for ungauged sites were subsequently estimated using multiple regression with CC's as descriptors. The DDD model has been further developed and in this paper we will discuss how the replacement of free calibration parameters with parameters estimated directly and independently from observed data influences the skill of the DDD model for PUB.

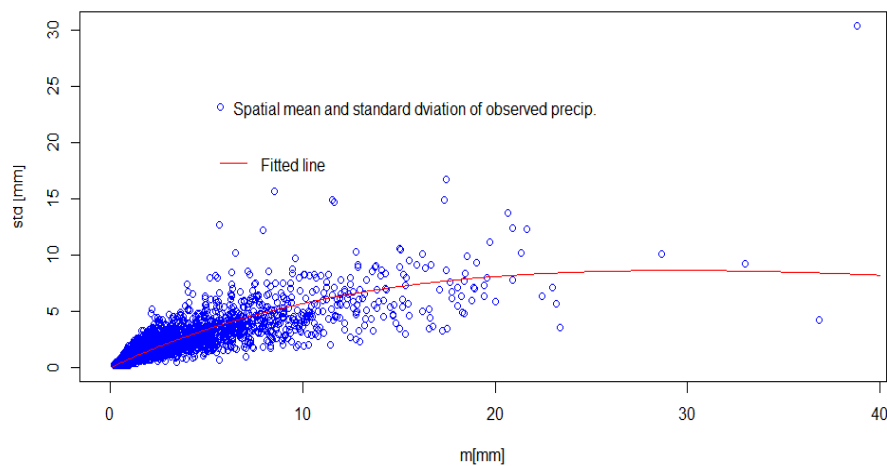


Figure 1: Observed spatial mean and standard deviation of precipitation over an area (blue circles). The red curve is the fitted function describing spatial variability as a function of spatial mean, decorrelation length and shape of the gamma distribution.

Calibrated vs estimated model parameters

Spatial distribution of snow

Catchment-based hydrological rainfall-runoff models, the DDD model included, often use a semi-distributed approach for the surface moisture accounting. Precipitation, snow accumulation and snowmelt are calculated for 10 elevation zones of equal area, whereas evapotranspiration and subsurface moisture is calculated for the catchment as a whole. Within each elevation zone the snow is distributed according to a statistical probability density function (PDF) specified by model parameters. There is a long tradition for using the log-normal distribution for the spatial distribution of snow (Killingtveit and Sælthun, 1996). In the HBV model (Hydrologiska Byråns Vattenbalansmodell: Bergström, 1972), the work-horse of operational hydrology in the Nordic countries, the skewness of the log-normal snow distribution is fixed and calibrated against runoff data. In Skaugen and Weltzien (2016), a gamma distribution was chosen as the model for the spatial PDF of snow. The spatial PDF of the accumulated snow is modelled as a summation of correlated gamma distributed snowfall events with identical parameters estimated from observed spatial variability of precipitation. Figure 1 shows how we can express the spatial variability of precipitation as a function of the spatial mean and the correlation between events. Adding and subtracting gamma distributed unit fields of snowfall and snow melt events provides a dynamical spatial PDF of snow which corresponds to its observed features (Alfnes et al. 2004). Using such a procedure for the spatial distribution of snow has made it possible to discard the calibrated parameter for the PDF of snow and to use instead the parameters estimated directly from observed data.

Groundwater capacity

In the 2015 version of the DDD model, the capacity of the ground water reservoir, M , was a parameter calibrated against runoff data. Skaugen and Mengistu (2016) described a method for estimating M from recession data and an estimate of the mean annual runoff (MAR). The method builds upon quite strong assumptions that the temporal distribution of groundwater fluctuations have a shape which is equivalent to the temporal distribution of the recession characteristic Λ , $\Lambda = \log(Q(t)) - \log(Q(t+1))$. Furthermore, a steady-state approach for the mean annual discharge, will give us an estimate of the mean subsurface storage. With the mean and shape of the distribution of groundwater fluctuations, we can estimate the capacity of the groundwater reservoir as the 99 % quantile of this distribution. This procedure gives us one less parameter to calibrate from runoff data.

Results and discussion: Predicting hydrology at ungauged basins

In this section we compare the PUB results using the DDD version of Skaugen et al. (2015) (DDD2015) with 7 parameters to estimate from regression equations an the DDD-PUB version developed during 2016 (DDD2016) in which 6 parameters are estimated from multiple regression equations based on catchment characteristics. One must recall that the model structures of DDD2015 and DDD2016 are quite different in that two quite influential parameters describing the spatial distribution of snow and the capacity of subsurface storage are not calibrated against runoff but estimated directly from observations. In DDD2016 we, unfortunately, introduced a calibration parameter, *gtcel*, the threshold for subsurface storage at which overland flow is initiated. In later versions of DDD, this threshold is (again) fixed as the 99% quantile of the subsurface storage distribution. The general procedure was to calibrate DDD for a number of catchments (84 for DDD2015) and 111 for DDD2016). A correlation analysis between model parameters and CC's was then performed in order to select promising CC's to use for estimating models parameters at ungauged catchments by multiple regression equations. Subsets of catchments (17 for DDD2015, located in Southern Norway and 25 for DDD2016 located from all over Norway) were used to evaluate the PUB skills of the two models. These subsets were not part of the catchments used for establishing the multiple regression equations needed to estimate the model parameters.

Model param	Mean elev	Mean d	L%	WeL%	EI%	C_len	Forest%	B_R %
Skorr				-0.26			-0.51	0.47
CX		-0.34	0.46		0.47	-0.27		
Cea		-0.43					0.38	-0.42
Gsh	-0.31		0.29		0.49		0.32	-0.38
Gsc		-0.27	-0.42		-0.40			
gtcel		-0.38		0.40			0.48	-0.44

Table 1: Correlation between model parameters and CC's for DDD2015. Only correlations significant at the p-value < 0.01 significance level are included

Model param	Mean elev	Mean d	L%	WeL%	El%	C_len	Forest%	B_R %
Skorr								
CX				-0.30	0.34	-0.35	-0.33	0.35
Cea	-0.45						0.32	-0.38
Gsh	-0.33		0.34		0.51	-0.27	0.41	-0.47
Gsc		-0.35	-0.31		-0.29	-0.34		
M		0.30	0.52		0.41			
CV_Snow				-0.27	-0.29		-0.38	0.40

Table 2: Correlation between model parameters and CC's for DDD2016. Only correlations significant at the p-value < 0.01 significance level are included

Tables 1 and 2 show correlations between model parameters and CC's. The CC's are: mean catchment elevation (Mean elev), mean of distance distribution (Mean d, see Skaugen and Onof, 2014), lake percentage (L%), percentage of wetlands (WeL%), effective lake percentage (EL%), catchment length (C_len), percentage of forest (Forest%) and percentage of bare rock (B_R%). The model parameters are: correction for precipitation as snow (Skorr), temperature-index factor for melting snow as a function of temperature (CX), temperature-index factor for evapotranspiration as a function of temperature (Cea), shape and scale parameters for the distribution of subsurface celerities (Gsh and Gsc), subsurface capacity (M), the coefficient of variation for the spatial distribution of snow (CV_Snow), and the subsurface storage threshold for initiating overland flow (gtcel).

From the tables above we see that all model parameters (except for Skorr in Table 1) are significantly correlated with more than one CC. The correlations are quite moderate and there are no significant differences in correlations between DDD2015 and DDD2016. The clear and significant correlations between model parameters of the DDD and CC's, contrasts with previous published findings of, for example Merz and Blöschl (2004), who found very weak correlations between model parameters of the HBV model and CC's. They further questioned if it was at all possible to find universal relationships between model parameters and CC's. The above results show that it is indeed possible, but it is our belief that the number of free calibration parameters needs to be kept at a minimum so that the limited information available (the CC's) stand a chance of explaining them. The effect of reducing calibration parameters, can further be seen when we run DDD2015 and DDD2016 at a 24 hours temporal resolution for the subsets of catchments with calibrated model parameters (DDD_CAL) and with parameters estimated from the CC's (DDD_PUB).

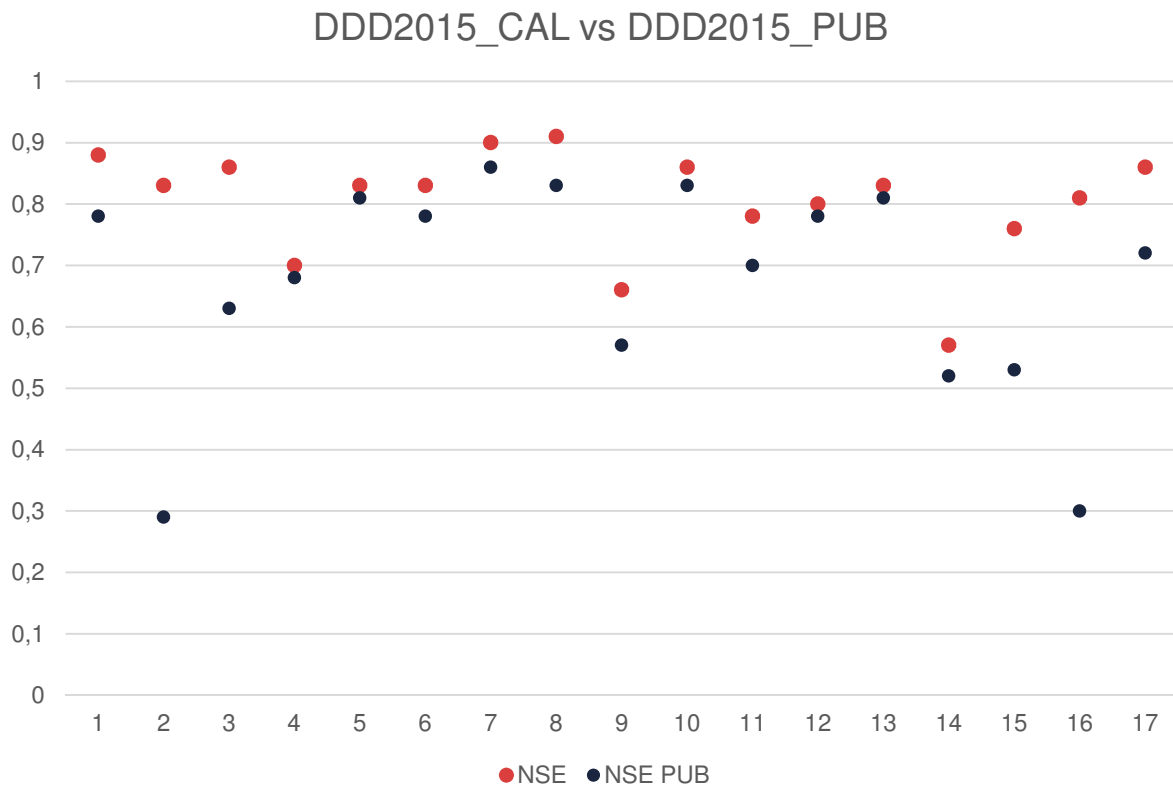


Figure 2 Nash-Sutcliffe (NSE) skill score for 17 catchments. Mean skill score is NSE=0.8 for calibrated DDD2015 (red markers) and mean skill score is NSE = 0.67 for PUB DDD2015 (black markers).

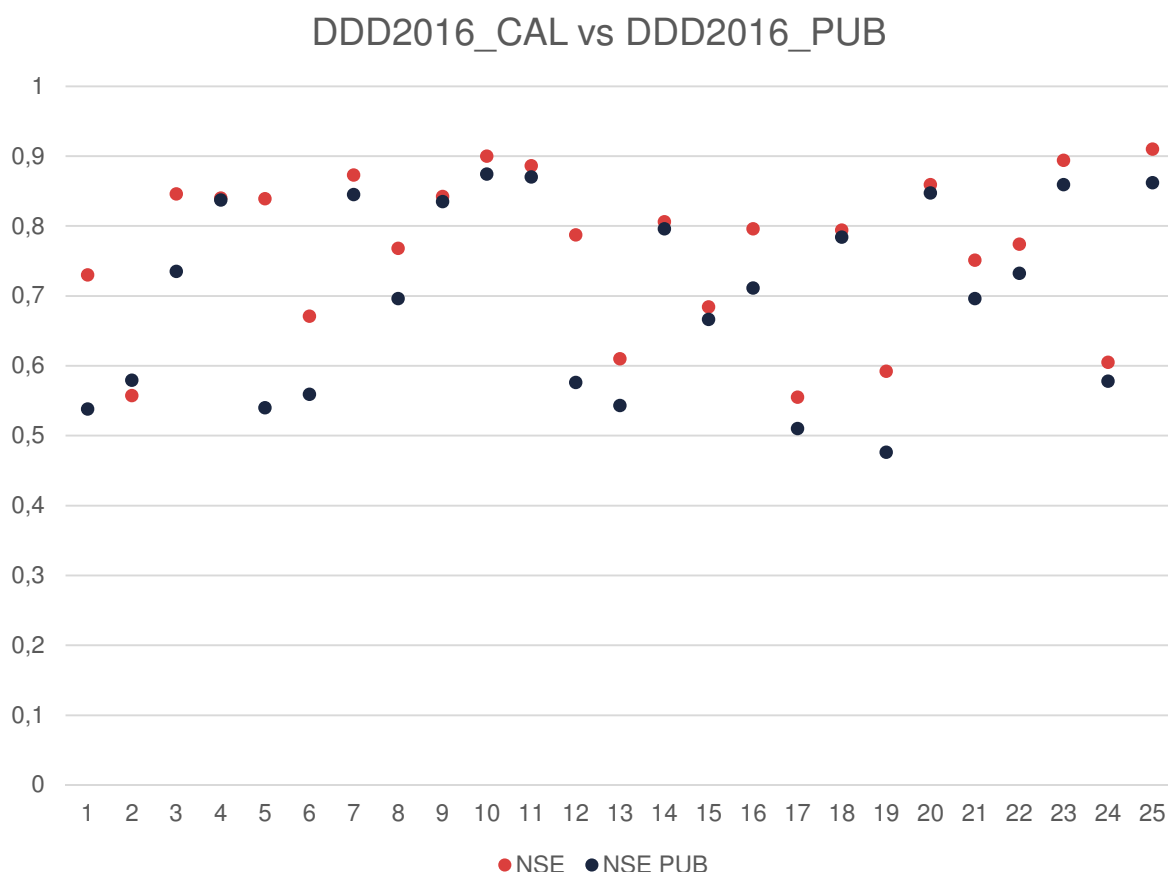


Figure 3 Nash-Sutcliffe (NSE) skill score for 25 catchments. Mean skill score is $NSE=0.77$ for calibrated DDD2016 (red markers) and mean skill score is $NSE = 0.70$ for PUB DDD2016 (black markers).

Figures 2 and 3 show the skill scores (Nash-Sutcliffe efficiency criterion (NSE), Nash and Sutcliffe, 1970) for calibrated and PUB versions of DDD2015 and DDD2016 run for 17 and 25 catchments. The NSE for calibrated versions of DDD2015 and DDD2016 are not directly comparable since the subsets of catchments are different and, in addition, the meteorological forcing (precipitation and temperature) is different. DDD2016 is forced by the new meteorological grid seNorge2 (Lussana et al. 2017) which employs new methods for interpolation as compared to seNorge1.1 (Mohr, 2009) which was used for DDD2015. What we should note here is the difference in NSE between the calibrated and PUB versions for the two generations of DDD. The difference in NSE for DDD2015 between calibrated and PUB version is $\Delta NSE = 0.13$, whereas the difference for DDD2016 is $\Delta NSE = 0.07$. The loss in performance between calibrated and PUB versions is reduced by almost 50% for DDD2016. Since this is not an ideal comparison, given that the sample of catchments and the meteorological forcing are different, we cannot state conclusively that the improved PUB skill of DDD2016 is entirely due to the reduction of calibration parameters. Nevertheless, the results show that improvements have been made in PUB and that the adopted approach of substituting parameters calibrated against runoff with parameters estimated directly from the data they are supposed to

represent is a good way to proceed. Finally, we find, in Figure 4, plots of NSE for DDD2016_CAL and DDD2016_PUB run on a 3 hourly temporal resolution. The average NSE is lower than for 24 hours, which is expected since the meteorological forcing is assumed to be more uncertain. The meteorological forcing is the grid developed from disaggregating 24 hours precipitation and temperature data using the fine temporal resolution of the NORA 10 atmospheric hindcast data (see Vormoor and Skaugen, 2013 and Skaugen and Dyrødal, 2018 (this report)). The difference between _CAL and _PUB versions of DDD is, however of the same order of magnitude as for the 24 hour version, $\Delta NSE = 0.09$.

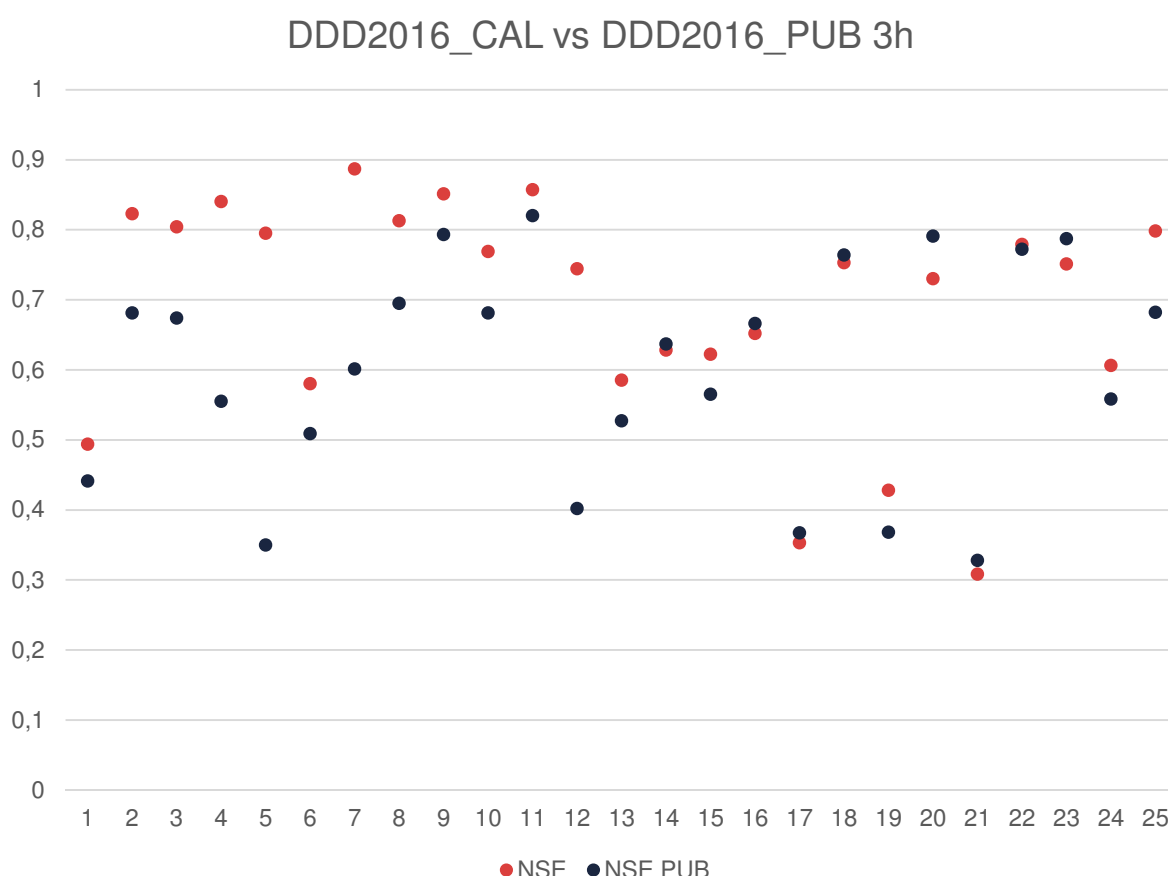


Figure 4. Nash-Sutcliffe (NSE) skill score for 25 catchments, 3 hourly forcing data. Mean skill score is $NSE=0.69$ for calibrated DDD2016 (red markers) and mean skill score is $NSE = 0.60$ for PUB DDD2016 (black markers).

Outlook

The full potential for substituting calibrated relationships for more physically based algorithms with parameters estimated from relevant data has not been realised. For example, we have already tested an energy balance approach for snowmelt implemented into DDD which gives quite reasonable and robust results (Skaugen et al, 2017). We use proxy-models for estimating the different energy balance elements so that the only forcing necessary is precipitation and temperature. A similar

approach will be considered for estimating evapotranspiration. The implementation of these algorithms will further reduce the dependence on calibration and possibly improve predictions in ungauged basins.

References

- Alfnes, E., Andreassen, L.M., Engeset, R.V., Skaugen, T. and Udnæs, H-C.(2004). Temporal variability in snow distribution. *Ann. Glaciol.* 38, p. 101-105.
- Bergström, S.(1992). The HBV model – its structure and applications. SMHI Reports Hydrology No. 4, Swedish Meteorological and Hydrological Institute, Norrköping, Sweden.
- Beven, K.J. and Binley, A., 1992. The future of distributed models: model calibration and uncertainty prediction. *Hydrological Processes*. 6, 279-298.
- Blöschl, G., M. Sivapalan, T. Wagener, A. Viglione and H. Savenije, (2013). Eds.in: *Runoff Prediction in Ungauged Basins- Synthesis across Processes, Places and Scales*, Cambridge University Press, New York.
- Hrachowitz, M., Savenije, H.H.G., Blöschl, G., McDonnell, J.J., Sivapalan, M., Pomeroy, J.W., Arheimer, B., Blume, T., Clark, M.P., Ehret, U., Fenicia, F., Freer, J.E., Gelfan, A., Gupta, H.V., Hughes, D.A., Hut, R.W., Montanari, A., Pande, S., Tetzlaff, D., Troch, P.A., Uhlenbrook, S., Wagener, T., Winsemius, H.C., Woods, R.A., Zehe, E., and Cudennec, C., (2013). A decade of Predictions in Ungauged Basins (PUB)—a review. *Hydrological Sciences Journal*, 58 (6), 1–58, doi: 10.1080/02626667.2013.803183.
- Killingtveit, Å. and Sælthun, N-R.(1995). *Hydrology*, (Volume No. 7 in *Hydropower development*). NIT, Trondheim, Norway.
- Kirchner J.W., (2006). Getting the right answers for the right reasons: Linking measurements, analyses and models to advance the science of hydrology. *Water Resour. Res.*, 42, W03S04, doi:10.1029/2005WR004362.
- Lussana, C., Saloranta, T., Skaugen, T., Magnusson, J., Tveito, O. E., and Andersen, J.(2017). Evaluation of seNorge2, a conventional climatological datasets for snow- and hydrological modeling in Norway, *Earth System Science Data Discussions*, 2017, 1–40, <https://doi.org/10.5194/essd-2017-64>, <https://www.earth-syst-sci-data-discuss.net/essd-2017-64/>.
- Merz, R.and G. Blöschl, (2004). Regionalisation of catchment model parameters. *J. Hydrol.*, 287, 95–123.
- Nash, J. E. and Sutcliffe, J.V.(1970). River flow forecasting through conceptual models, Part 1 – a discussion of principles, *J. Hydrol.*, 10, 282–290.
- Nilsson, A.L.K., E. Knudsen, K. Jerstad. O.W. Røstad, B. Walseng, T. Slagsvold and N.C. Stenseth (2011). Climate effects on population fluctuations of the white throated dipper *Cinclus cinclus*. *Journal of Animal Ecology*, 80, 235-243.
- Sivapalan, M., (2003) Prediction in ungauged basins: a grand challenge for theoretical hydrology. *Hydrol. Process.* 17, 3163-3170.
- Skaugen T. and Onof, C.(2014). A rainfall runoff model parameterized from GIS and runoff data. *Hydrol. Process.* 28, 4529-4542,D0I:10.1002/hyp.9968.
- Skaugen, T. and Z. Mengistu, (2016). Estimating catchment scale groundwater dynamics from recession analysis- enhanced constraining of hydrological models. *Hydrol. Earth. Syst. Sci.* 20, 4963-4981, doi: 10.5194/hess-20-4963-2016.
- Skaugen, T. and I.H. Weltzien, (2016). A model for the spatial distribution of snow water equivalent parameterised from the spatial variability of precipitation, *The Cryosphere*. 10, 1947-1963, doi:10.5194/tc-10_1947_2016.
- Skaugen, T., H. Luijting, T. Saloranta, D. V-Schuler and K. Müller (2018). In search of operational snow models for the future- comparing four snow models for 17 catchments in Norway. In review.
- Skaugen, T., I. O. Peerebom and A. Nilsson, (2015). Use of a parsimonious rainfall-runoff model for predicting hydrological response in ungauged basins. *Hydrol. Process.* 29, 1999-2013, DOI:10.1002/hyp.10315.
- Vormoor K. and T. Skaugen, (2013). Temporal disaggregation of daily temperature and precipitation grid data for Norway. *J.Hydrometeor*, 14, 989-999, doi: <http://dx.doi.org/10.1175/JHM-D-12-0139.1>

4. Future changes in short-term extreme precipitation and flooding

Projected changes in future short-duration extreme precipitation events using EURO-CORDEX simulations: Stationary and non-stationary analysis

S. Mayer^a, A.V. Dyrørdal^b and R.G. Skaland^b

^aUni Research AS, Climate and Bjerknes Centre for Climate Research, Norway

^bNorwegian Meteorological Institute, Norway

Summary

Future sub-daily extreme precipitation is projected to increase for most areas in Norway.

Here we study this change according to the EURO-CORDEX ensemble by fitting the GEV distribution to annual maximum precipitation from the simulations. Both stationary and non-stationary methods have been used. The results are little sensitive to the chosen methods.

Under the high emission scenario RCP8.5 climate factors range between 1.2 and 1.6. Climate factors increase with return period and shorter precipitation duration.

Introduction

Precipitation with extreme intensities is a potential hazard to infrastructure, such as roads, railways, and sewage systems. Especially convectively driven extreme precipitation - typically occurring within thunderstorms, heavy showers and cold fronts, passing within a few hours over a limited area - can cause damages to infrastructure or shorten its lifetime. Due to anthropogenically induced greenhouse gas (GHG) emissions into the atmosphere, the global mean temperature will increase by a few degrees Celsius depending on the GHG emission trajectory. In a warmer climate, it is likely that extreme

precipitation events will increase due to increases in the atmosphere's capacity to hold more water vapor.

Return value estimates, computed from extreme value theory (see article 2.1 and 2.4, this report) are usually applied for planning and design of infrastructure. In Norway, the majority of precipitation measurements show an increase in intense rainfall on a daily and sub-daily timescale (article 1.1, this report). However, today's return value estimates of extreme precipitation are calculated assuming stationarity, i.e. no temporal change in the statistics of extreme precipitation. Here, we test the sensitivity of return value estimates to stationarity and non-stationarity, i.e. statistics of extreme precipitation is changing with time. We analyze precipitation data available from regional climate model projections (see Data) to assess future changes of extreme precipitation in intensity, trend, return value and finally calculate

climate factors, both by stationary and non-stationary estimation methods. Climate factors, also sometimes called safety factors, are defined as the factor current design values to multiply with in order to get an estimate of future design values (Paus et al., 2015).

Data

Within the World Climate Research Program-initiative Euro-CORDEX high-resolution projections simulated with regional climate models (RCM) on a horizontal grid scale of $\sim 12 \times 12$ km (Jacob et al. 2014) are made available at <https://esg-dn1.nsc.liu.se/projects/esgf-liu/>.

An overview of currently available projections at different temporal resolutions for the emission scenario RCP8.5 is provided in Table 1. We have accumulated the 3-hour simulations to 6 and 12-hours, for the purpose of computing climate factors also for those durations. The Euro-CORDEX data set comprises the years 1971 until at least 2099, some simulations also include year 2100. The historical period 1971-2005 is run with observed GHG concentrations, while the future period 2006-2099/2100, is run under the assumption of the high GHG emission scenario, RCP8.5.

<i>GCM/ RCM</i>	CERFACS- CNRM- CM5 (r1i1p1)	ICHEC- EC- EARTH (r1i1p1, r12i1p1)	IPSL- CM5A- MR (r1i1p1)	MOHC- HadGEM2- ES (r1i1p1)	MPI- ESM-LR (r1i1p1)
RCA4	24, 3, 1	24, 3, 1	24, 3, 1	24, 3, 1	24, 3, 1
CCLM4-8- 17	24, 1	24, 1		24, 3, 1	24, 1
RACMO22E		24, 3, 1,1		24, 3, 1	

Table 1: Overview of dynamically downscaled GCM-RCM data (day-pr: 24, 3hr-pr: 3, 1hr-pr: 1) retrieved from the high-resolution Euro-CORDEX data set.

This data set enables the analysis of a relatively long time series of 129 years covering the European continent. Sub-daily precipitation has been processed from each RCM simulation to obtain time series of annual maxima precipitation intensities for Norway. Figure 1a) shows an example of projected annual block maxima and corresponding trends. 2-, 10-, 25-, 50- and 100-year effective return levels are shown as a linear function of time in Fig. 1b). It can be seen that today's return levels

increase linearly by approximately 2 mm under the RCP8.5 scenario until the end of this century.

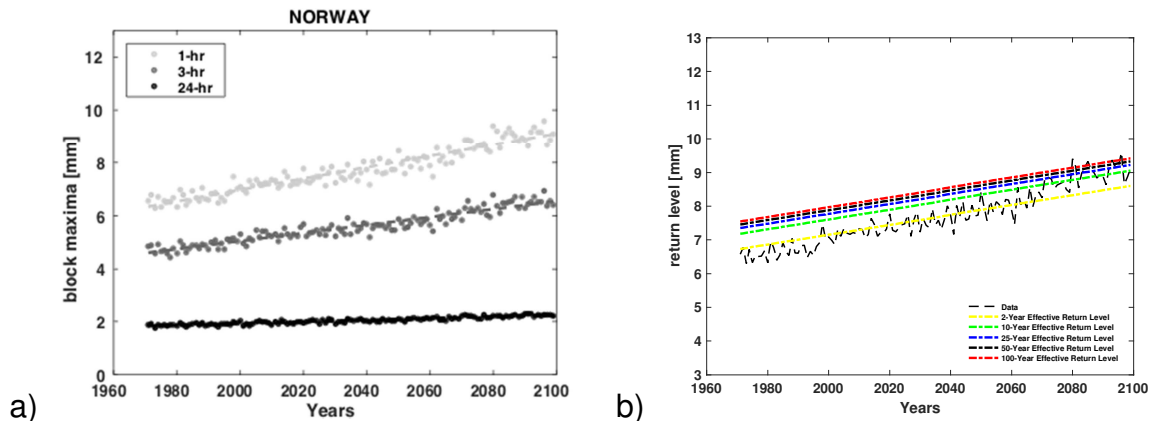


Figure 1: a) Projected annual block maxima values [mm] of 1-hr, 3-hr and 24-hr precipitation in Norway; b) effective return levels for 1-hr precipitation.

Extreme value analysis

To estimate extreme precipitation, we fit the three-parameter Generalized Extreme Value (GEV) distribution to annual maxima (e.g. Coles, 2001). The parameters location, scale and shape, can be estimated through a variety of methods, introduced in article 2.1 (this report), Estimation of return levels/precipitation design values at single sites in Norway. The location parameters can be estimated as a constant (stationary method) or it can be allowed to change linearly with time (non-stationary method). First, we applied the non-stationary extreme value analysis tool, NEVA, introduced by (Cheng et al. 2014), to detect any trend in the data. This MATLAB[®] code can be freely downloaded at <http://amir.eng.uci.edu/neva.php>. The software tests the data set for significant trends by applying the Mann-Kendall trend test (Mann, 1945) at a 0.05 level of significance. The non-stationary method is applied only if a significant positive trend is detected. For estimating the GEV parameters, the priors for the Bayesian method are constrained by a maximum likelihood estimation (MLE) performed for the 19 counties within Norway. As a result, the range of the scale parameter is set from 0 to 5, and the range of the shape parameter is set from -0.5 to 0.4, as suggested by Martins and Stedinger (2000). The other priors are left default. The statistical model parameters are set to 5000 number of random samples for parameter estimation, and 3000 of burned samples in 5 chains. Return levels of the maximum precipitation within each Norwegian county have been calculated. As an example, Fig. 2 shows return levels for the county of Vestfold in Southern Norway. For the non-stationary calculated return levels (Fig. 2a and 2b), the location parameter from the middle of the timeseries, i.e. year 2036 has been chosen. The resulting return level curves show very similar behavior for the four methods, i.e. the results are not very sensitive to the chosen parameter estimation method. However, it

is noteworthy that the confidence intervals become slightly broader taking non-stationarity into account.

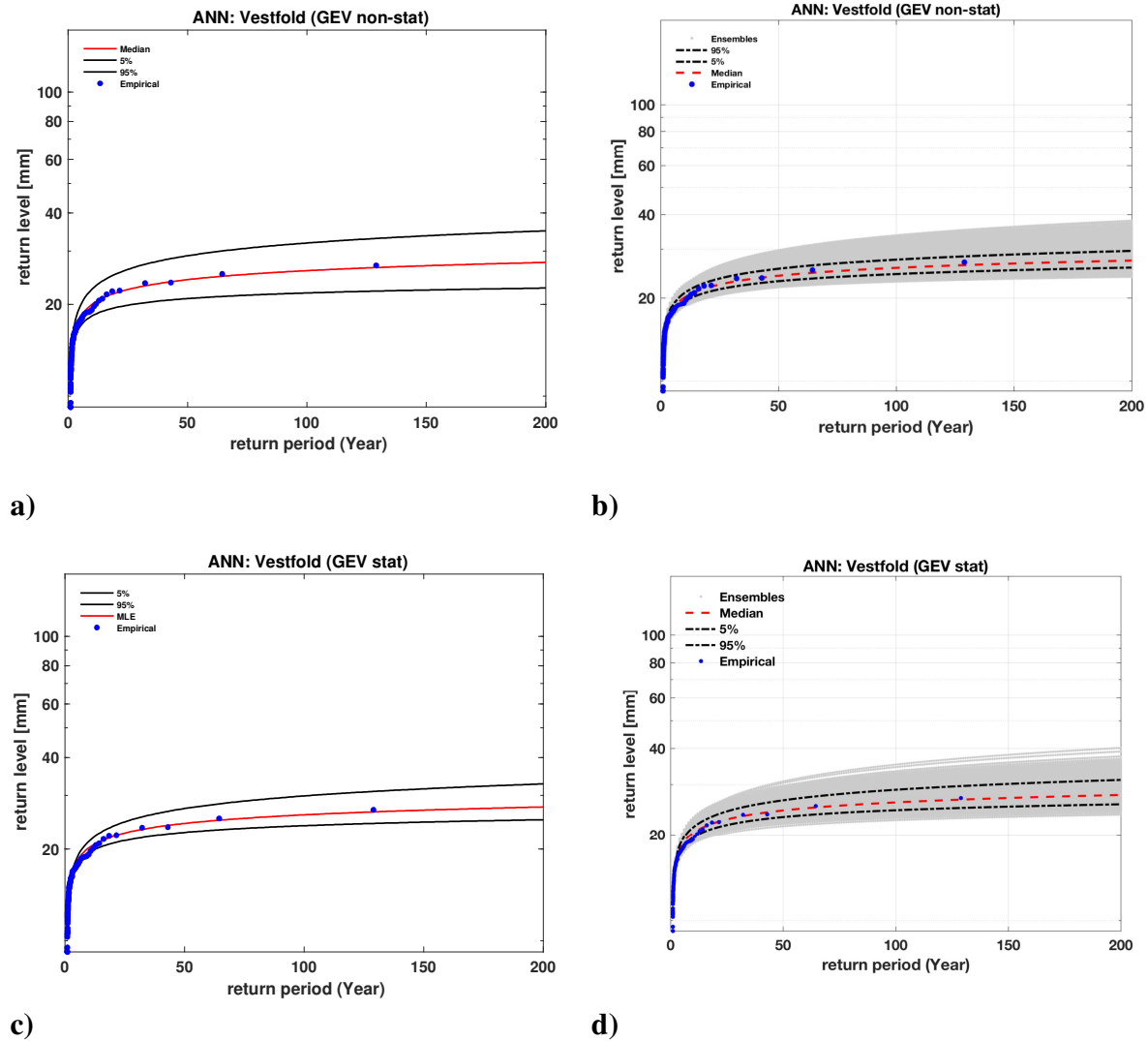


Figure 2: a)-d) return values as a function of return period; black lines indicate the 5th and 95th confidence bounds; red line: median; blue dots: annual block maxima data. a) method: maximum likelihood non-stationary; b) method: Bayesian non-stationary; c) method: maximum likelihood stationary; d) method: Bayesian stationary.

Climate factors

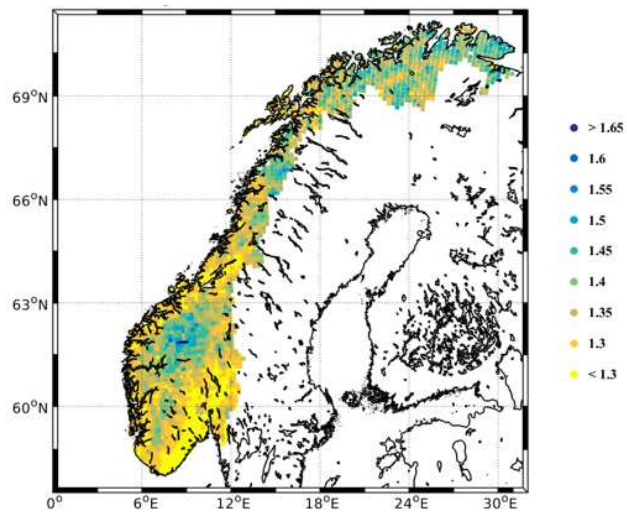
Climate factor maps are calculated by using time slices of 30 years. For the historical period the years 1971-2000 are considered, while for the future period the years 2070-2099/2100 are used. Since the time slices are rather short, we apply only the *stationary* method. We fit the GEV distribution to annual maxima using both the Bayesian and the MLE approach to estimate the GEV parameters and compute return levels for different return periods on each RCM simulation. Finally, we computed mean values from the RCM ensemble. Note that, as the GEV shape

parameter is especially hard to estimate and may become unstable for short time series, the MLE approach includes a beta prior on this parameter as suggested in Martins and Stedinger (2000).

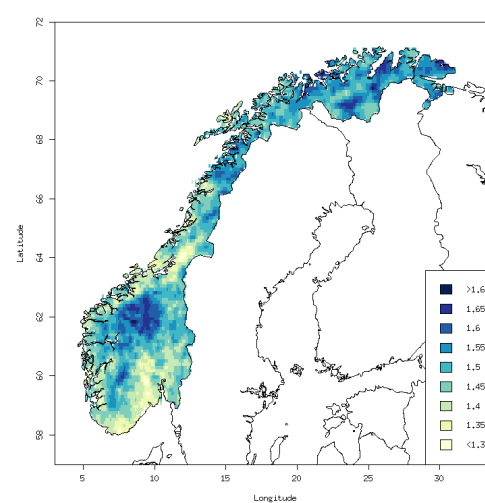
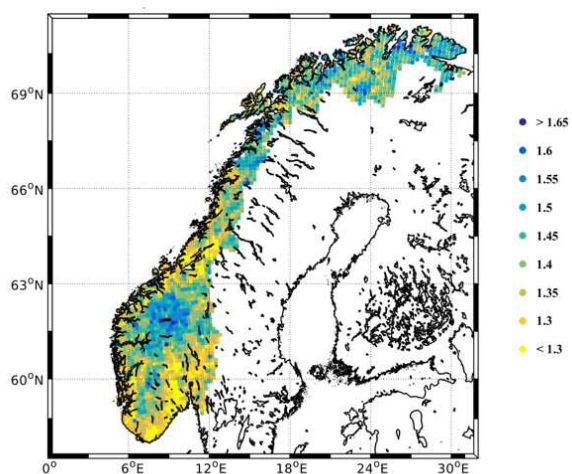
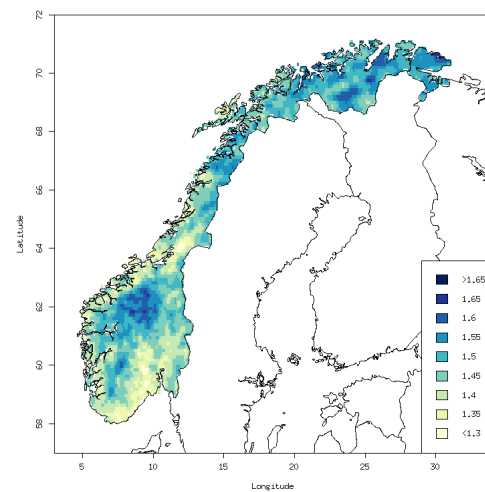
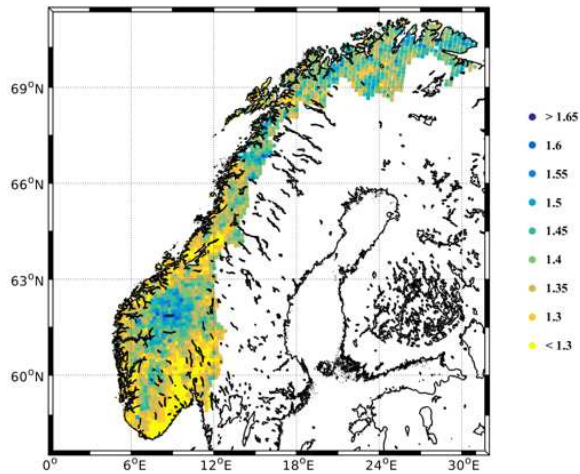
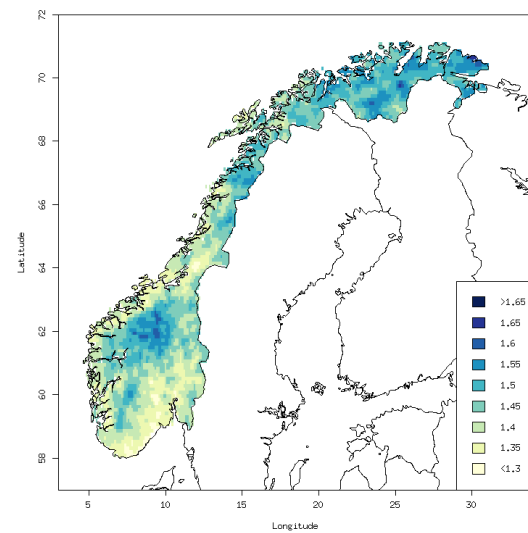
The climate factor, CF, is then defined as the ratio of the mean future return levels, RL, relative to the mean historical return levels: $CF = RL_{\text{future}} / RL_{\text{historical}}$ (e.g. Paus et al., 2015). This calculation is performed for each grid box over Norway and the ensemble mean is shown in Fig. 4 for the return periods of 5-, 10-, 20-, 50-, 100- and 200-years for the precipitation duration of 1-hour. Climate factors calculated with the stationary Bayesian approach are shown in the left column, and climate factors calculated with the MLE method are shown in the right column. Both methods show very similar climate factors for all return periods, both in terms of magnitudes and spatial distribution. The highest climate factors are found in the mountainous region northeast of Sognefjorden and in Finnmark (relatively dry areas). Regions with climate factors > 1.5 expand with longer return periods. In general, the climate factors increase with return period, i.e. return levels of very rare events (e.g. 200-year event) will increase more than rare events (e.g. 2-year event). In Table 2 we summarize spatially averaged climate factors for different durations (hourly to daily). Climate factors for short durations tend to be higher than climate factors for longer durations, indicating that the more intense rainfall will increase the most. This can be expressed in an exponential relationship shown in Fig. 5.

Climatic changes in short duration extremes - implications for design values

Baysian method (stationary):



MLE method (stationary):



Climatic changes in short duration extremes - implications for design values

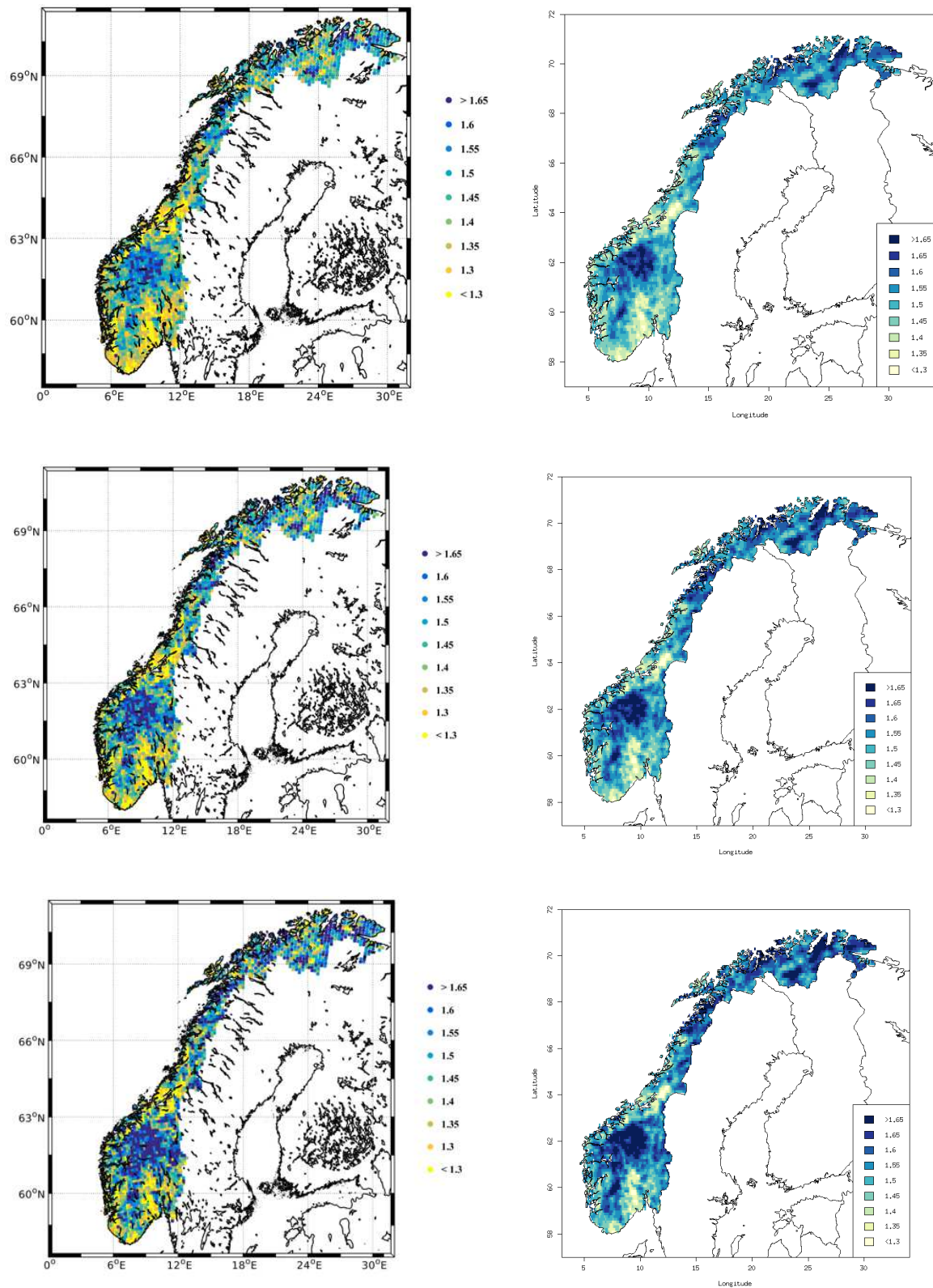


Figure 4: Climate factors under the emission scenario RCP8.5 for 1hr-pr and the 5-year, 10-year, 20-year, 50-year, 100-year, and 200-year return periods. Left: Bayesian method. Right: MLE.

	5-year	10-year	20-year	50-year	100-year	200-year
1hr-pr	1.37 (B) 1.42 (M)	1.39 (B) 1.44 (M)	1.41 (B) 1.46 (M)	1.44 (B) 1.49 (M)	1.47 (B) 1.51 (M)	1.50 (B) 1.54 (M)
3hr-pr	1.35 (B) 1.35 (M)	1.37 (B) 1.36 (M)	1.38 (B) 1.38 (M)	1.41 (B) 1.40 (M)	1.43 (B) 1.41 (M)	1.45 (B) 1.43 (M)
6hr-pr	1.31 (M)	1.32 (M)	1.34 (M)	1.35 (M)	1.37 (M)	1.39 (M)
12hr-pr	1.28 (M)	1.29 (M)	1.30 (M)	1.31 (M)	1.32 (M)	1.34 (M)
24hr-pr	1.24 (B) 1.26 (M)	1.25 (B) 1.27 (M)	1.26 (B) 1.27 (M)	1.28 (B) 1.28 (M)	1.30 (B) 1.29 (M)	1.32 (B) 1.30 (M)

Table 2: Climate factors of extreme precipitation for Norway for different durations (1- to 24-hours) and different return periods (5 to 200-years). B: Bayesian stationary method; M: maximum likelihood estimation.

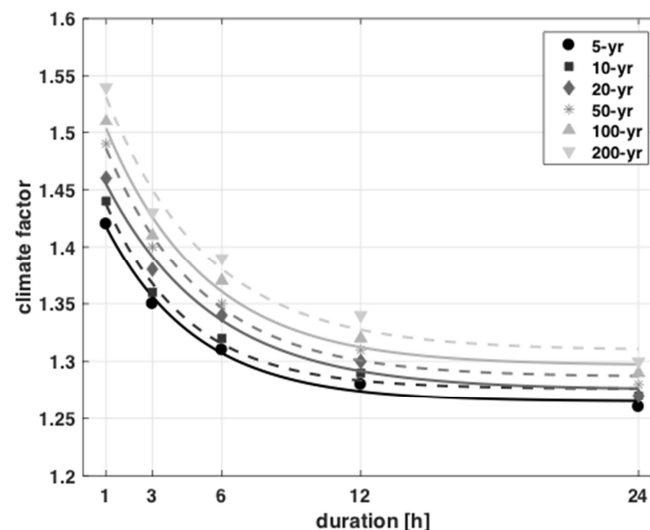


Figure 5: Climate factors for different return periods (5- to 200-years) shown as an exponential function of rainfall duration (h).

Conclusions

We have used the high-resolution Euro-CORDEX dataset to estimate changes in future short-duration extreme precipitation under the high emission scenario RCP8.5. We have tested the MLE and Bayesian method on annual maxima precipitation time series under the stationary and non-stationary assumption. We find the estimated return values little sensitive to the chosen method, although the data shows an increase in extreme precipitation. However, the projected positive trends are much weaker than the observed trends. For example, at the MET station Oslo-Blindern, an increase of 10 mm from 1968 until 2017 has been observed (article 1.1, this report). The RCM projections show only an increase of 2 mm in Oslo until the end of the century.

Climate model projections are afflicted with uncertainties that can be attributed to the choice of the GHG scenario, and model uncertainties origin from model imperfectness. This can be partly accounted for by using an ensemble of projections and is often shown as model spread, e.g. shown in Hanssen-Bauer, et al. 2015. Compared to Hanssen-Bauer, et al. (2015) we find slightly higher climate factors due to the fact that the ensemble of climate models has grown over the last three years. Note also, with the calculation of return levels we introduce an additional uncertainty accompanied with the GEV model. In this study, we find that return levels are not very sensitive to the chosen method, but uncertainties (shown as confidence bounds in Fig. 2) increase to some extent, when we account for the non-stationary behavior in the time series.

The change of the magnitude of extreme precipitation can be expressed as climate factors. For Norway, we find climate factors ranging between 1.2 and 1.6 depending on duration and magnitude which can be expressed as exponential functions of the duration (see Fig. 5).

References

- Cheng, L. Y., et al. (2014). "Non-stationary extreme value analysis in a changing climate." *Climatic change* **127**(2): 353-369.
- Coles S. G. (2001). *An Introduction to Statistical Modeling of Extreme Values*, Springer Series in Statistics: Springer-Verlag London.
- Hanssen-Bauer, I., et al. (2015). "Klima i Norge 2100 Kunnskapsgrunnlag for klimatilpasning oppdatert i 2015." NCCS report, NCCS, Oslo, Norway: 203.
- Jacob, D., et al. (2014). "EURO-CORDEX: new high-resolution climate change projections for European impact research." *Regional environmental change* **14**(2): 563-578.
- Martins, E.S. and J.R. Stedinger (2000). "Generalized maximum-likelihood generalized extreme-value quantile estimators for hydrologic data." *Water Resources Research* **36**(3): 737-744.
- Paus, K., E.J. Førland, A. Fleig, O Lindholm og SO Åstebøl (2015). *Metoder for beregning av klimafaktorer for fremtidig nedbørintensitet*. Miljødirektoratet, Rapport M-292/2015

4.2 Sensitivity of historical extreme precipitation events to a temperature change

A. Sorteberg and M. I. Sandvik

Geophysical Institute and Bjernes Center for Climate Research, University of Bergen, Norway

Summary

We present a method for perturbing historical extreme precipitation events to see the isolated effect of a warmer atmosphere on extreme precipitation.

Using a set of orographically enhanced extreme events we found the change in daily extreme precipitation to be on average around 5% per degree warming with a distinct geographical pattern. The most extreme hours within the extreme days changed on average with around +7% per degree. As these were autumn and winter extremes there was a large increase in rainfall (over 20% per degree) on the expense of snowfall.

Introduction

Estimating future changes in precipitation is complicated due to the variety of processes with different spatial and temporal scales that might affect the precipitation. In general, precipitation is formed due to cooling of humid air until saturation is reached and subsequent microphysical processes generating raindrops/snow crystals large enough that they fall under gravity.

Thus, any process that can alter the amount of water the atmosphere can hold before saturation, the rate of cooling or the efficiency of the microphysical processes can affect precipitation. Figure 1 lists some of

the most important processes ranging from large scale changes in planetary and synoptic flows to small scale changes in the cloud microphysics.

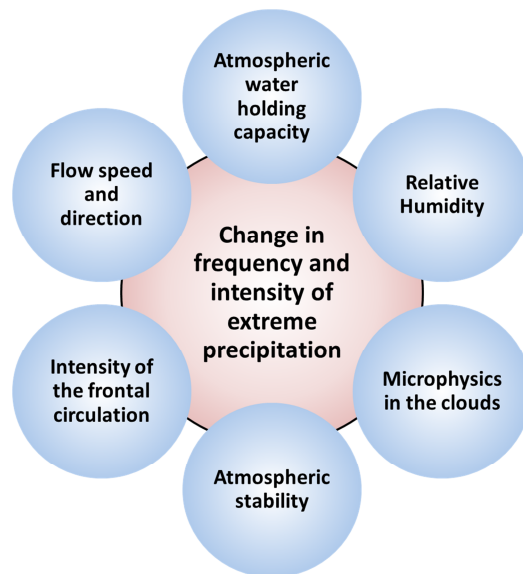


Figure 1: Factors potential influencing local changes in the frequency and intensity of extreme precipitation

Method

It is still very uncertain as to what extent and how some of the processes outlined in Figure 1 may change in a changing climate. In this paper we report some simplified simulations that have been set up under the following assumptions:

- The large scale flow is not changing,
- The temperature of the atmosphere and ocean/land surface is uniformly changed (and therefore the water holding capacity of the atmosphere).
- The relative humidity (% of water holding capacity) is not changed.
- Since the water holding capacity will change, but not the relative humidity the amount of water in the atmosphere will change according to Clausius-Clapeyrons equation with approximately 7-8% increase in water per degree warming

Such a setup will provide useful information about how an historical extreme event may look in a warming climate if the large scale flow is exactly the same as in the historic event (i.e. exactly the same strength, positioning etc. of the low-pressure centers, the fronts etc.). In such a scenario the warmer atmosphere will contain more water and have the potential for increased condensation and rainfall.

The model used is the Advanced Research WRF (ARW) model (version WRF3.6.1). WRF is a fully compressible non-hydrostatic model, with a terrain-following hydrostatic pressure vertical coordinate system. The model domain covers southern Norway, parts of the United Kingdom, Sweden and Denmark as well as the Norwegian Sea, North Sea and Skagerrak with a 2×2 km horizontal resolution. The high resolution enables explicit calculation of convection. This is in contrast to regional climate models which due to coarser resolution have to parameterize this

important process. Details of the model and experiment setup can be found in Sandvik et al., 2017.

We consider 11 historical extreme precipitation events along the west coast of Norway (Table 1) and look at how a uniform +2C warming will influence the precipitation in these events given that the atmospheric flow is not changing. All values are averages over the shaded area in Figure 2 and the events are the 11 most extreme precipitation events since 1990 (extreme based on 1-day accumulated precipitation). Due to a lack of high quality boundary data for the modelling prior to 1990 we discarded earlier events.

Dates (dd.mm.yyyy) and maximum observed precipitation (mm)					
05.03.1990	11.01.1992	19.10.1995	27.10.1995	02.03.1997	04.02.1999
109.4	206.0	121.2	184.6	175.0	140.6
29.11.1999	15.11.2004	14.09.2005	15.11.2005	12.012.009	
135.8	195.0	179.5	223.0	123.5	

Table 1: Dates (dd.mm.yyyy) and maximum observed 24h precipitation accumulated from 06 UTC-06UTC (mm) for the events investigated. Dates are the dates at the end of the accumulation period.

The events and quality of the simulations are discussed in detail in Sandvik et al. (2017) and put in a longer time perspective in Azad and Sorteberg (2017). All events are characterized by an incoming front and a strong westerly/south-westerly flow hitting the west coast mountains which produces an additional lift and a strong orographic enhancement of the precipitation (Figure 2).

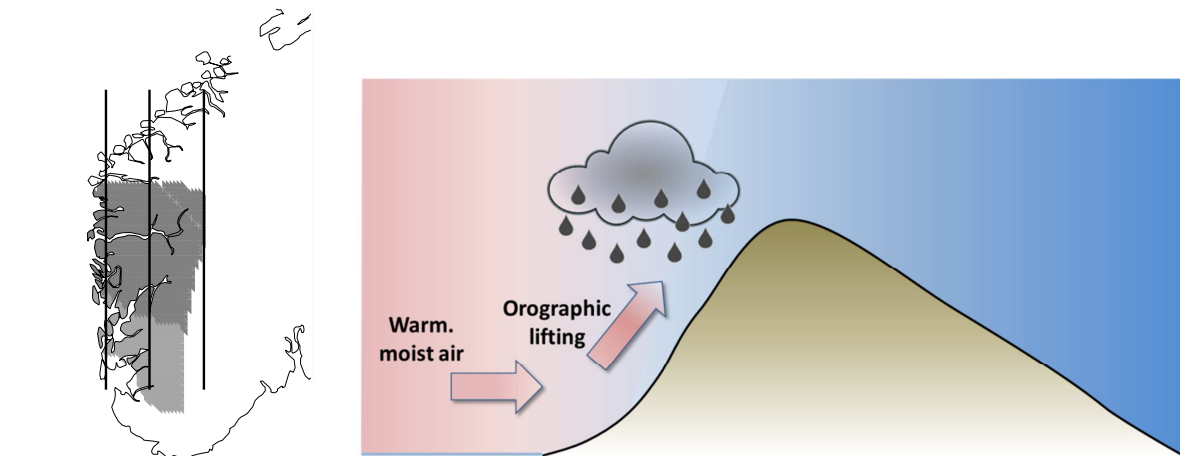


Figure 2: Right: The shaded area (spanning the two of the precipitation regions in Norway outlined in Hanssen-Bauer et al. (2015) is the area analyzed in this report. Left: Schematic drawing showing the typical situation analyzed with an incoming front bringing in moist, warm air and the forced orographic lifting enhancing the frontal precipitation.

Sensitivity of the historic events to a warming

The regionally averaged sensitivity

If we think of this system as more or less isolated air parcels that get lifted and cooled with immediate fallout of the condensed water when it passes the mountains we can get some simple theoretical estimates as to what will happen. The first and simplest idea is that if nothing else happens, the increase in water holding capacity with 7-8%/K will increase the condensation which will translate into a 7-8%/K increase in precipitation. If we take into account that the increase in condensation will warm the air parcel (condensation is a process that releases heat) the cooling will be reduced as the air parcel is lifted and the condensation increase will be less than 7-8%/K. If the air parcel is totally isolated from the surrounding air it can easily be shown that the condensation will increase with around 5%/K. Thus we expect the overall result to be somewhere between a +5 and +8% increase in precipitation per degree warming if the simulations do not produce changes in the small scale flow or the effectiveness of the cloud microphysics. Figure 3 shows that the average change in precipitation was 5.2%/K. This is close to the simple estimates assuming air parcels totally isolated from the surrounding air. This strongly suggest that on the larger spatial scales the change in extreme precipitation for orographically enhanced events due to climate change can be approximated with the simple theory of closed air parcels if the large scale flow does not change.

As all the extreme events on the west coast are autumn and winter events the warming gave a pronounced increase in rainfall at the expense of snowfall. The relative change in rainfall was on average +21.1%/K, which was partly compensated by a reduction in snowfall of -29.7%/K. This change in precipitation type may have a pronounced effect on the hydrology of these events.

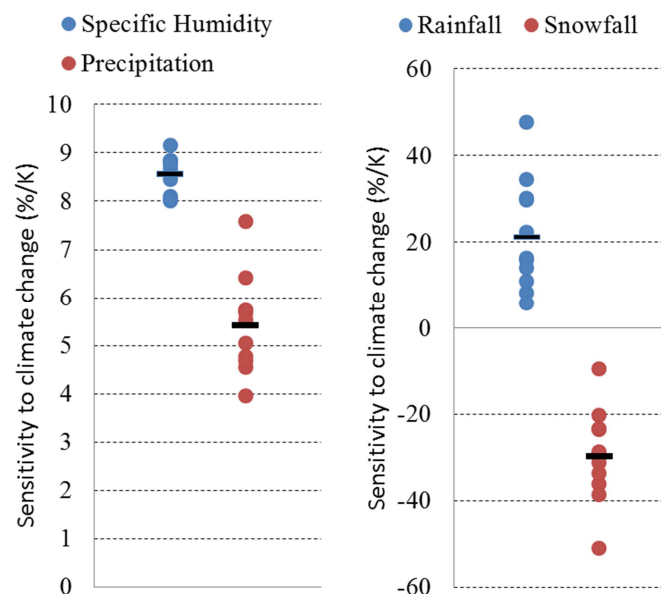


Figure 3: Changes in climatic variables averaged over the west coast (see Figure 2) due to a +2C temperature perturbation of 11 historic extreme events. Left: specific humidity (blue dots) and 1-day precipitation (red dots) Right: Changes in 1-day rainfall (blue dots) and 1-day snowfall (red dots). All values are given in %/K.

If we look into the hourly values we find that the sensitivity is dependent on the intensity of the precipitation. It is the most extreme hours within the extreme days that are most sensitive to the temperature change. Regionally averaged the change for the 5% most extreme hours within the extreme days is almost +7%/K while the less extreme hours have a change that is only half of that (Figure 4).

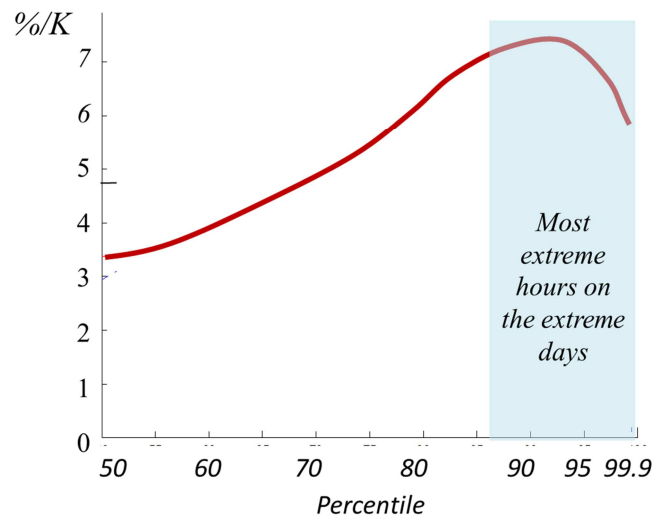


Figure 4: Changes in hourly precipitation due to a warming (%/K) averaged over the west coast (see Figure 2) and the 11 events. Changes are calculated for different percentiles from the 50 percentile (median) to the 0.1% most extreme hours given by the 99.9 percentile).

The geographical spread in sensitivity

Due to the high spatial resolution of the simulations (grid of 2km*2 km) it was possible to investigate the geographical spread in the precipitation response. The west coast region was divided into 3 sectors (coastal, near coastal and inland) and four elevation heights (lines on map in Figure 5). A very consistent pattern emerged with relatively small changes in the coastal areas, and the largest changes in the high elevation regions of the near coastal mountains (the region of Kvamskogen, Bergsdalen and western part of Stølsheimen). The coastal response was typically +3%/K while the high elevation regions of the near coastal mountains had a response of around +7%/K. The response was reduced to around +5.5%/K in the inland mountains (See Figure 5 for details).

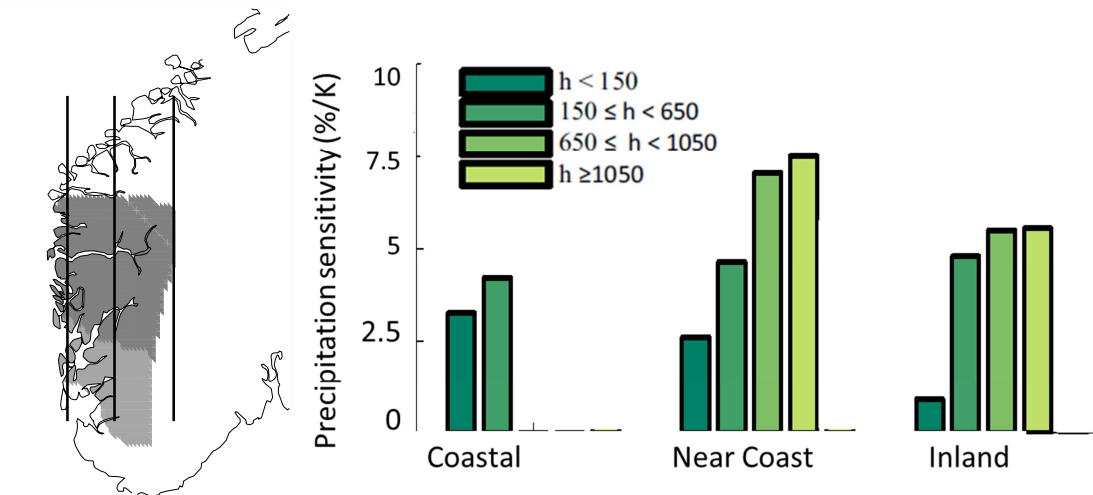


Figure 5: Left: map showing the lines separating the coastal, near coastal and inland regions only the shaded area is analyzed. Right: Average changes in 1-day precipitation per degree warming (%/K) for the different regions and different altitude bands (m.a.s.l.) within each region. Values are averages over the 11 extreme events.

The reason for the geographic response pattern is the increased response in the higher elevations that can be attributed to a couple of processes. The +2°C warming shifted the cloud microphysics towards more “warm cloud” processes as the atmospheric 0°C isotherm was elevated with approximately 200 m per degree warming. Snow and ice crystals have a lower saturation pressure than liquid droplets, and therefore grow more efficiently than liquid droplets growth through collision-coalescence processes. The shift towards more liquid droplets would therefore delay the droplet growth which would mute the coastal changes, bring more moisture into the near coastal areas and strengthen the response in this region. Secondly the sensitivity of condensation to a temperature change is higher at lower temperatures (around +1.5%/K higher for an air parcel which is -15°C compared to one with a temperature of -5°C). This would also increase the near coastal response and explain why the largest response is for the highest elevations where the overlying atmosphere is the coldest.

Conclusions

Simplified climate change simulations where a +2°C warming has been imposed on historical extreme precipitation events for the west coast of Norway, keeping the large scale flow and relative humidity unchanged have been performed. The results can be summarized as follows:

- The response was very similar for the selected extreme events.
- The change in precipitation on the extreme day was +5.2%/K averaged over the west coast of Norway
- The most extreme hours within the extreme days changed with around +7%/K.
- There was a huge increase in rainfall (over 20%/K) at the expense of snowfall.

- The changes had a distinct geographical pattern with the high elevation regions of the mountain chains closest to the coast having the largest changes.

These types of simulations act as a supplement to long climate simulations. The pros are that the simulations relates to historic events which are easy for users to relate to. As we do not have to do run long multi-decadal simulations, the horizontal and vertical resolution can be much higher than in traditional classic regional climate simulations. This enables important processes such as convection to be modelled explicitly and not parameterized. As the flow is taken from historic events the flow bias in these simulations are much smaller than in regional climate models which are forced with global climate models that may have considerable flow biases. The major drawback of the method are the assumption that the large scale flow and relative humidity on the border of the model domain is held at historic values even when the temperature has changed. Thus, the results are conditional on these assumptions. The event-based simulations precludes the analysis of the frequency of extreme events and analysis of type of extreme events that are not common in the historic period. Thus, the simulations should not be seen as alternatives to long climate simulations, but rather as an easier to understand supplement that can be used to explain the far more complex results that may emerge as the large scale flow possibly change in the future.

References

- Azad R. and Sorteberg A (2017). Extreme Daily Precipitation in Coastal Western Norway and the Link to Atmospheric Rivers. *Journal of Geophysical Research, Atmosphere*, 122, 1–16, doi:10.1002/2016JD025615
- Sandvik, M.I., Sorteberg, A. and Rasmussen, R. (2017). Sensitivity of historical orographically enhanced extreme precipitation events to idealized temperature perturbations. *Climate Dynamics* pp 1-15. doi:10.1007/s00382-017-3593-1
- I. Hanssen-Bauer, E.J. Førland, I. Haddeland, H. Hisdal, S. Mayer, A. Nesje, J.E.Ø. Nilsen, S. Sandven, A.B. Sandø, A. Sorteberg og B. Ådlandsvik (2015). *Klima i Norge 2100. Kunnskapsgrunnlag for klimatipasning* (2015). Norwegian Centre for Climate Services (NCCS) Report no. 2/2015 pp. 204

4.3 Modelling the effects of projected changes in sub-daily precipitation intensities on flooding in small catchments

D. Lawrence

Hydrology Department, Norwegian Water Resources and Energy Directorate (NVE), Oslo, Norway

Summary

Hydrological projections for 65 small (< 160 km²), rapidly responding catchments developed using bias-corrected EUROCORDEX data and the DDD hydrological model point towards increases in the 200-yr 3-hr flow that are at least 20 - 25% higher than increases in the daily-averaged 200-yr flow. The largest projected increases are found in western Norway and in coastal areas. Simulations using quantile perturbation methods suggest that catchments with a 'mixed' flood regime under the current climate (i.e. with contributions from both rainfall and snowmelt) can have increases in the annual maximum flood of over 40%, i.e. much higher than the anticipated increases in precipitation. The results presented here confirm previous speculations that in small catchments, the instantaneous flood can increase more than the daily flood under a future climate.

Introduction

Projected changes in precipitation under a future climate in Norway indicate larger increases in short-term precipitation intensities than in daily, especially for the higher quantiles (Hanssen-Bauer et al., 2015, Table 5.2.6). In small, rapidly responding catchments, this can lead to increases in peak discharge that are larger than changes estimated using models run with a daily timestep. Climate change adaptation to flooding in Norway is currently based on estimates for changes in the daily averaged flood magnitude (e.g. Lawrence, 2016) and the effect of increases in short-duration (i.e. sub-daily) precipitation intensities on peak flows is unquantified. Two factors contribute to this shortcoming: 1) precipitation and temperature time series from Regional Climate Models (RCMs) with a sub-daily temporal resolution have only recently become available to climate impact researchers; and

2) the availability of observed precipitation and temperature series required for the calibration of hydrological models at a high temporal resolution has also been limited. The release of some of the EUROCORDEX RCM (Jacob et al., 2014) output with a 3-hr time step has however made analyses of sub-daily hydrological processes under a future climate feasible. In addition, NVE has developed disaggregated 3-hr precipitation and temperature series following the procedure proposed by Vormoor and Skaugen (2013) for the 1 x 1 km gridded data available from www.seNorge.no.

This has been further used to calibrate and validate the DDD hydrological model (Skaugen and Onof, 2013) using a 3-hr time step for a range of catchments distributed across Norway. Within the ExPrecFlood project, we have taken advantage of both the availability of EUROCORDEX climate projections at a sub-daily temporal resolution and the DDD calibrations for a 3-hr time step to investigate possible climate change impacts on peak flows in small catchments under a future climate. The principal research questions for this work are: 1) are small catchments likely to have larger increases in maximum 3-hr peak flows than in maximum averaged daily flows under a future climate?; 2) is the spatial pattern of expected increases across Norway similar for peak flows and daily flows?; and 3) is there a clear relationship between projected increases in short-term precipitation and increases in peak flows in small catchments, or are there other factors which either mitigate or enhance the changes in precipitation?

Data and methods

Adjustment of climate model data

3-hr precipitation and temperature series from 5 SMHI-RCA4 RCM runs based on the EUR11 domain (i.e. with a grid resolution of approximately 12 km), representing 5 different GCMs and two Representative Concentration Pathways (RCP 4.5 and RCP 8.5) were extracted for 65 small catchments (with area less than 160 km²) distributed across Norway. As it is well established that uncorrected time series from climate models cannot be used directly in hydrological models due to biases in the climate model data, these data were processed using two alternative techniques. The first technique is bias correction using Empirical Quantile Mapping (Gudmundson et al., 2013) to adjust precipitation and temperature series from climate models based on their cumulative distribution functions. The adjustment is made relative to the cumulative distribution of the 'observed' series for each of the 65 catchments. For the work reported here, we have used 3-hr disaggregated precipitation and temperature series for the period 2000-2010 to develop the bias adjustment. Quantile corrections were developed using precipitation and temperature data grouped into standard seasonal 3-month periods (i.e. DJF, MAM, JJA, SON). Bias adjustment was then applied to climate data for a reference period (1970-2000) and a future period (2070-2100). The adjustment was applied to residual values after removing trends between periods, following the recommendations given by Hempel et al. (2013). The bias correction also included an adjustment of the fractional number of wet days, based on the ratio between the seasonal number of wet days in the observed vs. the climate data series during the correction period.

Bias correction is, nevertheless, an imperfect procedure with many shortcomings (Ehret, et al., 2012; Maraun, 2016). We have therefore also applied a second technique, quantile perturbation (Willems and Vrac, 2012; see also comparison with other methods in Sunyer et al., 2015) to consider the effect of changes in extreme

precipitation on the hydrological response in small catchments. In this method, changes in precipitation quantiles between the reference and the future period are estimated based on a comparison of the cumulative distribution functions for the data from the climate model for each period. These changes are used to adjust the cumulative distribution function of the observed precipitation series for the catchment and thereby create a 'perturbed' precipitation series representing the future climate. An advantage of this technique is that it interprets changes directly from uncorrected precipitation series, thus avoiding potential interferences in the signal introduced by bias correction. It can also be used to separately assess the role of temperature vs. precipitation changes on changes in the hydrological response. A disadvantage, however, is that the precipitation and temperature sequences found in the observed data are also used for the future climate such that potential changes in storm tracks and weather patterns, for example, are not reproduced. For the application reported here, quantile perturbations for 3-hr precipitation values were estimated based on the differences between the 1970-2000 reference period and the 2070-2100 future period and these were applied to the 2000-2010 observed precipitation series. The perturbations were developed for seasonal 3-month periods, as was done for the bias correction. For temperature, however, a monthly change factor was estimated and applied to the observed temperature series to simulate the effect of future changes in temperature.

Hydrological modelling

The DDD (Dynamical Distance Distribution) hydrological model (Skaugen and Onof, 2013) is a lumped, conceptual hydrological model which shares many similarities with the widely used HBV hydrological model (see Sælthun, 1996 for details), but has also some important differences. In particular and in contrast with the HBV model, the distribution of distances to and within the channel network (which can be extracted using a GIS analysis of a given catchment) determines the runoff dynamics for the catchment. Saturation states are tracked at four subsurface levels and on the surface, and the saturation states control the celerities of the water flux through the system. This both introduces a higher degree of physical realism than is found in traditional lumped, conceptual models and reduces the number of arbitrary parameters that must be calibrated for individual catchments. The DDD model has previously been calibrated and validated relative to observed discharge for the 65 small catchments and the disaggregated 3-hr precipitation and temperature series also used here. Calibration was performed for the period 2005-2010 and validation for the period 2000-2005 relative to observed discharge data, and the Kling-Gupta criterion (Gupta et al., 2009) was used as the objective function for the optimisation. Calibration and validation have also been performed relative to 24-hr data, for which longer precipitation and temperature series are available (1985-2014) for these catchments. The calibrated parameter were used to run hydrological simulations for each catchment for: 1) bias corrected 3-hr and 24-hr precipitation and temperature series, where the 24-hr bias corrected series was constructed by aggregating the 3-

hr bias corrected series; and 2) observed and perturbed 3-hr precipitation and temperature series for each catchment.

The annual maximum series were extracted from the simulated discharge series for each model run, and the mean annual flood was estimated for the reference and the future period for each simulation. For simulations based on bias-corrected climate data, the annual maximum series were also used to estimate the 5-yr and 200-yr flood magnitudes using a 2-parameter Gumbel extreme value distribution. This distribution was used due to the limited length of the available series (i.e. 30 years), potential problems with the stability of the shape parameter for 3-parameter distributions (Kobierska et al., 2017) and in order to be consistent with previous estimates for changes in flooding based on 24-hr simulations (i.e. Lawrence, 2016). Expected percentage changes in the mean annual flood, the 5-yr flood and the 200-yr flood were estimated by comparing the values estimated for the reference and the future periods for each simulation. For the observed and perturbed 3hr series, changes in only the mean annual flood were estimated due to the limited length of the available record (10 years).

Results

Hydrological simulations with bias-adjusted EUROCORDEX data

A comparison of the expected changes in the mean annual flood, the 5-yr flood and the 200-yr flood based on simulations using the bias-adjusted EUROCORDEX data is shown in Table 1. Each value represents the average for all 65 catchments for all 5 SMHI-RCA4 runs for the RCP indicated. The results indicate that the estimated average increase in both the 3-hr flow and the 24-hr flow for a given flood quantile is twice as large under the RCP 8.5 concentration pathway in comparison with RCP 4.5. The results further suggest that the simulations based on 3-hr input data and a 3-hr model time step give increases that are 22-30% higher than do the simulations with the lower, 24-hr temporal resolution. There is, however, a significant spread in the results for individual climate projections and this is shown in Fig. 1, which illustrates differences between the results for individual climate models for the 24-hr and 3-hr simulations for each catchment.

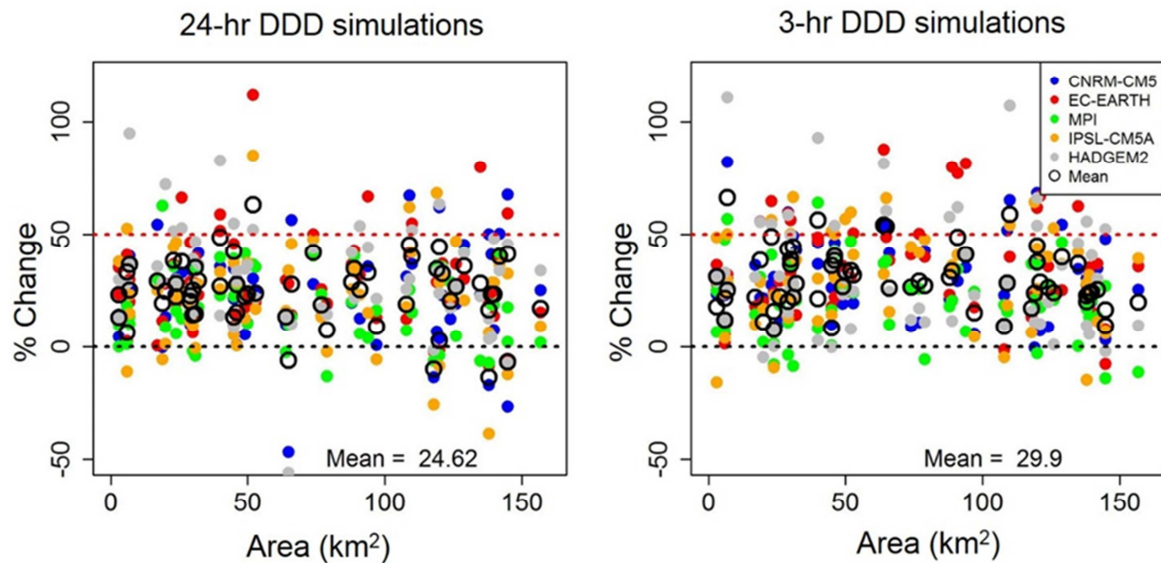


Figure 1: Estimated percentage changes in the 200-yr flood as function of the GCM used as boundary conditions for the RCM EUROCORDEX simulations (colours) and as a function of area for 65 catchments for hydrological simulations using a) a 24-hr time step and b) 3-hr time step. The open circles show the average value for all 5 climate model data sets for an individual catchment. The results shown here are for the difference between the reference period 1971-2000 and the future period 2071-2100 for projections based on the RCP 8.5 concentration pathway. All climate projections are from the SMHI-RCA4 RCM model.

	RCP 4.5		RCP 8.5	
	24-hr	3-hr	24-hr	3-hr
Mean annual flood	11	14	22	29
5-year flood	12	14	24	29
200-year flood	12	15	25	30

Table 1: Estimated percentage changes (increases) in the flood quantiles indicated for 24-hr vs. 3-hr simulations based on climate model projections for RCP 4.5 and 8.5. The values given are average values for all 65 catchments for all five EUROCORDEX RCM models considered in this study.

It can also be seen, however, that although a few catchments show a mean value that indicates a decrease in the 24-hr 200-yr flood level, all of the mean values for the 3-hr flood level indicate an increase of at least 5%. The results are plotted as a function of catchment area so that potential trends as a function of area can be highlighted. Although the mean values for the 3-hr simulations indicate a very weak tendency towards larger mean increases in smaller catchments, this effect is not

statistically significant. The spatial distribution of the mean projected changes in the 200-yr flood for the 65 small catchments (i.e. open circles in Fig. 1) are shown in Fig. 2 for the 24-hr and the 3-hr simulations. The results confirm the somewhat higher values for the expected change in the 200-year 3-hr flow level relative to the 24-hr flow. There is evidence for a clustering of the highest values of projected changes (i.e. > 40%) in western Norway, although there is also one catchment in southern Norway, one in south-eastern Norway and one in northern Norway with projected increases in the 200-year 3-hr flow in this range. Otherwise, the majority of catchments in southern and eastern Norway have projected changes in the 200-year 3-hr flow in the range 20-40%, and in northern Norway in the range 10-30%.

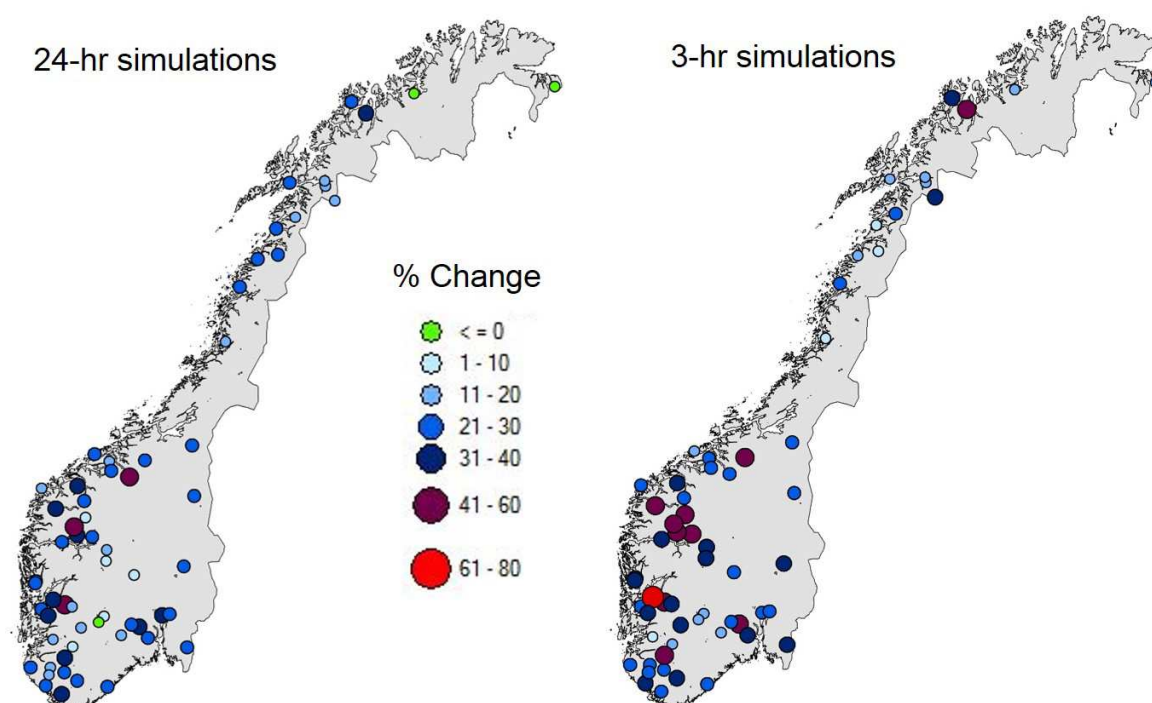


Figure 2: Estimated mean percentage changes in the 200-yr flood for 24-hr (left) and 3-hr (right) hydrological simulations with the DDD model. Changes are estimated for the future period (2071-2100) relative to reference period (1971-2100) for RCP 8.5.

Hydrological simulations with perturbed observed series

The percentage change in the mean annual 3-hr flood level based on the mean of the 5 perturbed observed series for each of the 65 catchments is shown in Figure 3. The results are plotted as a function of area and of the percentage of over threshold flows in the observed series that are driven predominantly by rainfall (as opposed to snowmelt). This quantity has been previously shown to be a good indicator of the flood generating process (FGP) in the catchment and is an important factor driving

the direction of changes in flooding under climate change (e.g. Vormoor, et al., 2015, 2016). Projected changes are shown for simulations in which only precipitation is perturbed (left-hand side) and in which both precipitation and temperature are perturbed (right-hand side) following the procedures explained in the Data and Methods section.

The results of the simulations with the perturbed series indicate striking differences between the two sets of simulations and as a function of how dominant rainfall is in driving high flows in the catchment. The maximum values of percentage change for the series in which only rainfall is perturbed are in the range 31-40% and most values are below 30%, whereas when both rainfall and temperature are perturbed most of the highest values are in the range 41-60% and one catchment has a mean change of > 60%. Although the mean value of change for all catchments is somewhat higher for the simulations in which only precipitation is perturbed (22% as opposed to 18%), this is due to the 8 catchments which show a decrease in the mean value of change when both precipitation and temperature are perturbed.

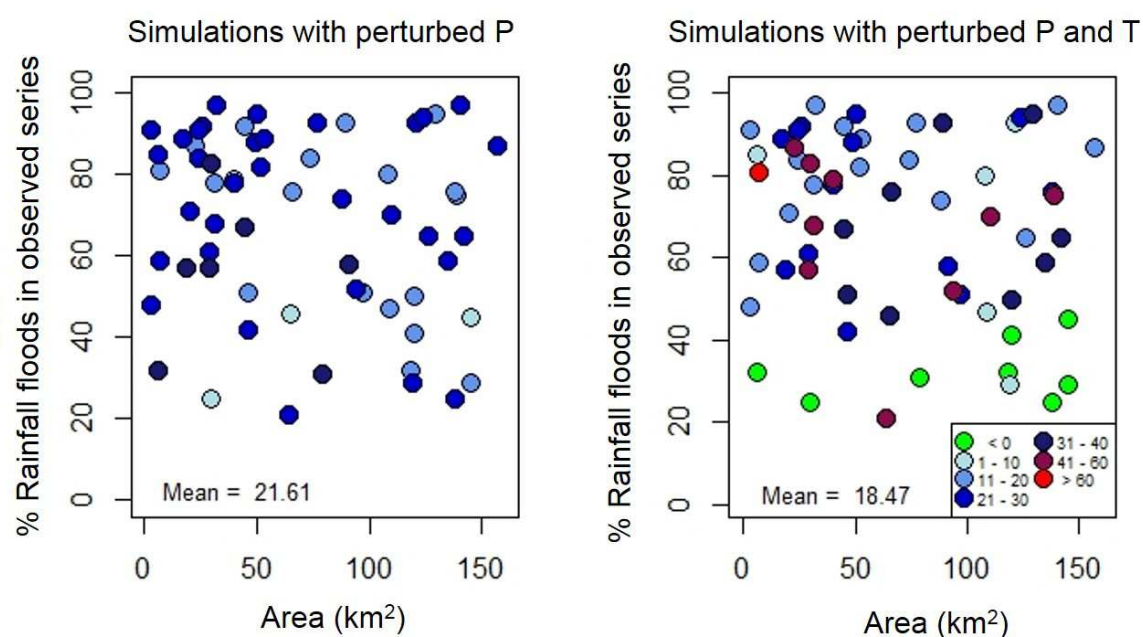


Figure 3: Estimated mean percentage changes in the mean annual flood for 3-hr simulations in which only precipitation intensities are perturbed (left) and in which both precipitation and temperature are perturbed. Hydrological simulations were performed for the 65 catchments using the DDD hydrological model. The perturbations applied to the observed series were estimated based on changes between the reference period (1971-2000) and the future period (2071-2100) relative to reference period (1971-2100) for RCP 8.5.

There is again very little evidence for variation as a function of catchment area, although it can be noted that all of the catchments with an increase of > 30% are smaller than 100 km². There are, however, distinguishable patterns in the results as a

function of flood generating process (FGP). Firstly, the simulations with perturbed precipitation suggest that the largest increases are found for catchments for which the percentage rainfall floods in the observed series is less than 80-85%, and this tendency is also seen for the simulations in which both precipitation and temperature are perturbed. In addition, the perturbation of temperature leads to decreases in most of the catchments that have a snowmelt dominated flood regime, i.e. with a value of percentage rainfall floods of less than 45%.

Discussion

Reported changes in precipitation intensities vs. in extreme flows

The results for the 3-hr vs. the 24-hr simulations based on bias corrected EUROCORDEX data (Table 1 and Figs. 1 and 2) indicate an increase the magnitude of 3-hr extreme flood quantiles which is 22-30% higher than that estimated for the 24-hr quantiles. We have only considered catchments with an area of less than 160 km² here, and it is reasonable to expect that in such catchments the larger changes that are projected for 3-hr precipitation intensities relative to 24-hr intensities will contribute to this. The average value of the projected changes in the 3-hr discharge (Table 1) are, however, somewhat less than projected changes in the 5-yr and 200-yr 3-hr precipitation reported in Hanssen-Bauer et al., 2015 (Table 5.2.6). In that report, the expected changes in 3-hr 200-yr precipitation intensities are, for example, reported as 19 and 38% for RCP 4.5 and 8.5, respectively. There are several factors which potentially contribute to this: 1) the effects of bias correction on the precipitation values; 2) the use of differing extreme value functions for estimating the 5-yr and 200-yr values; 3) that the values reported in Hanssen-Bauer et al., 2015 are based on an average of all grid cells for the whole of Norway, whereas in this study we have used areally-averaged values from 65 specific locations not uniformly distributed across Norway (Fig. 2); and 4) the selection of RCMs considered differs slightly between the two studies. We consider the first two issues by comparing the estimated changes in 3-hr and 24-hr precipitation intensities for uncorrected and bias corrected values for the 99.5 percentile and for extreme quantiles using both a 2-parameter Gumbel and a 3-parameter GEV distribution. The latter two issues can also contribute to small differences, but will not be discussed here.

A comparison of the estimated changes in precipitation intensities for the 99.5 percentile and for the 5-yr and the 200-yr flood for uncorrected and bias correction precipitation for 24-hr and 3-hr durations is shown in Table 2. The values are given as the average for all 65 catchments for all 5 RCMs for RCP 8.5. The values in parentheses refer to the values reported in Hanssen-Bauer et al., 2015 (Table 5.2.6).

	Uncorrected P		Bias corrected P	
	24-hr	3-hr	24-hr	3-hr
99.5% quantile	19 (20)	21 (20)	19	22
5-yr (Gumbel)	20	28	22	29
200-yr (Gumbel)	21	29	23	29
5-yr (GEV)	21 (22)	32 (28)	23	33
200-yr (GEV)	27 (26)	40 (38)	30	41

Table 2: Estimated percentage changes (increases) in the precipitation quantiles indicated for 24-hr vs. 3-hr intensities based on climate model projections for RCP 4.5 and 8.5. Changes estimated from uncorrected and bias corrected data are compared. The values given are average values for all 65 catchments for all five EUROCORDEX RCM models considered in this study. The number in parentheses is taken from Table 5.2.6 in Hanssen-Bauer, et al., 2015.

The values reported in Table 2 suggest that the changes in the 99.5% quantile and the 5-yr and 200-yr return levels for precipitation intensity estimated from the uncorrected precipitation series used here are very similar to those reported in Hanssen-Bauer et al. (2015) if one uses a 3-parameter GEV distribution to estimate the extreme values. If one uses a 2-parameter Gumbel distribution, however, the estimated changes in the 200-yr precipitation intensities for both the 3-hr. and the 24-hr. durations are considerably lower. Thus, the higher values for the expected changes in both the 200-yr 3-hr and 24-hr precipitation intensities reported in Hanssen-Bauer relative to those we report here for flooding can to some degree be a consequence of the choice of the extreme value function. The comparison of the average values for change estimated from uncorrected and bias corrected data suggest that bias correction does not significantly alter the projected changes in the extreme values. The largest discrepancies (i.e. 2 to 3 percentage points) are between the estimates for the projected change in the 5-yr and 200-year 24-hr. precipitation intensities, for which the mean values estimated from the bias corrected data are slightly higher.

Role of flood generation regime

The results for the perturbed series (Fig. 3) indicate that if one only introduces changes in precipitation intensities in the observed series, the resulting mean value of change in the 3-hr mean annual flood for all catchments (i.e. 22%) is very similar to the mean value of changes in the 99.5% quantile of precipitation (i.e. 21%) given in Table 2. If one also introduces changes in temperature, a very different pattern of

change is apparent, with several catchments showing increases of 40-60% and several showing decreases. By perturbing temperature one also simulates the effects of a) increased evapotranspiration leading to larger soil moisture deficits during certain times of the year, and b) changes in the duration and magnitude of the snowmelt contribution to streamflow. There is some minor evidence for the first of these effects in Fig. 3 (right-hand side) in that the values for many, but not all, rainfall-dominated catchments (with FGP > 85%) are slightly lower than for the simulations which only consider the change in precipitation (left-hand side). This would occur if, for example, warmer temperatures in late summer and early autumn produce a significant soil moisture deficit capable of attenuating the largest increases in precipitation intensities.

Evidence for the effects of changes in the snowmelt contribution are more apparent in Fig. 3. in that most catchments with an FGP < 40% have a projected decrease in the mean annual flood, including the smallest catchments. Thus, even though precipitation intensities increase, the role of snowmelt in driving high flows dominates in both the present and the future climate such that decreases in the duration and peak values of snowmelt produce an overall decrease in the mean annual flood. More strikingly, in many catchments with a mixed regime (i.e. both rainfall and snowmelt, with an FGP between 50 and 85%) the projected changes are higher than for the simulations in which only precipitation is perturbed. Possible reasons for this include that a) precipitation falls as rain rather than snow during a longer period of the year, and b) the percentage of the catchment area that receives precipitation as rain, rather than snow, during a storm event is larger under the future climate. The first of these factors will lead to high streamflow values during, for example, the winter period, such that the catchments are more vulnerable to precipitation events with high intensity during this period. The second factor will produce a larger rainfall volume which must be routed through the catchment during such periods and events.

Implications for climate change adaptation for flooding in small catchments

The results presented here show a similar spatial pattern in the expected increase in the 24-hr 200-yr flood (Fig. 2 left-hand side) to that which is currently used for climate change adaptation in Norway (i.e. Lawrence, 2016). In addition, the results for the 3-hr 200-year flood suggest an increase which is 20-25% higher than for the 24-hr flood. The current recommendations for climate change adaptation given in Lawrence (2016) suggest that for small catchments (and other catchments which respond quickly to intense rainfall) the climate factor used for adjusting flows to account for future climate change effects should be AT LEAST 20%. The data used to inform this recommendation are shown in Fig. 4 (left-hand side). Given that about half of catchments under 100 km² have projected increases of at least 20%, and that it has been recognised that processes in small catchments are not fully accounted for in the 24-hr. simulations, the recommendation of 'at least 20%' is given for small

catchments. The results of this study using 3-hr simulations, which in principle are better suited for characterising the sub-daily response to extreme rainfall in small catchments, support the recommendation and further suggest that a minimum value of 30% may be more suitable if one bases the lower bound on the results for at least half of the catchments considered.

It should be kept in mind that the simulations presented here include a larger number of smaller catchments than was available for Lawrence (2016). In addition, those projections are based on a larger number of EUROCORDEX RCMs (10 instead of 5) and a different hydrological model (HBV). The results shown in Fig. 2 and Fig. 3 also suggest that different types of catchments in different locations will have differing responses to increases in precipitation intensity and this should be investigated more thoroughly in further work.

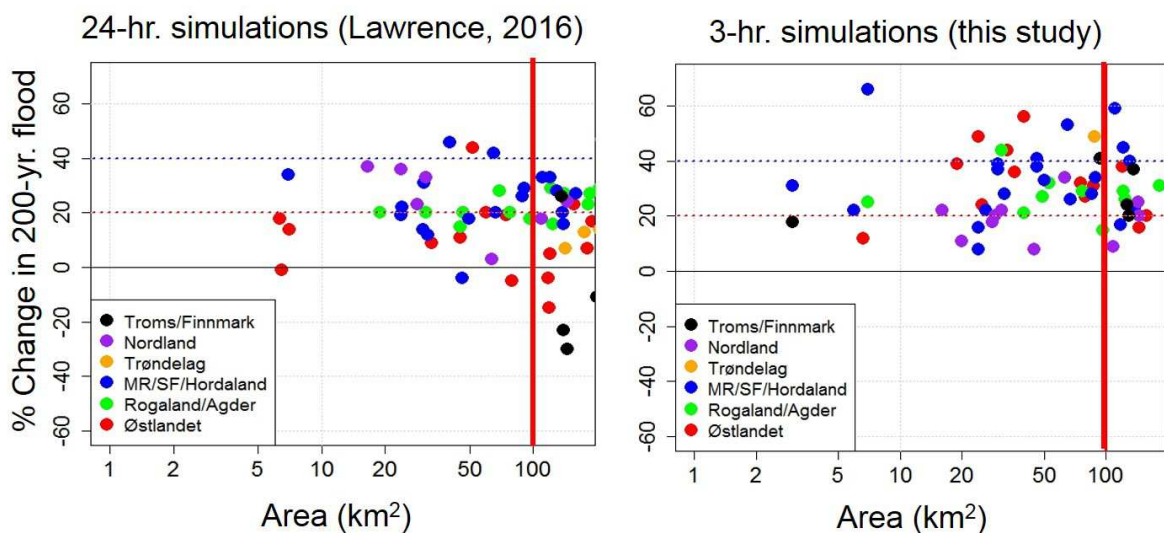


Figure 4: Estimated percentage change in the 200-yr flood as a function of catchment area and region for catchments under 160 km². The results on the left-hand side are from Lawrence, 2016 and on the right-hand side from the work presented here. The estimated changes are between the reference period (1971-2000) and the future period (2071-2100) for RCP 8.5.

Acknowledgements

Thomas Skaugen (NVE) is thanked for making the DDD hydrological model and the 24-hr and 3-hr model calibrations available for this work. Wai K. Wong and Hong Li (both NVE) are thanked for extracting the 3-hr precipitation and temperature time series for the required grid cells from the 5 EUROCORDEX RCMs used here and for preparing areal-averaged uncorrected time series for each of the 65 catchments.

References

- Ehret, U., E. Zehe, V. Wulfmeyer, K. Warrach-Sagi, J. Liebert, (2012), HESS Opinions “Should we apply bias correction to global and regional climate model data?”, *Hydrology and Earth System Sciences*, 16, 3391-3494.
- Gudmundsson, L., J. B. Bremnes, J. E. Haugen, T. Engen-Skaugen, (2012), Technical Note: Downscaling RCM precipitation to the station scale using statistical transformations – a comparison of methods, *Hydrology and Earth System Sciences*, 16, 3383-3390.
- Gupta, H. V., H. Kling, K. K. Yilmaz, G. F. Martinez, (2009), Decomposition of the mean squared error and NSE performance criteria: Implications for improving hydrological modelling, 377, 80-91.
- Hempel, S., K. Frieler, L. Warszawski, J. Schewe, F. Piontek, (2013), A trend-preserving bias correction – the ISI-MIP approach, *Earth System Dynamics*, 4, 219-236.
- Jacob, D., J. Petersen, B. Eggert, A. Alias, O. B. Christensen, L. M. Bouwer, A. Braun, A. Colette, M. Deque, G. Georgievski, E. Georgopoulou, A. Gobiet, L. Menut, G. Nikulin, A. Haensler, N. Hempelmann, C. Jones, K. Keuler, S. Kovats, N. Kröner, S. Kotlarski, A. Kriegsmann, E. Martin, E. van Meijgaard, C. Moseley, S. Pfeifer, S. Preuschmann, C. Radermacher, K. Radtke, D. Rechid, M. Rounsevell, P. Samuelsson, S. Somot, J-F. Soussana, C. Teichmann, R. Valentini, R. Vautard, B. Weber, P. Yiou, (2014), EURO-CORDEX: new high-resolution climate change projections for European impact research, *Regional Environmental Change*, 14, 563-578.
- Hanssen-Bauer, I., E. J. Førland, I. Haddeland, H. Hisdal, S. Mayer, A. Nesje, J. E. Ø. Sandven, A. B. Sandø, A. Sorteberg, B. Ådlandsvik (Editors), (2015), *Klima i Norge 2100: Kunnskapsgrunnlag for klimatilpasning oppdatert i 2015*, Norwegian Climate Services Centre Report 2/2015.
- Kobierska, F., K. Engeland, Th. Thorarindsdottir, (2017), Evaluation of design flood estimates – a case study for Norway, *Hydrology Research* doi:10.2166/nh.2017.068
- Lawrence, D. (2016), *Klimaendring og framtidige flommer i Norge*, NVE Rapport 81/2016.
- Maraun, D. (2016), Bias correcting climate change simulations – a critical review, *Current Climate Change Reports*, 2, 211-220.
- Skaugen, T. and C. Onof (2014), A rainfall-runoff model parameterized from GIS and runoff data, *Hydrological Processes*, 28, 4529-4542.
- Sunyer, M., Y. Hunecheda, D. Lawrence, H. Madsen, P. Willems, M. Martinkova, K. Vormoor, G. Bürger, M. Hanel, J. Kriaciuniene, A. Loukas, M. Osuch, I. Yücel (2015), Intercomparison of statistical downscaling methods for projection of extreme precipitation in Europe, *Hydrology and Earth System Sciences*, 19, 1827-1847.
- Sælthun, N. R. 1996. The Nordic HBV Model, NVE Publication No. 7.
- Vormoor, K. and T. Skaugen, (2013), Temporal disaggregation of daily temperature and precipitation grid data for Norway, *Journal of Hydrometeorology*, 14, 989-999.
- Vormoor, K., D. Lawrence, M. Heistermann, A. Bronstert, (2015), Climate change impacts on the seasonality and generation processes of floods – projections and uncertainties for catchments with mixed snowmelt/rainfall regimes, *Hydrology and Earth System Sciences*, 19, 913-931.
- Vormoor, K., D. Lawrence, L. Schlichting, D. Wilson, W. K. Wong, (2016) Evidence for changes in the magnitude and frequency of observed rainfall vs. snowmelt driven floods, *Journal of Hydrology*, 538, 33-48.
- Willems, P. and M. Vrac, (2011), Statistical precipitation downscaling for small-scale hydrological impact investigations of climate change, *Journal of Hydrology*, 402, 193-205.

4.3 Uncertainty introduced by flood frequency analysis in the estimation of climate change impacts on flooding

D. Lawrence

Hydrology Department, Norwegian Water Resources and Energy Directorate (NVE), Oslo, Norway

Summary

Analysis of the variance in ensembles of hydrological projections for 115 catchments distributed across Norway suggest that although differences between climate models generally dominate uncertainty in projections for the 200-yr. flood under a future climate, the uncertainty introduced by flood frequency estimation is of a similar order of magnitude. Hydrological model parameterisation is generally less important than the other two factors, although it can be locally important, particularly for non-inland catchments in the southern half of Norway. A comparison of projected changes using a 2-parameter Gumbel vs. 3-parameter GEV and GPD extreme value distributions indicates that the 3-parameter functions give higher projected changes in areas where flood magnitudes are expected to increase. The GEV and GPD distributions produce very similar results (judged by the median of the ensemble of projections) even though they are applied to differing extreme value series (annual maxima vs. over threshold events).

Introduction

Estimates of likely changes in extreme flooding under a future climate are often based on extreme value analyses using the annual maximum series or peak over threshold series extracted from hydrological simulations based on climate input data (e.g. Prudhomme et al., 2003; Veijalainen et al., 2010). Although numerous studies have investigated the uncertainty introduced in such estimates due to differences between climate models, bias correction methods and hydrological models (e.g. Lawrence and Haddeland, 2011; Bosshard et al., 2013; Osuch, et al., 2016;), little attention has been paid to the uncertainty underlying the extreme value estimates and the methods used to derive those estimates. The quantification of uncertainty in flood estimates is a well-established research topic (e.g. Renard et al, 2013; Kobierska et al., 2017). Two general issues are particularly relevant for climate change impacts research: 1) uncertainty in higher flood quantiles, particularly when the return period is significantly longer than that represented by the time

series used; and 2) uncertainty introduced by selecting a particular extreme value distribution to estimate the higher flood quantiles. In the work reported here, we

present preliminary results evaluating the magnitude of the first of these factors relative to uncertainty introduced by other factors in an ensemble of hydrological projections for future changes in flooding in Norway. We also considering the second factor by assessing whether or not three standard types of extreme value functions give a similar overall magnitude and spatial pattern of projected changes in flooding across Norway.

Data and methods

Ensemble of hydrological projections for changes in flooding

Input data for hydrological simulations were obtained from 10 RCM runs generated by the EUROCORDEX initiative (Jacob, et al., 2014) for RCP 4.5 and 8.5 on the EUR11 grid. The RCM runs used here are the same as those reported in Klima i Norge 2100 (Hanssen-Bauer, et al., 2015, Table A.5.1.1). Daily precipitation and temperature series were extracted for 115 catchments distributed across Norway for a reference period (1971-2000) and a future period (2071-2100), and these were bias corrected using two techniques: a) empirical quantile mapping (Gudmundsson et al., 2013); and b) a distribution-based mapping using a double gamma function (Yang et al., 2010). Correction was performed on residual values after trend removal following the procedures recommended by Hempel et al. (2013). The bias corrected time series were used as input to the HBV hydrological model (Sælthun, 1996), previously calibrated for each of the 115 catchments. Calibration was performed using PEST optimization routines (Lawrence, et al., 2009) and this produced 25 best-fit parameter sets for each catchment, all with values of the Nash-Sutcliffe efficiency criterion of within 2 percentage points of each other for a given catchment. These multiple best-fit parameter sets constitute the basis for assessing uncertainty introduced by the parameterization of the HBV hydrological model. In total, the 10 climate projections, 2 bias correction procedures and 25 hydrological model parameter sets produce an ensemble of 500 simulations for each of the 115 catchments for both RCP 4.5 and 8.5. Only selected results from the full ensemble are reported here.

Flood frequency analysis methods

Previous hydrological projections for future patterns of flooding in Norway (e.g. Lawrence, 2016) have used a 2-parameter Gumbel distribution for estimating return levels for the 200-year flood due to its robustness for extreme value series of limited length (30 years in this case). Other European studies have also used this distribution (e.g. Dankers and Feyen, 2008) and justified its use by applying a likelihood ratio test to assess the value added by including a 3rd parameter, in this case a shape parameter, in the distribution (resulting in a 3-parameter GEV distribution). However, as discussed by Renard et al., (2013), there are several issues that can be considered when assessing the most suitable extreme value distribution for estimating flood quantiles. Extreme value distributions with a shape parameter are often more reliable than simpler distributions, both for streamflow (e.g.

Kobierska et al., 2017) and for precipitation (e.g. Blanchet et al., 2015), although they are also less stable. Changes in the tail of the distribution are, however, of particular interest in climate change impact studies, and these may be better captured using an extreme value function which also models the skewness of the distribution. Estimates for the projected change in the 200-year flood developed using a 2-parameter Gumbel distribution and a 3-parameter GEV distribution are therefore compared in this study. In addition, a GPD (Generalised Pareto Distribution) is also used to estimate the 200-year flood. In that case, a fixed threshold corresponding to the 98.5 percentile of streamflow is used to select events. Events were assumed to be independent if they were separated by at least 6 days, a value which has previously been shown to be suitable for the 115 catchments considered here (with the exception of two large catchments with an area $> 10,000 \text{ km}^2$ and having a predominantly snowmelt flood regime). This procedure was found to result in an average of approximately 2 events per year for the catchments considered.

Quantification of uncertainty in return level estimates

The 200-year flood was estimated for each of the 500 simulations for each of the 115 catchments for both the reference and the future period using the L-moment method for all three extreme value distributions considered. The L-moment method was implemented in R using the 'lmomco' package (Asquith, 2017).

Parametric bootstrapping following the procedure described in Kuczera and Franks (2006) was then used to quantify the empirical distribution of estimates for the 200-yr return level using 5000 resamples. An

example of the results for one simulation is shown in Fig. 1 and illustrates both the large spread in the estimates for a given simulation period and the significant overlap between periods. For use in the ensemble modelling for each catchment, 100 samples with replacement were drawn from the empirical distribution for the 1971-2000 reference period and for the 2071-2100 future period and used to generate 100 estimates of the percentage change between the two periods.

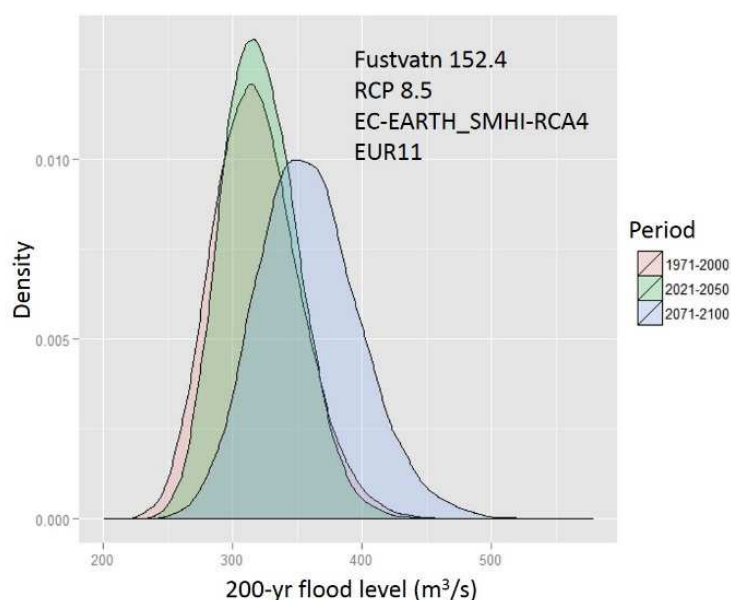


Figure 1: Distribution of estimates for the 200-yr flood based on the climate projection indicated for one catchment for three periods.

Variance decomposition

An ensemble consisting of 50,000 estimates (i.e. 500 simulations with 100 extreme value estimates for each simulation) for the percentage change in the 200-yr flood was generated for each of the three extreme value functions for each of the 115 catchments. The contributions of each of three factors (differences between climate models, hydrological model parameterization, and uncertainty in the extreme flood estimate) to the total spread in the ensemble of results for a given catchment were assessed using variance decomposition (see Déqué et al., 2007 or Sunyer et al., 2016 for full details). The decomposition procedure uses an ANOVA linear model for the ensemble variance and estimates the variance introduced by individual factors and the so-called 'interaction' terms between the factors. The interaction terms arise when the variance introduced by multiple factors cannot be explained using a simple linear combination of the individual factors. Examples of the decomposed variance for the ensembles for a selection of eight catchments distributed across Norway for flood estimates with a 2-parameter Gumbel distribution and a 3-parameter GEV distribution are shown in Figure 2. For the ensemble with flood estimates using Gumbel distribution, the variance is dominated by two components, differences between climate models (light blue) and differences in the FFA estimates (blue) in all catchments. In addition, the variance introduced by the 10 climate models is larger than that associated with the flood frequency analysis in 6 of the 8 catchments. When a GEV distribution is used, the interaction term between the climate models and the FFA estimates becomes non-negligible in all catchments and the variance introduced by FFA estimation increases. It can also be seen that the variance introduced by considering alternative parameterisations of the hydrological model is negligible relative to FFA estimation and differences between climate models in all but one of the eight catchments. It is nevertheless small ($< 10\%$ of the total variance) also in that catchment.

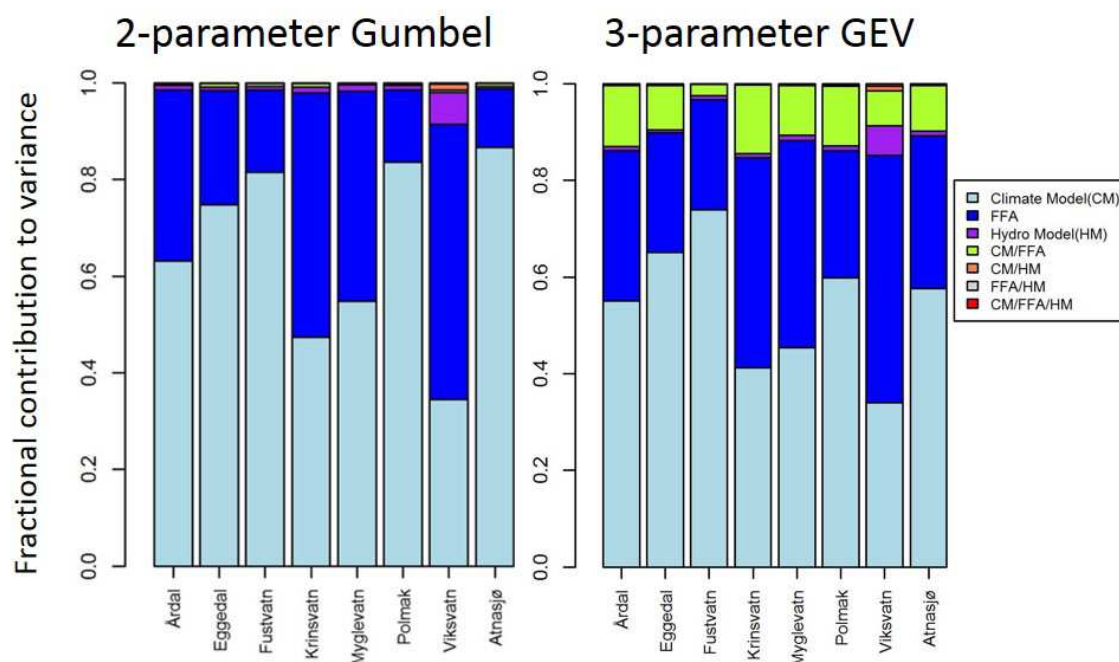


Figure 2: Fractional contribution to the total variance for the three factors considered, i.e. Climate Models (CM), Flood Frequency Analysis (FFA), and Hydrological Model parameterisation (HM), and the interactions between these components. The variance is estimated from ensemble estimates for the change in the 200-yr. flood under RCP 8.5 for the eight catchments indicated.

Results

Alternative flood frequency estimation methods

The ensemble of 500 simulations for each of 115 catchments was used to estimate the median percentage change in the 200-yr. daily flood discharge for the three alternative extreme value distributions: 1) 2-parameter Gumbel distribution applied to the annual maximum series; 2) 3-parameter Generalised Extreme Value (GEV) distribution applied to the annual maximum series; and 3) 3-parameter Generalised Pareto distribution (GPD) for RCP 8.5. The median values for all catchments for the three distributions are shown in Figure 3. All of the distributions give a somewhat similar regional pattern of variation in that the highest projected median increases are found in western Norway, along the coast and in Nordland, whilst lower projected increases and, in some cases decreases, are found in inland regions of eastern Norway and in Troms and Finnmark. The two distributions with a shape parameter (GEV and GPD) give, however, much higher median values of expected change than does the Gumbel distribution. In addition, the results for these two distributions are remarkably similar, even though they represent different types of extreme value series in each case (annual maxima vs. over threshold events). The comparison of the three distributions indicates that the inclusion of the shape parameter does indeed lead to higher estimated changes, and that these higher values vary systematically between regions. Thus, although individual estimates based on 3-

parameter distributions may suffer from problems of stability, the ensemble estimates give a coherent regional signal.

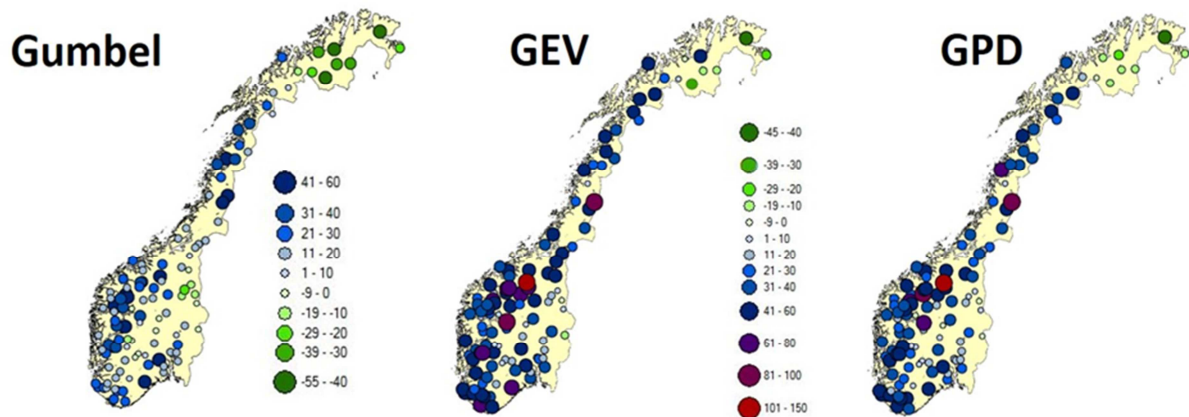


Figure 3: Median value of estimated percentage change in the 200-year flood based on an ensemble of 500 simulations for each of 115 catchments for RCP 8.5. Flood estimates are based on the three different extreme value distributions indicated: Gumbel, Generalised Extreme Value (GEV) and Generalised Pareto Distribution (GPD).

Relative contributions to total variance

The fractional contributions to the total variance in the ensemble for each of the 115 catchments are illustrated in Figure 4 for estimates for the change in the 200-yr. flood (under RCP 8.5) based on the GEV distribution. To simplify the presentation, the interaction terms have been divided equally between the 2 (or 3) factors they represent and added to the individual term for that factor. The results indicate that in more than half of the catchments, the variance introduced by differences in climate models dominates the total variance (i.e. is more than 60%), whilst flood frequency analysis is of secondary importance (in the range 21-40%) and hydrological model parameterisation is of tertiary significance (generally 10% or less). This is nevertheless some evidence for regional patterns in the catchments which do not follow this general pattern. For example, nearly all of the catchments for which the contribution of flood frequency analysis to the total variance is in the range 41-60% are found in non-coastal locations. Many of these catchments are dominated by 'mixed' flood regimes (i.e. both heavy rainfall and snowmelt can contribute to high flows, see Fig. 1 in Vormoor and Lawrence in this report) and may well undergo a transition to a rainfall-dominated flood regimes in the future climate. This issue will be explored in further work.

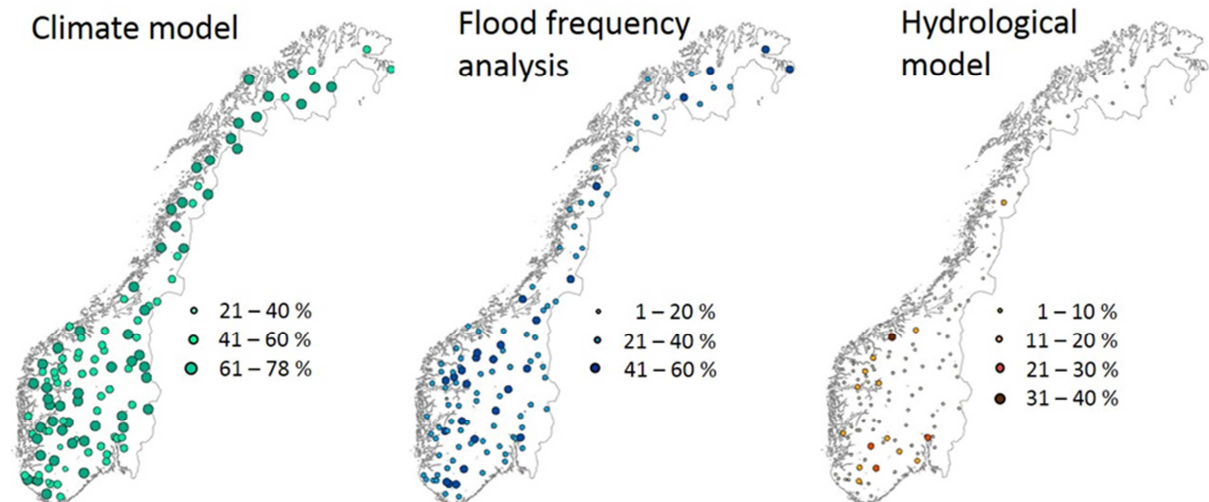


Figure 4: Relative contributions of the three factors distinguished in the variance decomposition as a percentage of the total variance of the ensemble for estimates of the future change in the 200-yr. flood for 115 catchments. Simulations are based on RCP 8.5.

With respect to the parameterisation of the hydrological model, almost all catchments which show a relative contribution from this factor which is greater than 10% are located in the southern half of Norway, specifically in western, south-eastern and southernmost Norway. No catchments in the inland region of southern Norway or in northern Norway (with one exception) have relative contributions from this factor which are greater than 10%. This is consistent with previous experience of HBV hydrological model calibration for these catchments (e.g. Fig. 9, Lawrence et al., 2009), which suggests more robust model parameterisations for the snow-dominated catchments found in those areas.

References

- Asquith, W.H., (2017), Imomco: L-moments, censored L-moments, trimmed L-moments, L-comoments, and many distributions. R package version 2.2.9, Texas Tech University, Lubbock, Texas.
- Blanchet, J., J. Touati, D. Lawrence, F. Garavaglia, E. Paquet, (2015), Evaluation of a compound distribution based on weather pattern subsampling for extreme rainfall in Norway, *Natural Hazards and Earth Systems Science*, 15, 2653-2667.
- Bosshard, T., M. Carambia, K. Goergen, S. Kotlarski, P. Krahe, M. Zappa, C. Schär, (2013), Quantifying uncertainty sources in an ensemble of hydrological climate-impact projections, *Water Resources Research*, 49, 1523-1536.
- Dankers, R. and L. Feyen, (2008), Climate change impact on flood hazard in Europe: An assessment based on high-resolution climate simulations, *Journal of Geophysical Research*, 113, D19105, doi:10.1029/2007/JD009719.
- Déqué, M., S. Somot, E. Sanchez-Gomez, C. M. Goodess, D. Jacob, G. Lenderink, O. B. Christensen, (2007), An intercomparison of regional climate simulations for Europe: assessing uncertainties in model projections, *Climate Change*, 81, 53-70.
- Gudmundsson, L., J. B. Bremnes, J. E. Haugen, T. Engen-Skaugen, (2012), Technical Note: Downscaling RCM precipitation to the station scale using statistical transformations – a comparison of methods, *Hydrology and Earth System Sciences*, 16, 3383-3390.

- Hanssen-Bauer, I., E. J. Førland, I. Haddeland, H. Hisdal, S. Mayer, A. Nesje, J. E. Ø, Sandven, A. B. Sandø, A. Sorteberg, B. Ådlandsvik (Editors), (2015), Klima i Norge 2100: Kunnskapsgrunnlag for klimatilpasning oppdatert i 2015, Norwegian Climate Services Centre Report 2/2015.
- Hempel, S., K. Frieler, L. Warszawski, J. Schewe, F. Piontek, (2013), A trend-preserving bias correction – the ISI-MIP approach, *Earth System Dynamics*, 4, 219-236.
- Jacob, D., J. Petersen, B. Eggert, A. Alias, O. B. Christensen, L. M. Bouwer, A. Braun, A. Colette, M. Deque, G. Georgievski, E. Georgopoulou, A. Gobiet, L. Menut, G. Nikulin, A. Haensler, N. Hempelmann, C. Jones, K. Keuler, S. Kovats, N. Kröner, S. Kotlarski, A. Kriegsmann, E. Martin, E. van Meijgaard, C. Moseley, S. Pfeifer, S. Preuschmann, C. Radermacher, K. Radtke, D. Rechid, M. Rounsevell, P. Samuelsson, S. Somot, J-F. Soussana, C. Teichmann, R. Valentini, R. Vautard, B. Weber, P. Yiou, (2014), EURO-CORDEX: new high-resolution climate change projections for European impact research, *Regional Environmental Change*, 14, 563-578.
- Kobierska, F., K. Engeland, Th. Thorarindsdottir, (2017), Evaluation of design flood estimates – a case study for Norway, *Hydrology Research* doi:10.2166/nh.2017.068
- Kuczera, G., S. Franks, (2006), Australian rainfall and runoff book IV, Estimation of Peak-Discharge, Revision draft (online), Engineers Australia. Available from www.arr.org.au.
- Lawrence, D. (2016), Klimaendring og framtidige flommer i Norge, NVE Rapport 81/2016.
- Lawrence, D. and I. Haddeland, (2011), Uncertainty in hydrological modelling of climate change impacts in four Norwegian catchments, *Hydrology Research* 42, 457-471.
- Lawrence, D., I. Haddeland, E. Langsholt, (2009), Calibration of HBV hydrological models using PEST parameter estimation, NVE Report 1/2009.
- Osuch, M., D. Lawrence, H. K. Meresa, J. J. Napiorkowski, R. J. Romanowicz, (2016), Projected changes in flood indices in selected catchments in Poland in the 21st century, *Stochastic Environmental Research and Risk Assessment*, DOI 10.1007/s00477-016-1296-5.
- Prudhomme, C., D. Jakob, C. Svensson, (2003), Uncertainty and climate change impact on the flood regime of small UK catchments, *Journal of Hydrology*, 277, 1-23.
- Renard, B., K. Kochanek, M. Lang, F. Garavaglia, E. Paquet, L. Neppel, K. Najib, J. Carreau, P. Arnaud, Y. Aubert, F. Borchi, J.-M. Soubeyroux, S. Jourdain, J.-M. Veysseire, E. Sauquet, T. Cipriani, A. Auffray, (2013), Data-based comparison of frequency analysis methods: A general framework, 49,825-843.
- Sunyer, M., Y. Hundecha, D. Lawrence, H. Madsen, P. Willems, M. Martinkova, K. Vormoor, G. Bürger, M. Hanel, J. Kriaciuniene, A. Loukas, M. Osuch, I. Yücel (2015), Intercomparison of statistical downscaling methods for projection of extreme precipitation in Europe, *Hydrology and Earth System Sciences*, 19, 1827-1847.
- Sælthun, N. R. 1996. The Nordic HBV Model, NVE Publication No. 7.
- Vejjalainen, N., E. Lotsari, P. Alho, B. Vehviläinen, J. Käyhkö, (2010), National scale assessment of climate change impacts on flooding in Finland, *Journal of Hydrology*, 391, 333-350.
- Yang, W., J. Andreasson, L. P. Graham, J. Olsson, J. Rosberg, F. Wetterhall, (2010), Distribution-based scaling to improve the usability of regional climate model projections for climate change impact studies, *Hydrology Research*, 41, 211-222.

5. New tools for design flood analysis

5.1 The Intensity-Duration-Frequency (IDF) tool – combining point and grid estimates

A. V. Dyrørdal and E. J. Førland

Norwegian Meteorological Institute, Norway

Summary

A new web tool for extracting IDF-statistics at any point in Norway is presented at the Norwegian Centre for Climate Services website. This interactive tool will assist local authorities and engineers in deciding the best possible precipitation design values for their region, and is to our knowledge the first of its kind. IDF-statistics can be downloaded as figures and tables. Further development of the IDF-tool involves, a measure of uncertainty in different regions, implementing climate factors for future design values, as well as improving the methodology for estimating design values for current climate.

Introduction

Intensity-Duration-Frequency (IDF) precipitation statistics are widely used for planning purposes in Norway. The relatively sparse network of pluviometer stations that have recorded short-duration rainfall long enough to estimate IDF statistics (minimum ten years), represents a challenge, as damaging rainfall is not limited to those locations with stations. Thus, we aim to meet the need for local IDF-statistics at any point in Norway through gridded precipitation design values. These are, along with station design values, presented on Norwegian Centre for Climate Services (NCCS) website (<https://klimaservicesenter.no/faces/desktop/idf.xhtml>). The purpose of

the new IDF-tool is to help local authorities decide on the best possible precipitation design values for their region.

Norwegian Centre for Climate Services

NCCS is a collaboration between Norwegian Meteorological institute (MET, leader), Norwegian Water Resources and Energy Directorate (NVE), Uni Research and the Bjerknes Centre for Climate Research (BCCR). The Norwegian Environment Agency represented in the board. The main aim of NCCS is to provide decision makers in Norway with relevant information regarding climate change adaptation, under the motto: “Prepare for the weather of the future”. The NCCS website presents climate and hydrological data for use in climate adaptation and further research on the effect

of climate change on nature and society. The front page of the NCCS websites is shown in Figure 1.

New IDF-tool

The newest asset on the NCCS website is a tool presenting IDF-statistics for meteorological stations and arbitrary points on a 1 x 1 km grid. The gridded estimates are described in article 2.2 (this report) In Figure 2 we see a map with pluviometer stations (green markers) where IDF-statistics have been estimated. The warning ("OBS") relates to an ongoing evaluation and improvement of the gridded estimates, implying they are not to be used for planning purposes for now.

The very detailed geographical map enables the user to easily locate the site of interest. By clicking on a green marker or searching the location, as shown in Figure 3, the map zooms to the station which is indicated in dark green. Some meta information appears below the map, along with the estimated IDF-curve for the station. The curve can be shown for durations 1 – 60 minutes, 60 – 1440 minutes, or for all durations, and return periods not of interest can be removed by clicking on the label. The default unit is mm, but can be changed to l/sha. The IDF-curve can be downloaded as a png and the table as csv.

For estimated IDF-curves at arbitrary points, the user can click in the map, or search coordinates or location name; a purple marker then appears in the map. As described in article 2.1 and 2.4 (this report), estimated precipitation design values in terms of return levels can differ significantly depending on methodology. As of today, station estimates and gridded estimates are based on different methods, resulting in large deviations at some locations. MET is currently working on better and more comparable estimates.

Three clickable information boxes are available on the website, where more detailed information on functionality and methodology is presented.

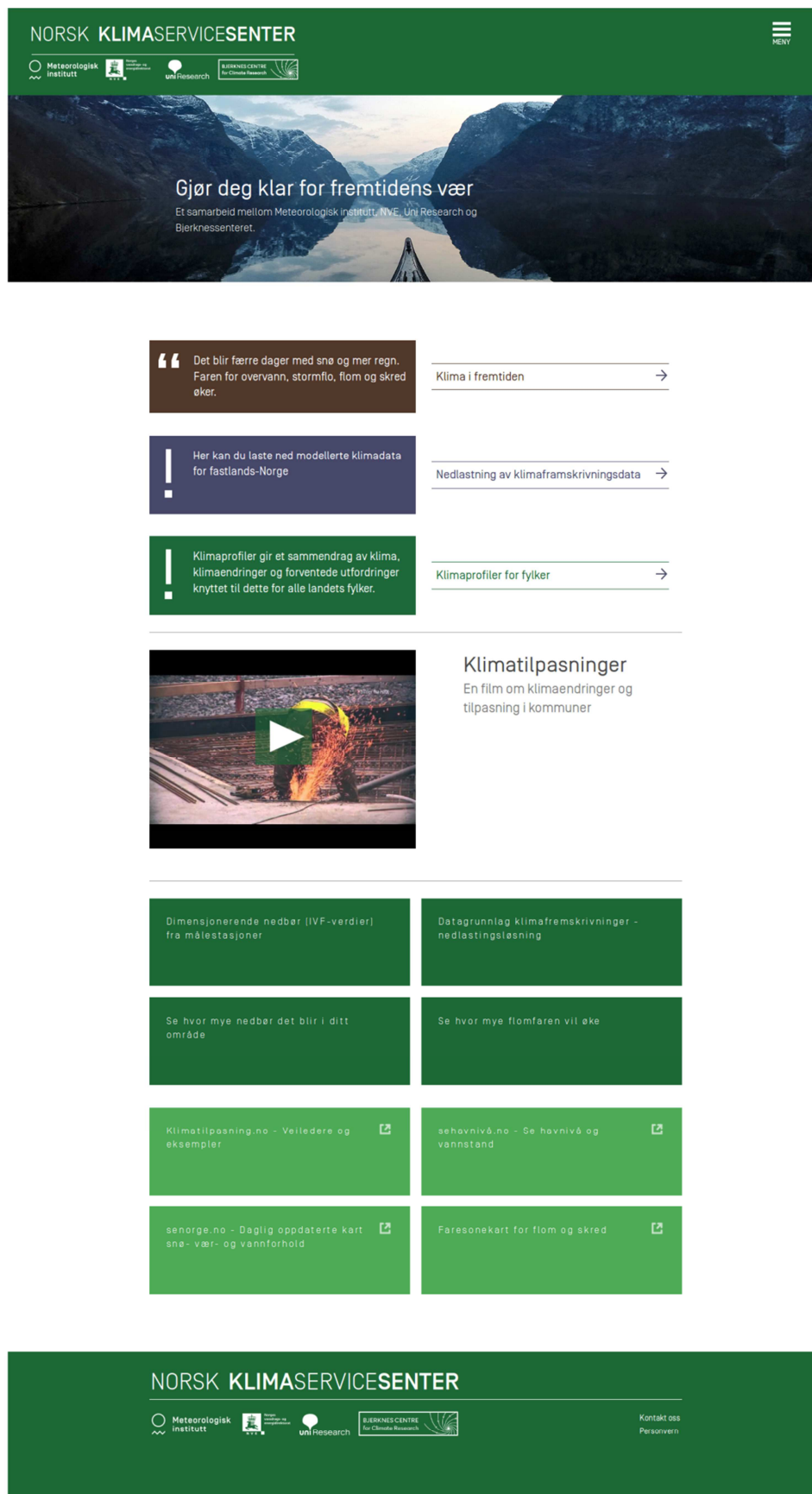


Figure 2: Front page of NCCS website (in Norwegian)

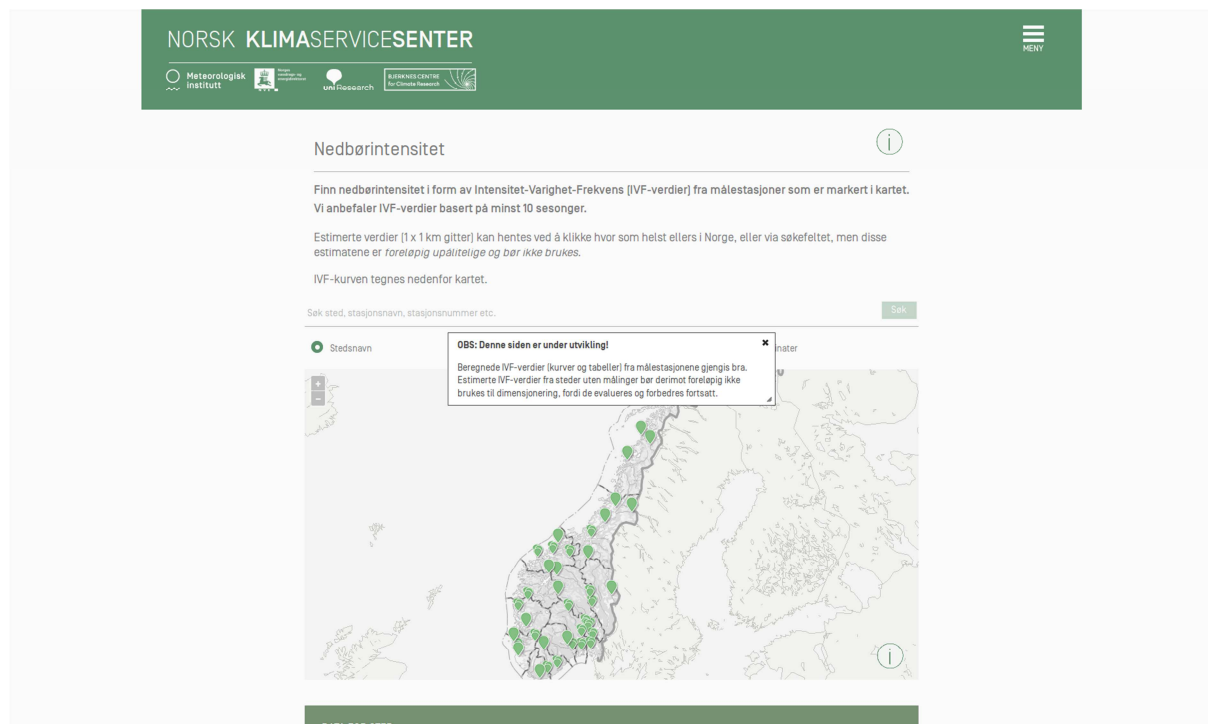


Figure 3: Front page of the IDF-tool, including a warning.

Nedbørintensitet



Finn nedbørintensitet i form av Intensitet-Varighet-Frekvens [IVF-verdier] fra målestasjoner som er markert i kartet. Vi anbefaler IVF-verdier basert på minst 10 sesonger.

Estimerte verdier (1 x 1 km gitter) kan hentes ved å klikke hvor som helst ellers i Norge, eller via søkefeltet, men disse estimatene er foreløpig upålitelige og bør ikke brukes.

IVF-kurven tegnes nedenfor kartet.

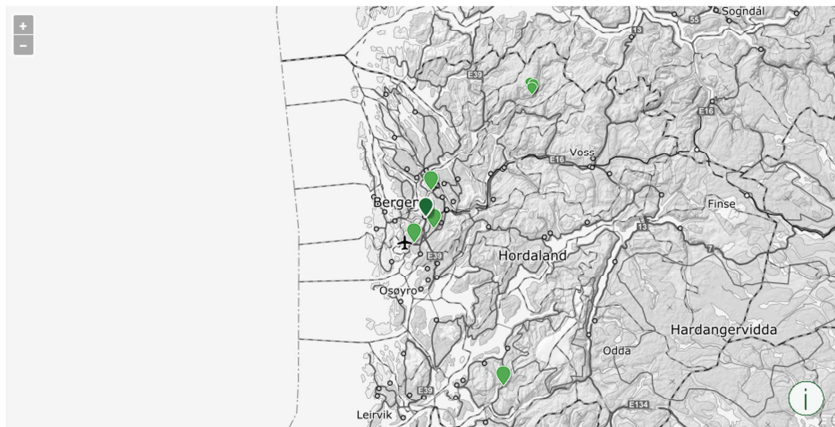
BERGEN - FLORIDA UIB

Søk

Stedsnavn

Bredde-/lengdegrad

UTM-koordinater



STEDSINFO

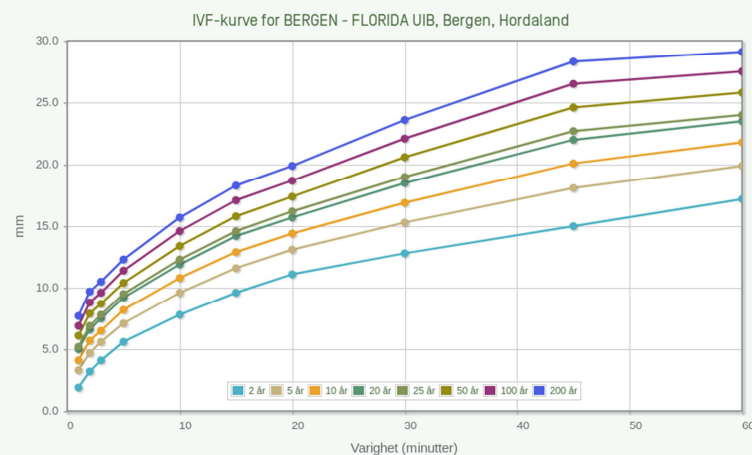
BERGEN - FLORIDA UIB (SN50539)
Bergen, Hordaland
Høh.: 46 m
Måleperiode for stasjonen: 2003-06-17 - 2018-01-10. [Se alle måleperioder.](#)
Antall sesonger i IVF-statistikk: 13

DATA FOR STED

NEDBØRSINTENSITET OG RETURVERDIER

Varigheter 1-60 min.

mm



Last ned figur (png)

Tabellvisning

Last ned data



Figure 4: Figure 3: Map zoomed over Hordaland, indicating the station Bergen - Florida in dark green. Meta data and IDF-curve are shown below the map. This is for durations 1 – 60 minutes.

Further development

As soon as gridded estimates are of acceptable quality, and methodologies for stations and grid have been harmonized, we will present a measure of uncertainty associated with the estimated return levels. We will include a color code indicating the level of uncertainty depending on degree of variability in the region and the density of the station network. Four levels seem reasonable, representing (very) uncertain and (very) certain.

In article 4.1 (this report), so-called “climate factors” are presented. These are factors with which to multiply today's design values to obtain an estimate of future design values, as given by fine-scale climate models. We intend to present climate factors on the IDF website to facilitate the planning of installations with a long life time.

5.2 NEVINA

K. Engeland, T. Væringstad, N.K. Orthe, A. Voksø, D. Lawrence

Hydrology Department, Norwegian Water Resources and Energy Directorate (NVE), Norway

Summary

NEVINA is a public, interactive map-based service providing estimates of streamflow characteristics including low flow indices and design flood values as well as key physiographic and climatic characteristics for ungauged catchments. In NEVINA, users can easily extract catchment boundaries for a self-chosen point in a river system. For this user-specified catchment, key characteristics and flow indices are calculated. Recommendations for climate factors for design floods in small catchments are also provided.

NEVINA aims to be an efficient tool for extracting catchment information and obtaining estimates of important flow indices required by end-users. In addition, NEVINA represents an efficient and accessible platform for the implementation and dissemination of research results related to catchment hydrology and its applications.

Introduction

In order ensure that results from research projects will be useful for and applied by end users, implementation in efficient, robust and user friendly tools is a solution. Such tools also serve as a channel for dissemination of research project results. For the ExPrecFlood project, NEVINA is one of the tools used for implementation of results and provides a first step towards operational climate services.

NEVINA is an interactive map-based tool where the user can extract catchment boundaries upstream of any point in a river network. For the selected catchment, NEVINA calculates a range of climatic and physiographic parameters. Based on this information, statistical models can be applied to estimate flow characteristics.

The predecessor to NEVINA is the low flow map for Norway (Engeland et al, 2008) where the aim was to

provide estimates of low flow indices in ungauged catchments. The results were implemented in a web-based tool available for the public. This tool has been popular among end-users since it is efficient, user friendly and provides much needed information. For several projects related to design flood estimation (FlomQ and Flomkart, in addition to ExPrecFlood), it was decided that the low flow map application could also be used for estimating design floods in ungauged catchments. The name of the low flow map tool was therefore changed to NEVINA (Nedbørfelt-

Vannføring-Indeks-Analyse) in 2015 in order to reflect this broader goal. At that time, design flood estimates for peak floods in small catchments developed in the NIFS-project were implemented (Glad et al., 2014)

An important challenge when providing a tool such as NEVINA, that is based on existing information and algorithms and provides estimates of flow indices for any arbitrary catchment in Norway, is that there may be errors in the underlying data. In addition, the statistical model used for the estimation, may be biased. Users are therefore asked to give feedback on obvious errors and are allowed to edit much of the information that is automatically generated. In its current version, NEVINA is well suited for use in preliminary assessments of possible measures. For more detailed planning of a proposed measure, the values from NEVINA must be supplemented with a professional hydrological assessment. The extent of such an assessment depends on the nature of the measure.

Brief user guide to NEVINA

The web-address for NEVINA is <http://nevina.nve.no>. Once NEVINA is opened, the user will need to zoom into the map to a scale sufficient to see the necessary details of the river network in the area of interest. The user then needs to follow the menu to the left, starting at the top. The first step is to choose a point in a river network ("VELG PUNKT"). The point should not be more than 100 meters from a river segment and should be more than 100 meters from a river intersection or outlet. The upstream catchment boundaries are then generated by running "GENERER NEDBØRFELT". In the third step ("REDIGER NEDBØRFELT"), the catchment boundaries can be edited if errors in the automatically-generated catchment boundaries are found (Figure 1).

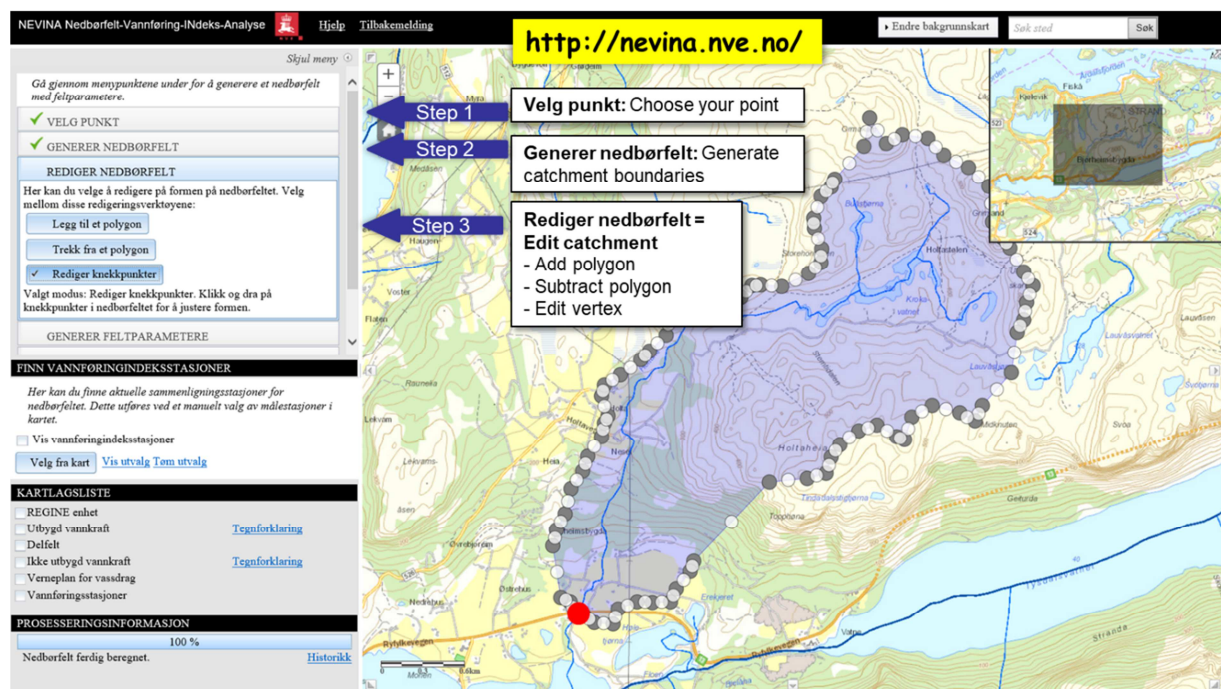


Figure 1: The first three steps are to select a point in or close to a river segment, generate catchment boundaries and, if necessary, edit the catchment boundaries.

The fourth step is to generate the catchment parameters. Several of the parameters can be edited by the user if errors are found (Figure 2). The fifth step is to generate the indices, including design flood estimates, and in the sixth step the results can be exported either as a pdf-report or to a shape file containing all derived information (Figure 3). Design flood estimates and/or low flow indices from nearby gauging stations can also be extracted using a map-based selection tool as illustrated in Figure 4. This allows the user to compare the estimated design flood from the regional model to estimates based on local flood frequency analysis.

The pdf report from NEVINA also gives recommended values for a climate factor for use in assessing the future effects of climate change on the flood estimates generated by NEVINA. These factors are currently only given for catchments with area < 50 km². The recommended factors for small catchments are 1.2 for the daily flood and 1.4 for the instantaneous flood (i.e. the peak flow). The first of these is based on the results and recommendations for assessing climate change impacts on future flooding in Norway published by NVE (Lawrence and Hisdal, 2011; Lawrence, 2016) where use of a climate factor of at least 20% is recommended for small catchments. The use of 1.4 for the instantaneous flood is based on analyses of future changes in 3-hr. vs. daily precipitation intensities undertaken by the Norwegian Meteorological Institute (see Hanssen-Bauer, et al., 2015, Table 5.2.6) which suggest that 3-hr. precipitation intensities will increase more than daily (38% vs. 26%) for the 200-yr. return period. Small, rapidly responding catchments will be most vulnerable to the larger increase in sub-daily precipitation intensities, so a climate factor of 1.4 is currently recommended by NEVINA. The results from the ExPrecFlood project (see article 4.3, this report) generally support the current recommendations given by NEVINA for climate change factors for small catchments and will be reviewed by NVE.

Climatic changes in short duration extremes - implications for design values

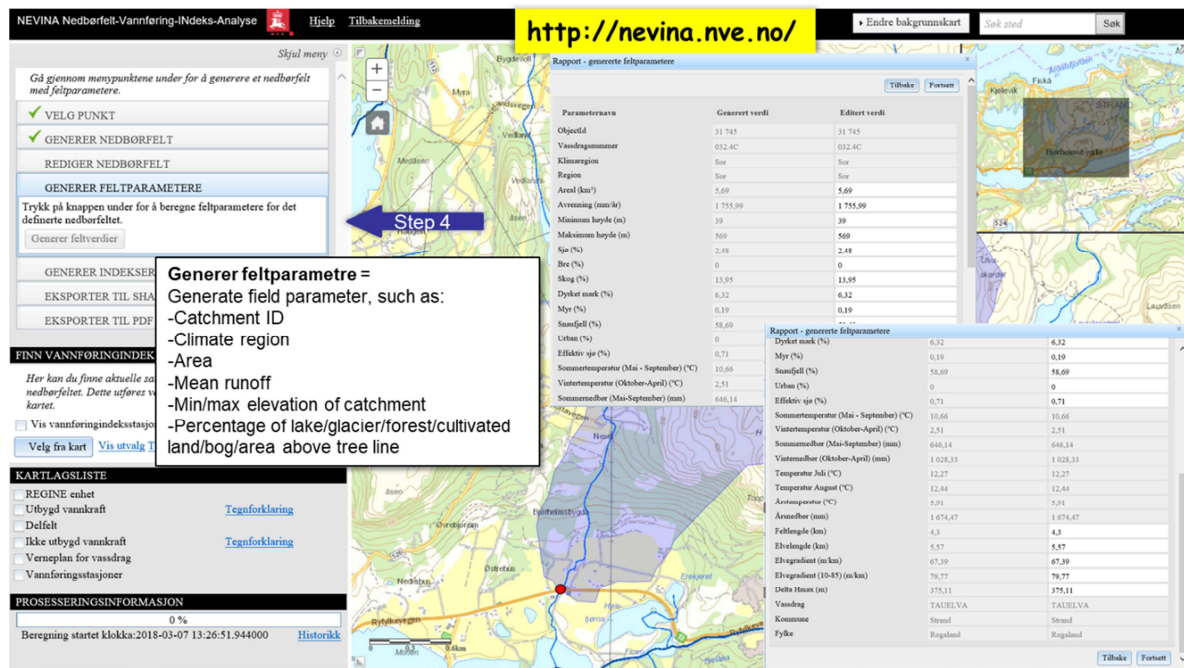


Figure 2: The fourth step is to generate the catchment parameters. Several of the parameters can be edited by the user.

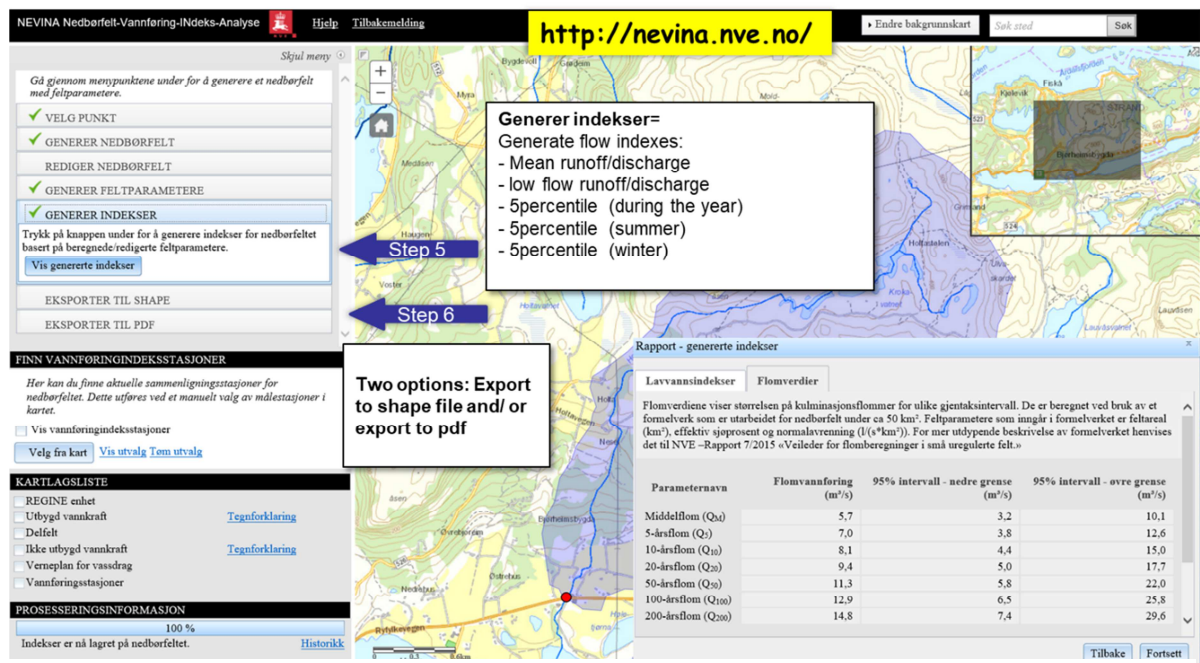


Figure 3: The fifth step is to generate the flow indices for the catchment. This includes low flow indices and design flood estimates. The sixth step is to export the results to a shape file or to a pdf-file with a standard report.

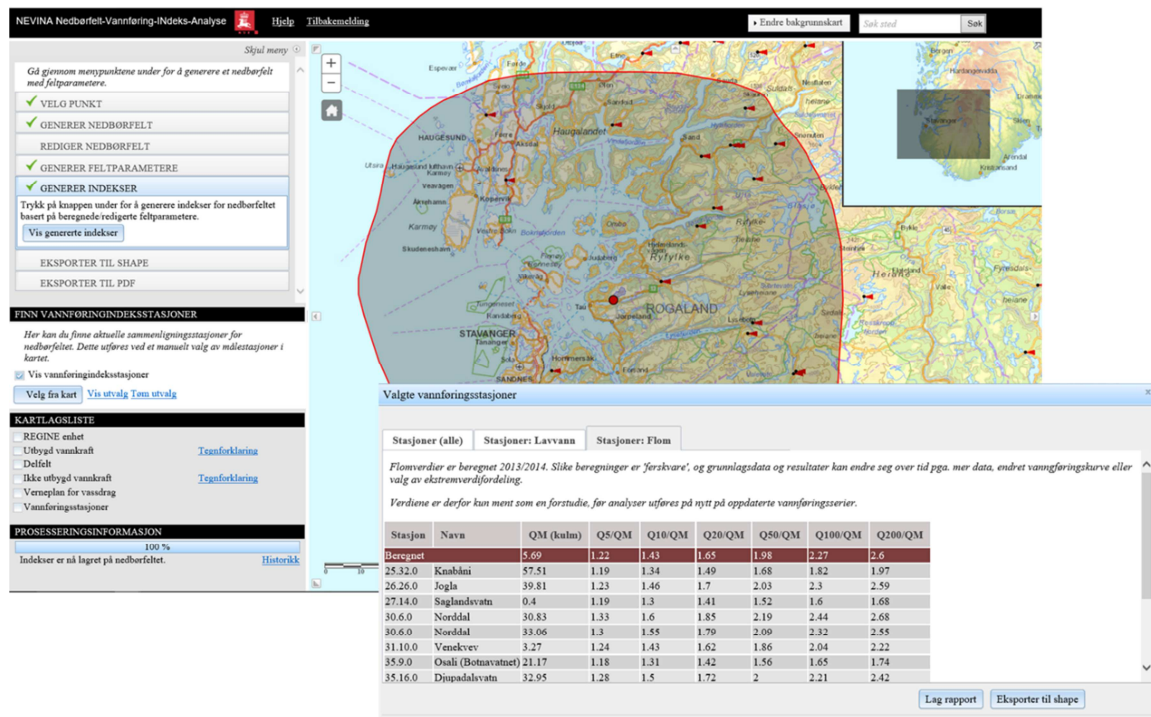


Figure 4: Nearby gauging stations can be selected and design flood estimates from these stations are then provided.

Data and algorithms

Delineation of upstream catchment

The calculation of upstream catchment boundaries is based on the following GIS-datasets covering all Norway and, where necessary, trans-boundary catchments flowing into Norway from Sweden, or Finland.

- Flow direction and flow accumulation grids at a spatial resolution of 25 meters calculated at NVE based on a DTM from the Norwegian mapping authorities and a map of river network that is lower the grid cells crossed by a river segment by 30 meters.
- REGINE – polygons with boundaries for approximately 30 000 sub-catchments in Norway, included catchments which drain to Norway from neighbouring countries.
- River network – a geometric network of river segments including flow direction. For lakes, centrelines are used as river segments.

The point selected by the user has to be within a maximum of 100 meters from a river segment and more than 100 meters from a river intersection or outlet. The flow

direction grid is used to delineate upstream catchment boundaries up to the nearest catchment boundaries defined in the REGINE dataset.

Calculating catchment characteristics

The following datasets are used to extract catchment characteristics

- DTM25 for calculation of the hypsographic curve.
- Digital data from maps at 1:50.000 used for calculating percentages of land cover.
- River network with linear referencing for calculating river length and gradients.
- Gridded datasets (1x1 km²) of climatology for the period 1961-1990 for calculating precipitation, temperature and runoff statistics.

Calculating design floods

The design flood estimates are based on the algorithm presented in Glad et al (2014). An index flood approach is applied in which a regression equation is used to estimate the mean annual flood (used as the index flood) and the growth curve is subsequently calculated based on catchment properties. 95% credibility intervals are also provided. The equations are estimated using annual maximum peak flow data from 165 stations with catchment areas smaller than 50 km².

Planned extensions of NEVINA

Within 2018 the following extensions of NEVINA are planned in order to implement results from FlomQ and ExPrecFlood:

- New catchment characteristics. In particular, climatology will be calculated from the SeNorge dataset Version 2.1
- New algorithms for estimating design floods in ungauged catchments by implementing results from FlomQ / Flomkart
- New algorithms for estimating climate factors in ungauged catchments.
- New one-page tailored reports
- A dynamic link to the hydrological database for extracting observed floods
- from quality controlled streamflow stations

References

- Engeland, K., Hisdal, H., Orthe, N.K. Petersen-Øverleir, A. Voksø, A. (2008) Low flow map for Norway (in Norwegian: Lavvannskart for Norge), NVE oppdragsrapport A No. 5/2008, 60 pp.
- Glad, P. Reitan, T. and Stenius, S. (2014) Regional equations for flood estimation in small catchments (in Norwegian: Regionalt formelverk for flomberegninger i små nedbørfelt), NVE Rapport 62/2014, 52 pp.

- Hanssen-Bauer, I., E. J. Førland, I. Haddeland, H. Hisdal, S. Mayer, A. Nesje, J. E. Ø, Sandven, A. B. Sandø, A. Sorteberg, B. Ådlandsvik (Editors), (2015), Klima i Norge 2100: Kunnskapsgrunnlag for klimatilpasning oppdatert i 2015, Norwegian Climate Services Centre Report 2/2015.
- Lawrence, D., Hisdal, H. (2011), Hydrological projections for floods in Norway under a future climate, NVE Report 5/2011.
- Lawrence, D. (2016), Klimaendring og framtidige flommer i Norge, NVE Rapport 81/2016.

